Chem Soc Rev

REVIEW ARTICLE

View Article Online
View Journal | View Issue

Cite this: *Chem. Soc. Rev.*, 2019, **48**, 2216

Artificial photosynthesis: opportunities and challenges of molecular catalysts

Biaobiao Zhang [a] and Licheng Sun *[ab]

Molecular catalysis plays an essential role in both natural and artificial photosynthesis (AP). However, the field of molecular catalysis for AP has gradually declined in recent years because of doubt about the long-term stability of molecular-catalyst-based devices. This review summarizes the development history of molecular-catalyst-based AP, including the fundamentals of AP, molecular catalysts for water oxidation, proton reduction and CO_2 reduction, and molecular-catalyst-based AP devices, and it provides an analysis of the advantages, challenges, and stability of molecular catalysts. With this review, we aim to highlight the following points: (i) an investigation on molecular catalysis is one of the most promising ways to obtain atom-efficient catalysts with outstanding intrinsic activities; (ii) effective heterogenization of molecular catalysts is currently the primary challenge for the application of molecular catalysis in AP devices; (iii) development of molecular catalysts is a promising way to solve the problems of catalysis involved in practical solar fuel production. In molecular-catalysis-based AP, much has been attained, but more challenges remain with regard to long-term stability and heterogenization techniques.

Received 12th November 2018

DOI: 10.1039/c8cs00897c

rsc.li/chem-soc-rev

[a] *Department of Chemistry, School of Engineering Sciences in Chemistry, Biotechnology and Health, KTH Royal Institute of Technology, 10044 Stockholm, Sweden. E-mail: lichengs@kth.se*

[b] *State Key Laboratory of Fine Chemicals, Institute of Artificial Photosynthesis, DUT-KTH Joint Education and Research Center on Molecular Devices, Dalian University of Technology (DUT), 116024 Dalian, China*

1. Introduction

Over the last hundred years, approximately 80% of worldwide energy consumption has been based on fossil fuels, including coal, oil, and natural gas.[1] However, humankind now has to face the consequences arising from this dependence on fossil fuels. Worldwide energy consumption is expected to increase

Biaobiao Zhang

Dr Biaobiao Zhang received his PhD in Applied Chemistry from Dalian University of Technology in 2015 under the guidance of Prof. Licheng Sun and is currently a postdoc at KTH Royal Institute of Technology. His current work focuses on the development of manganese oxide based WOCs, molecular WOCs and molecular WOC engineered materials for artificial photosynthesis devices.

Licheng Sun

Prof. Licheng Sun received his PhD in 1990 from Dalian University of Technology. He went to Germany as a postdoc at Max-Planck-Institut für Strahlenchemie with Dr Helmut Görner (1992–1993), and then as an Alexander von Humboldt fellow at Freie Universität Berlin (1993–1995) with Prof. Dr Harry Kurreck. He moved to KTH Royal Institute of Technology, Stockholm, in 1995 and became an assistant professor in 1997, an associate professor in 1999 (at Stockholm University) and a full professor in 2004 (KTH). He is presently also a distinguished professor in DUT. His research interests cover artificial photosynthesis, molecular catalysts for water oxidation and hydrogen generation, functional devices for total water splitting, dye sensitized, quantum dot/rod sensitized solar cells, and perovskite solar cells.

by over 50% by the mid-2000s.[2] Because fossil fuels are finite and regional around the world, it is greatly challenging to ensure that this demand can be met, in the face of possible political tensions and other potential problems with energy supplies. Due to the usage of fossil fuels, large quantities of emissions, *e.g.*, CO_2, SO_2, and oxide particles, are the predominant reasons for global warming and severe pollution. Recent reports from the Intergovernmental Panel on Climate Change emphasized the necessity of decreasing CO_2 emissions on a global scale to the zero level before the next century.[3] These arguments make the development of sustainable and carbon-neutral energy technologies one of the most urgent challenges facing humankind all over the world. The most abundant renewable energy source on the planet is solar energy: solar illumination on Earth every hour is greater than the worldwide energy consumption for a whole year.[4] Therefore, the conversion and utilization of solar energy is a promising solution for energy problems.

The nature of a solar-energy carrier is that of a photon moving at light speed. A fundamental step for using solar energy is to harvest these high-energy particles with light absorbers to generate separated electrons and holes, *i.e.*, charge separation. In photovoltaic cells, these photogenerated electrons and holes can be collected to produce potential and current; in consequence, the harvested solar energy is directly converted into electricity, which is an important energy format in daily life. However, electricity is not readily stored on a large scale, and cannot realize a complete replacement of fossil fuels, because the energy density of batteries is far below that of chemical fuels with respect to both weight and volume.[3] Therefore, electricity is not an ideal energy source for applications such as large oversea vessels and long-distance air transport. Inspired by the natural photosynthesis, rather than being collected for electricity, the photo-generated electrons and holes can be used to drive chemical reactions; thus the harvested solar energy can be converted into chemical energy (solar fuel) stored in the form of chemical bonds. This multiple-step process, which mimics the function of natural photosynthesis, is generally named artificial photosynthesis (AP).[3,5]

Since the proposal of the AP concept and the modeling of AP devices, chemists have believed that developing molecular catalysts is one promising way to solve the problems of catalysis involved in AP, because of the abundant advantages of molecular catalysts.[6] Over the past few decades, hundreds of catalysts have been developed and investigated for the reactions involved in AP. However, it seems that the devices assembled from molecular catalysts are less stable and perform less efficiently than those built from material catalysts. On the other hand, it has been found that, under certain experimental conditions, the involved molecular catalysts decomposed into metal-based inorganic materials that were the true catalysts. Because of the underachievement of molecule-based AP devices, the research on development of molecular catalysts has been gradually losing focus over the last five years.

We believe that molecular catalysts are still promising for the future of AP. The real bottleneck problems for realizing applicable AP have obviously not been solved. The achievement of molecule-based AP should include several stages, such as development of efficient molecular catalysts, heterogenization of molecular catalysts, and engineering of applicable devices. In previous decades, scientists have expended much effort on the first stage, and several highly efficient and promising molecular catalysts have been developed for water oxidation, hydrogen evolution and CO_2 reduction. However, studies into the second stage, which is equally important and challenging, have largely been inadequate. Many problems and factors have not been researched and have not even been well considered. We have therefore written this review article to summarize previous research on molecular catalysts for AP, to emphasize the significance of molecular catalysts, and to discuss the opportunities, challenges and future of molecular catalysts, with the aim of providing readers with some guidelines on how to choose catalysts when they start to design their systems for AP.

2. Artificial photosynthesis and functional devices inspired by nature

For billions of years, plants and organisms on Earth have provided oxygen and foods for aerobic life cycles *via* photosynthesis, a process that produces O_2 and carbohydrates (*e.g.*, sugar $C_6H_{12}O_6$) from CO_2 and H_2O by utilizing sunlight.[7] Consequently, solar energy is converted into chemical energy and stored in carbohydrates. Photosynthesis occurs through the cooperation of photosystem II (PSII) and photosystem I (PSI).[8,9] Driven by sunlight, H_2O is oxidized in PSII into O_2, releasing four protons and four electrons. The electrons and protons are transferred *via* cytochrome *b6f* to PSI, in which the separated electrons and protons are finally consumed by CO_2 reduction to produce carbohydrates (Fig. 1a).

The photosystems and photosynthesis are extremely complicated. It is unachievable to exactly mimic their structures and components. However, the functions and chemical processes can be replicated to realize AP to convert solar energy into chemical energy and store it as synthetic chemical fuels (Fig. 1b). Solar energy can be directly converted into chemical fuels *via* photoelectrocatalytic reactions, or it can be converted into fuels indirectly by using the electricity generated from solar energy to drive electrocatalytic reactions. Water splitting to produce hydrogen fuel ($2H_2O \rightarrow O_2 + 4e^- + 4H^+$; $2H^+ + 2e^- \rightarrow H_2$) and CO_2 reduction to produce carbon-neutral fuel (*e.g.* $CO_2 + 6H^+ + 6e^- \rightarrow CH_3OH + H_2O$) are widely investigated reactions in artificial photosynthesis. In this review, we mainly focused on water splitting and CO_2 reduction reactions. However, it should be noted that the production of other types of fuels and high-value-added chemicals can also be achieved with AP by driving the corresponding reactions,[10] such as ammonia production from nitrogen fixation,[11] epoxide production from hydrocarbon oxygenation,[12–14] hydrogen peroxide production from oxygen reduction,[15] and polymer production from biomass related 5-hydroxymethylfurfural (HMF) conversion reactions.[16]

Two types of devices have been designed for the production of solar fuels, the photoelectrochemical (PEC) cell (Fig. 2a) and

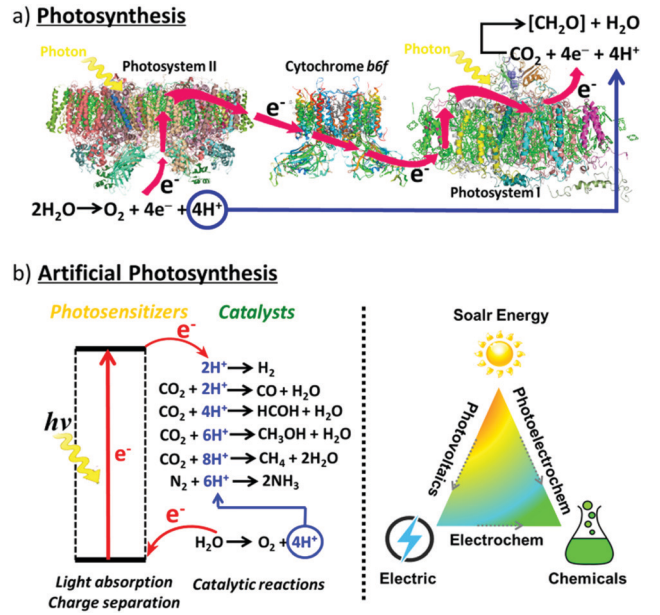

Fig. 1 Schematic representation of (a) the natural photosynthetic chain in photosystems; (b) general concept of AP.

the photovoltaic-coupled electrolyzer (PVE) device (Fig. 2b).[17] An ideal PEC cell consists of a photoanode and a photocathode. The photoanode can be a molecular dye sensitized TiO_2 electrode[18–20] or n-type visible-light-absorbing semiconductors[21] (*e.g.*, α-Fe_2O_3,[22] WO_3[23] and $BiVO_4$[24]) with enough driving force or valence band potential for water oxidation. The photocathode can be a molecular dye sensitized NiO electrode[25] or other p-type visible-light-absorbing semiconductors[26] (such as InP[27] and Cu_2O[28]) with conduction bands that are negative enough to reduce the reactants to chemical fuels. Under illumination, the generated holes and electrons are directly transferred to the catalysts loaded on the surface of the photoanode and photocathode to drive the photocatalytic reactions and produce fuels (Fig. 2a). In practice, a PEC cell can also be fabricated with a single photoelectrode, either one photoanode or one photocathode. Because of the challenge of assembling full PEC cells, most of the reported PEC cells to date are single-photoelectrode cells. For the PVE devices (Fig. 2b), the light absorption and charge separation are completed by a solar cell, which can be separated from the electrolyzer cell.[29] Potentials generated by the solar cell are applied to the electrolyzer to drive the electrochemical water-oxidation reaction on the anode and the electrochemical reduction reactions for fuel production on the cathode. In the PVE device, solar energy is indirectly converted into chemical fuels in two steps.

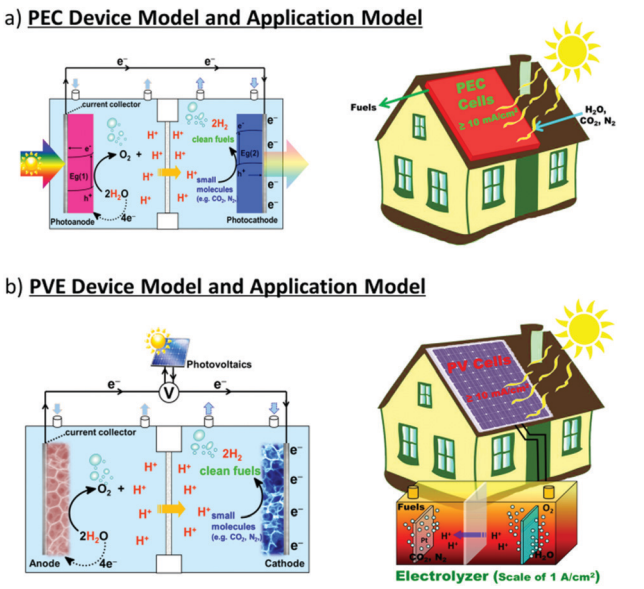

Fig. 2 Schematic representation of (a) PEC device model and application model; (b) PVE device model and application model.

Fig. 2 also shows two possible ways to domestically apply PEC and PVE devices in the future. The required performances of each device are marked in the figures.[30] To meet the forecasted worldwide annual energy consumption in the year 2050, only 1% of the earth's surface needs to be covered by solar energy converting devices with $\geq$10% solar-to-fuel efficiencies.[30,31] Accordingly, in the PEC device, the photo-generated current densities of water splitting need to be over 10 mA cm^{-2}. In the PVE device, the lowest demand on the ability of the solar cell in general is a photocurrent density over 10 mA cm^{-2} and a potential high enough to load the electrolyzer. Moreover, the electrolyzer cell needs to be a highly integrated device, which can generally generate a current for electrochemical synthesis with a current density in the region of 1 A cm^{-2}.

Four main processes, namely, light harvesting by light absorbers, charge separation in the light absorbers, charge transfer from the light absorbers to the catalysts, and the occurrence of catalytic reactions, will be involved in complete AP. Accordingly, two fundamental components are necessary for building AP devices. Ideal light absorbers, with broad absorption in the solar spectrum, stable excited states and high charge carrier mobility, and efficient catalysts, with high intrinsic activity and stability, are the two essential components to realize AP. Photosensitizers or light absorbers, such as molecular dyes,[19,32,33] semiconductors[34] and quantum dots,[35,36] are needed to absorb the light and generate the charge separation. Moreover, efficient catalysts are the other key. If the half reactions shown in Fig. 1b are taken as examples, the reactions in AP all involve multiple electron and proton transfers, which make these reactions kinetically sluggish and require high overpotentials. Efficient catalysts are required to overcome the high reaction barriers, lower the requirement for overpotential, and accelerate the reaction rate. To achieve catalysts with high intrinsic activity, low overpotential, and a high catalytic rate, the development of molecular catalysts is the most promising way to go.

3. Why and how to engage molecular catalysts in applicable AP devices

3.1 Advantages of molecular catalysts

Complexes **1**, **2**, and **3** (Fig. 3a) are well-known examples of Fe-based molecular catalysts for water oxidation, hydrogen

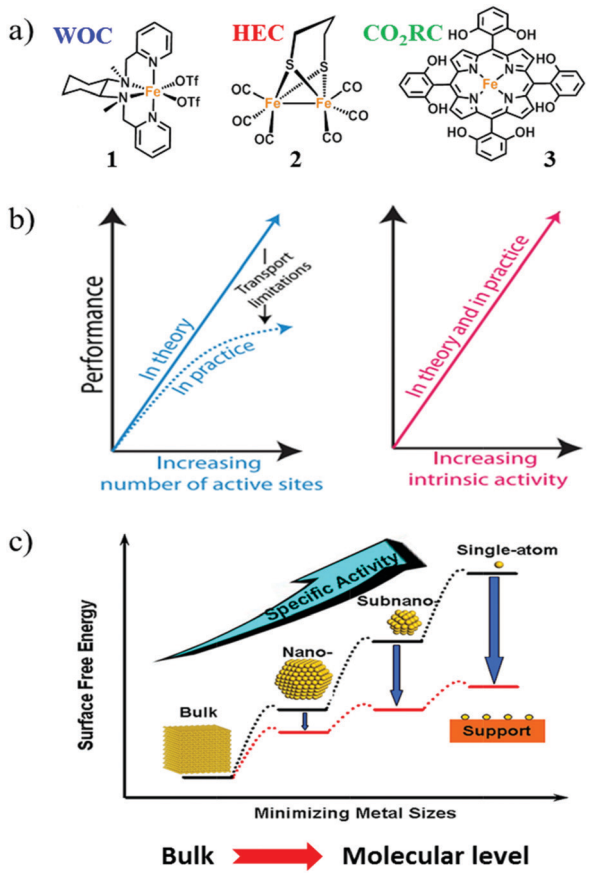

Fig. 3 (a) Molecular structures of Fe complexes **1**, **2**, and **3** as molecular catalysts. WOC: water-oxidation catalyst; HEC: hydrogen-evolution catalyst; CO_2RC: CO_2 reduction catalyst. (b) The enhancement of catalytic performance by increasing the number of active sites and/or increasing the intrinsic activity of each active site. Adapted with permission from ref. 37. Copyright 2017 American Association for the Advancement of Science (AAAS). (c) The positive effect on catalytic performance obtained by minimizing the size of nanoparticle catalysts. Adapted with permission from ref. 38. Copyright 2013 American Chemical Society.

evolution, and CO_2 reduction, respectively.[39–41] The metal centers of **1**, **2**, and **3** are all iron; however, these complexes can catalyze different reactions because the electronic structures of the iron cores are precisely adjusted by the particular coordination environments created by the ligands. Thus, a molecular catalyst usually comprises a metal center as the active site and specific organic ligand(s) to produce the correct coordination environment for regulating the electronic structure of the active site. Thanks to this configuration, molecular catalyst possesses plenty of advantages as partially listed below:

(1) Clear structure, active site and catalytic mechanism. For most molecular catalysts, their structures are readily characterized by conventional spectroscopy and X-ray crystallography. Their catalytic active sites are clearly identifiable. In general, the catalytic mechanism by molecular catalysts can be revealed by numerous common experiments based on standard laboratory techniques, such as spectroelectrochemistry, stopped-flow UV-Vis spectroscopy, *in situ* IR spectroscopy, *in situ* NMR spectroscopy and *in situ* MS.

(2) Tunability. Both the steric configuration and electronic structure of molecular catalysts can be appropriately adjusted by the specific coordination environment through ligand design. On the basis of the first advantage, molecular complexes can be accurately adjusted after an intensive study, to generate efficient molecular catalysts for various reactions, such as the examples shown in Fig. 3a.

(3) Direct improvement of the intrinsic activity. The activity of an electrode can generally be enhanced by two strategies: (i) increasing the number of active sites on it and (ii) improving the intrinsic activity of each active site.[42] The enhancement of activity from increasing the number of active sites can be achieved through increased loading of catalysts or by modifying catalyst structures to expose more active sites per gram (Fig. 3b). However, these two ways are physically limited because they affect other important processes, such as charge and mass transport.[42] For this reason, a plateau effect is viable in practice with a high loading amount of catalysts (Fig. 3b).

Jaramillo and co-workers have given a precise statement about the intrinsic activity in their review on material design. They have written that "increasing intrinsic activity leads to direct increases in electrode activity in a manner that mitigates transport issues arising from high catalyst loadings; with improved intrinsic activity, the catalyst loading can be decreased, which also saves on catalyst costs. Moreover, catalyst activity is measured across many orders of magnitude; the difference in intrinsic activity between a good catalyst and a poor catalyst can be more than 10 orders of magnitude, whereas the difference between a high-loading and a low-loading catalyst might only be one to three orders of magnitude" (Fig. 3b).[37]

Therefore, studies to effectively improve the intrinsic activity of catalysts are important for the advancement of AP. For molecular catalysts, every molecule is a single active site with suitable intrinsic catalytic activity based on its unique structure. In conjunction with the first two advantages of molecular catalysts, the development of molecular catalysts can directly promote their intrinsic activity.

(4) Selectivity. Product selectivity is one essential factor for the catalysis of CO_2 reduction. Molecular catalysts, with single, easy-to-identify, and readily adjustable active sites, provide sufficient possibilities to control the product selectivity of CO_2-reduction catalysis.[43–46]

(5) Metal-atom economy. With a view to the final application of AP, the most obvious and preponderant advantage of molecular catalysts is their metal-atom economy. Efficient utilization of metal atoms is meaningful for the application of catalysts, especially catalysts based on rare metals (*e.g.*, Pd, Rh, Pt, Ir and Ru). Metal utilization in homogeneous molecular catalysts can reach 100%, a value that may be several orders of magnitude higher than that in inorganic material-based catalysts. Nano-structures, the unit of inorganic material-based, are formed from aggregates of hundreds or thousands of metal atoms, only a small number of which can act as active sites, *i.e.*, the metal atoms at surfaces, edges, corners, and heterojunctions.[47] To pursue high metal-atom economy and good selectivity, minimization of the size of the nano-structures is one efficient strategy (Fig. 3c).

However, even sub-nanoclusters, *i.e.*, single-site catalysts, still contain multiple catalytically uninvolved metal atoms.[38] Accordingly, materials scientists have recently developed single-atom catalysts (SACs); this is the most effective approach to utilize each and every metal atom in supported metal catalysts (Fig. 3c).[38,47,48] In addition to SACs, dinuclear heterogeneous catalysts (DHCs) have also been reported recently, *e.g.*, iridium DHCs on metal-oxide semiconductors.[49,50]

Indeed, SACs and DHCs are similar to molecular catalysts, because they catalyze on a molecular level. The difference between them is that the chemical environment of the active metal center of molecular catalysts is provided by molecular ligands, whereas it is provided by the anchoring supports for SACs and DHCs. It is clear that the development of material catalysts is now focused deeply at the molecular level. In addition, nature also chose molecular catalytic centers for various enzymes to complete the catalysis of water oxidation,[9] proton reduction,[51] and CO_2 reduction reactions,[52] indicating that molecular catalysis is no doubt also promising for AP. Consequently, the development of molecular catalysts is one of the effective ways to achieve practical AP.

3.2 Stages prior to achieving applicable molecular AP devices

AP is a major project to solve the sustainable energy problem, which is a big issue facing all human beings. In this context, although research into molecule-based AP has been ongoing for over 30 years, we are still at the early stages, and many more stages have not been researched or have not even been well proposed. There are at least three stages involved in producing a final AP device based on molecular catalysts: development of efficient molecular catalysts, heterogenization of molecular catalysts, and engineering of applicable AP devices (Fig. 4). These stages are correlated but they also have their own totally different challenges. For the first stage, the research community in this field has accumulated a lot of methods, strategies, and principles. There are also several successful WOCs, HECs, and CO_2RCs in hand. However, for the remaining two stages, the investigations are far from complete.

First stage, development of efficient molecular catalysts. Highly efficient catalysis is the basis for realization of practical AP. To achieve efficient molecular catalysts, plenty of research has been conducted in the last 30 years.[4,43,53–55] The procedures of development of a molecular catalyst include ligand design, the synthesis and characterization of the ligands and the final metal complex, catalytic analyses, and revelation of the mechanism; the results, in turn, guide the design of more advanced catalysts (Fig. 4). Although the development of novel and efficient molecular catalysts is full of challenges, readily available routes make the synthetic modification of molecular catalysts possible; various experimental techniques are easily available for investigating catalytic kinetics and mechanisms. Fruitful results have been obtained from these studies, including several super active catalysts and a deep understanding of the catalytic mechanisms.

Second stage, heterogenization of molecular catalysts. Although several efficient molecular catalysts are available from the first stage, these homogeneous highly active units cannot be directly used in an AP device, because the use of a molecular catalyst in electrolytic solution or on an electrode prepared by simple drop casting may not result in an effective and stable device. In the first case, one main limitation is that only a small fraction of the catalyst in the diffusion layer is active. Catalyst leaking and uncontrollable aggregation of catalyst molecules are the big problems of the drop-casting method.

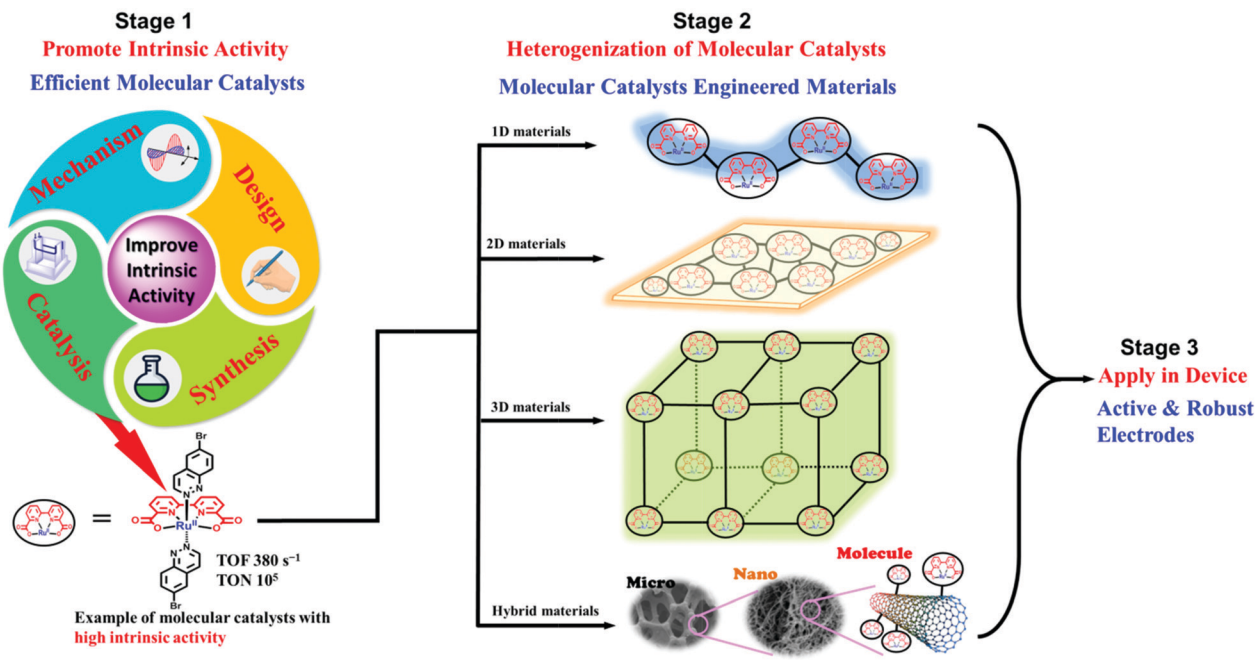

Fig. 4 Schematic representation of the stages involved in achieving applicable molecular AP devices. TOF: turnover frequency; TON: turnover number. The Ru complexes shown here are highly efficient molecular WOCs.

Therefore, investigations on how to heterogenize molecular catalysts are the second stage of the overall blueprint for molecular-catalyst-based AP.

Heterogenization of molecular catalysts, that is, from molecules to materials and from a homogeneous solution to a heterogeneous surface, is even more essential and challenging. However, there has been far from enough research on the heterogenization of molecular catalysts, in comparison with research on the first stage. Effective strategies for the heterogenization of molecular catalysts are needed to preserve the intrinsic high activity and selectivity of the homogeneous catalysts after heterogenization. In addition, the properties of the resultant heterogeneous surface or material, including the morphology (*e.g.*, particle size and surface area), density of active sites, hydrophobicity/hydrophilicity, and mass transfer limitations, require elaborate optimization. Without adequate methods, the molecular catalysts cannot be employed by the device effectively and stably. Indeed, this is the reason for the current poor situation of molecular catalyst based AP. Although several molecular catalysts with extremely efficient activities have been obtained, AP devices based on these molecular catalysts did not show any apparent superiority in performance; on the contrary, these devices were not comparable with material-based devices in terms of bulk current density and stability.

On the basis of success at the first stage, it is currently urgent and essential to explore applicable strategies for the heterogenization of molecular catalysts, as illustrated in the general representation in Fig. 4. In contrast to catalysts made of inorganic materials, the most prominent advantage of the materials obtained from the heterogenization of molecular catalysts is that each metal has the same coordination environment and is able to be the active site.

Third stage, engineering of an applicable AP device. Once a material generated from heterogenization of an efficient molecular catalyst is ready, there will be a chance to manufacture an applicable device. It should be noted that the laboratory test models made from simply dipping electrodes in beakers or electrolyte containers are unrelated to applicable AP devices, which are large scale devices with a two-electrode system, high current density and many other special factors. Engineering questions arise at this stage, such as how to integrate the device components (current collector, proton-transfer membrane, catalyst films, *etc.*), how to solve the problem of mass transfer and bubble removal, how to lower the contact resistance, and how to prevent electrode corrosion.

Obviously, the development of applicable AP devices based on molecular catalysts is now in the middle of the first stage, at the very beginning of the second stage, and far away from the third stage. Therefore, it is not reasonable to reject this promising pathway at such an early stage of the research and to miss the potential opportunities of AP devices with molecular catalysts.

4. Developing efficient molecular catalysts for AP

4.1 Overview of molecular water-oxidation catalysts (WOCs)

Water is the only ideal source of protons and electrons, which are necessary for the fuel-production reactions. No other alternative reducing substrate has the capacity to meet the heavy demands for fuel production on a global scale, while releasing no waste.[56] Therefore water oxidation is key for AP. However, it is also the bottleneck for the development of AP because it requires a high thermodynamic potential ($\Delta G \approx 237$ kJ mol^{-1} and $E_0 \approx 1.23$ V) and a high overpotential to overcome the kinetic barrier involved in the transfer of 4 H^+ and 4 e^-.[55] Efficient catalysts can reduce the kinetic barrier by forming low-activation-energy intermediates, and consequently, accelerate the rates of water oxidation. Due to the advantages of molecular catalysts mentioned above, development of molecular WOCs has attracted considerable attention in the field of AP, and major progress has been achieved.

4.1.1 Water-oxidation in PSII. In nature, water oxidation is catalyzed by the oxygen-evolving complex (OEC) in photosystem II (PSII), with a low overpotential of ~160 mV and a high reaction rate of 100–400 s^{-1}.[9,57–59] Thanks to the research effort of biophysicists, the structure of the OEC has been resolved at a resolution of 1.9 Å (Fig. 5a).[9,60] The core structure comprises a cubic Mn_3CaO_4 cluster linked to an additional dangling Mn *via* μ-O atoms. The Mn_4CaO_5 cluster is surrounded by ligands, including amino acid residues (Y_Z, D1-D61, D1-H190, *etc.*), two Cl^- ions, and several H_2O molecules.

Prior to the revelation of the OEC structure, it was only known that water oxidation at the OEC proceeds *via* the Kok cycle involving five intermediates, referred to as the S_i (i = 0–4) states, but the details of the catalytic mechanism were unknown (Fig. 5b).[61] Based on the clear crystal structure and the advanced physical techniques used in recent years, PSII scientists are in general agreement on the oxidation states[62] and structures of the metastable S_0, S_1, and S_2 intermediates (Fig. 5b).[9,63–65] Nevertheless, the mechanistic details of O–O bond formation remain unclear.[66–68] Currently, two main O–O bond formation mechanisms are widely considered for PSII: the oxo–oxyl radical coupling mechanism[69] and the nucleophilic attack mechanism,[68,70] involving a Mn^{IV}–oxyl radical and a Mn^{V}–oxo electrophile, respectively, as active S_4 intermediates. However, the existence of a Mn^{IV}–oxyl radical or a Mn^{V}–oxo electrophile has not been experimentally confirmed; the actual mechanism of water oxidation by the Mn_4CaO_5 cluster in PSII remains to be determined. Very recently, we proposed a new water oxidation mechanism involving a charge-rearrangement-induced Mn^{VII}–dioxo intermediate state.[71–73] Elucidating the catalytic mechanism in PSII will not only uncover the secret of water oxidation in nature, but also provide a blueprint for developing more efficient water-oxidation catalysts for AP.

4.1.2 Mechanisms of catalytic water oxidation by molecular WOCs. In general, molecular WOCs are redox-active transition-metal-based complexes with unsaturated first coordination spheres, which function as active sites for the substrate water molecule (Fig. 6).[74,75] To catalyze water oxidation, a catalyst must allow the accumulation of multiple charges to form a high-valent metal–oxo intermediate.

Fig. 6 shows that after binding with a substrate H_2O molecule and several steps of proton-coupled electron transfer (PCET), the WOC generates a high-valent M=O intermediate, which is essential for the next crucial O–O bond formation step.

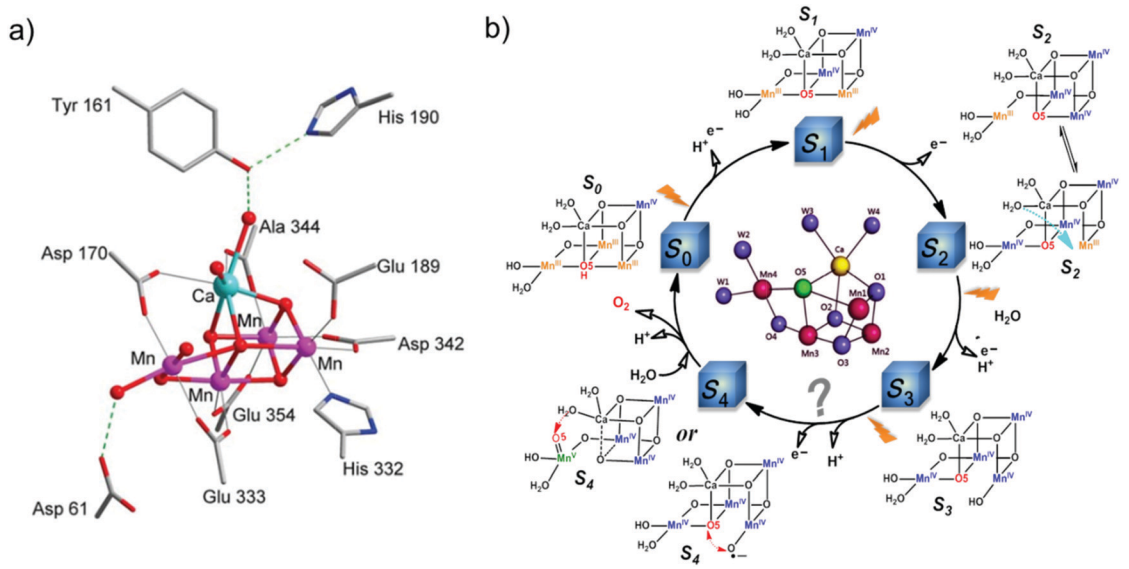

Fig. 5 (a) Structure of the Mn_4CaO_5 cluster of the OEC in PSII.[9] (b) Classic Kok cycle for water oxidation in PSII, with widely-proposed structures of the intermediate "S" states, electron transfer, and proton release.

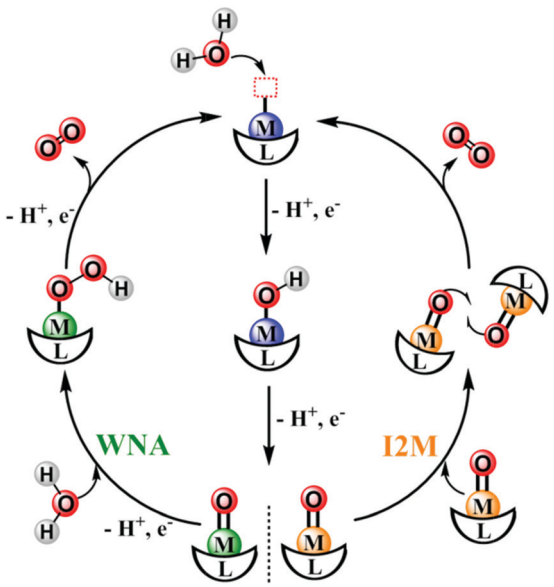

Fig. 6 Schematic representation of the water nucleophilic attack (WNA) and the interaction between two M–O intermediate (I2M) pathways to form O–O bonds catalyzed by molecular catalysts.

Depending on the nature of this M=O intermediate, there are two classic pathways for O–O bond formation: (i) water nucleophilic attack (WNA) and (ii) interaction of two M–O units (I2M).[76–79] In the WNA pathway, a second H_2O molecule, which acts as the nucleophile, attacks the electrophilic O on the M=O intermediate, resulting in a two-electron reduction of the metal center and O–O bond formation on a metal hydroperoxide intermediate (M–OOH). Next, O_2 evolution occurs after further oxidation of the M–OOH. In the I2M pathway, the O on the M=O intermediate may have higher electron spin and have more radical character. In this context, the O–O bond forms *via* coupling of two radical-like species, leading to an M–O–O–M species, which can release O_2 upon further oxidization.

Currently, the WNA mechanism is the most widely proposed mechanism for molecular catalysis and metal-oxide-based material catalysis, but the state-of-the-art catalyst Ru-bda (bda = 2,2′-bipyridine-6,6′-dicarboxylate) catalyzes water oxidation *via* the I2M mechanism.[80–83] Moreover, both these mechanisms have been considered as the possible water oxidation mechanism in PSII. We cannot conclude which mechanism is superior; however, there is no doubt that: (i) the catalytic mechanism of a WOC is dominated by its configuration and electronic structure, which are closely controlled by its coordination environment, for example, the ligands, and (ii) a better understanding of the catalytic mechanism of a WOC catalyst will significantly enhance catalytic activity.

4.1.3 Ru-Based molecular WOCs. Ru-Based molecular catalysts are the earliest and most studied molecular WOCs since 1982, when Meyer and co-workers reported the first molecular WOC, the so called "blue dimer" (BD) *cis,cis*-$[Ru^{II}(bpy)_2(H_2O)]_2(\mu\text{-}O)$ (**4**),[84] with a catalytic turnover number (TON) of 13 and turnover frequency (TOF) of 0.0042 s^{-1} by using Ce^{4+} as the oxidant.[85,86] Based on 27 years of research by the molecular WOC community, in 2009, the Sun group made a breakthrough regarding the catalytic efficiency of molecular WOCs by the successful development of the $Ru(bda)(pic)_2$ (**5**, pic = 4-picoline) catalyst with a TON of 2000 and a TOF of 41 s^{-1} by using Ce^{4+} as the oxidant.[80,83,87] This dramatic improvement is attributed to the introduction of carboxylate groups into the ligands and the special steric configuration of **5**, which provides an open site for the substrate water molecule and allows 7-coordination at this catalytic site. Here, we divide the history of development of Ru-based molecular WOCs into two periods to make the story of molecular WOC development clearer: the first period is from the invention of the BD to the Ru-bda catalysts, and the second

period is from after the development of the Ru-bda catalysts to the present (Fig. 7).

The blue dimer (BD). Although the BD showed modest catalytic activity for water oxidation, studies on the BD led to the development of various theories for the evolution of molecular WOCs. First, the mechanistic details of water oxidation catalyzed by transition metal complexes were established. The $O{=}Ru^{V}{-}Ru^{V}{=}O$ state is proved to be the final necessary state prior to oxygen evolution.[88–93] Three different mechanisms have been proposed for O–O bond formation by the BD: the intramolecular/intermolecular oxo–oxo coupling, the WNA pathway and a pathway involving the oxidation of the bpy-ligand.[93,94] Although several critical reaction steps remain open to interpretation, the WNA mechanism is preferred for the BD, and has been extensively studied by using various experimental techniques[92,95–97] and theoretical calculations.[98] It was subsequently proved that this general O–O bond formation mechanism is involved in the water oxidation catalysis by many different kinds of catalysts, including molecular catalysts[4,55,78] and metal-oxide-based material catalysts.[99,100] Second, these early studies emphasized the essential role of proton-coupling electron-transfer (PCET) processes for water oxidation catalysis.[84,101–104] In the PCET processes, oxidation of the metal center in a catalyst leads to a

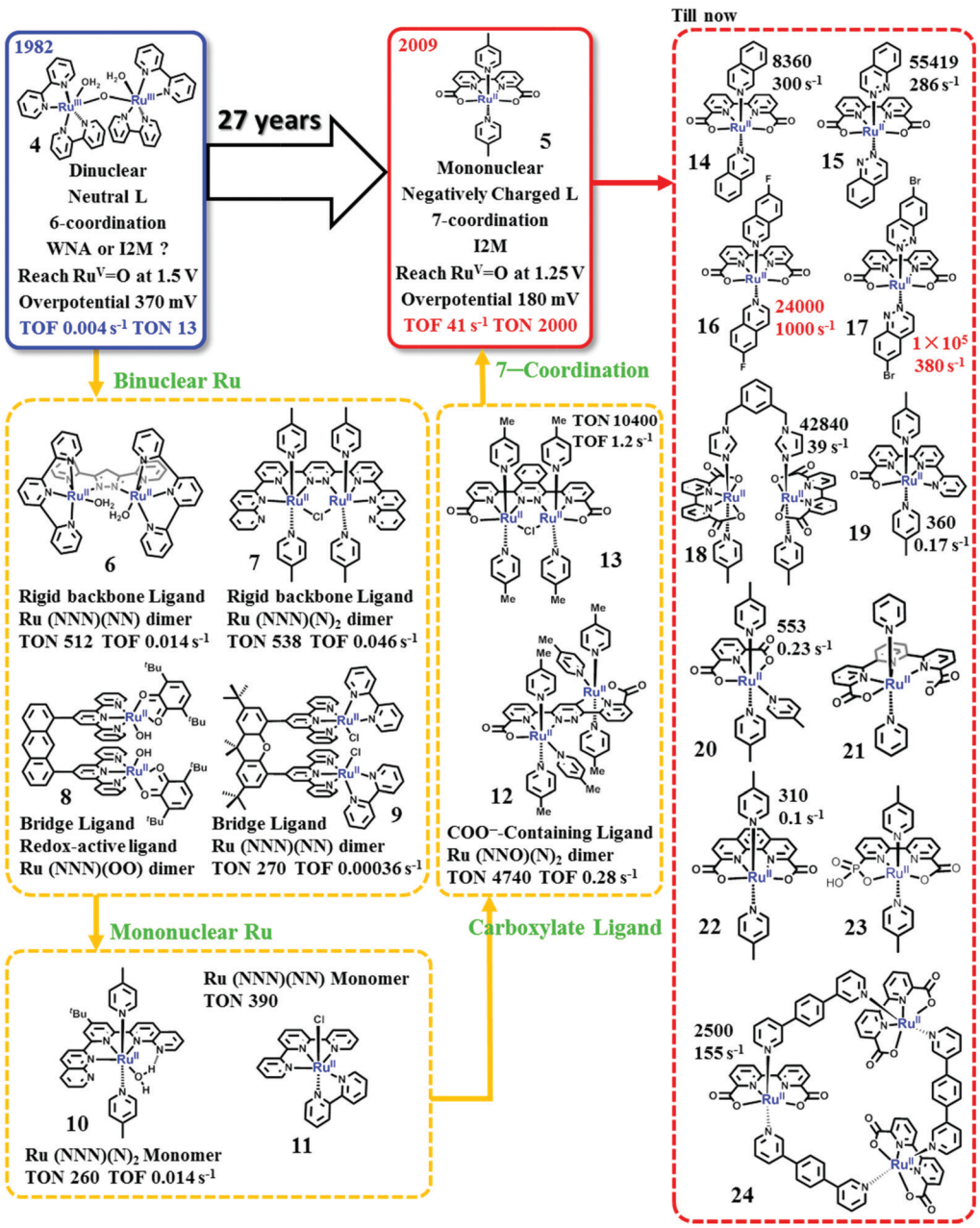

Fig. 7 Development history and recent status of Ru-based WOCs. Labelled TONs and TOFs are obtained from experiments using Ce^{4+} as the chemical oxidant.

reduction in the pK_a of the H_2O binding at the active site; this leads to the release of one proton, resulting in stronger donor ligands like hydroxo and oxo. This in turn stabilizes the high valent metal state and facilitates further oxidation of the metal center, thus advancing the multi-electron oxidation, which is necessary for water oxidation catalysis. Third, the success of the BD as a water oxidation catalyst also confirmed the suitability of polypyridine ligands, which are capable of tolerating harsh oxidation conditions and are stable towards hydrolysis, as a scaffold to build molecular WOCs.[103] Research studies on the BD have inspired the development of both binuclear and mononuclear Ru-based WOCs and molecular catalysts based on other transition metal complexes.[4,55]

Ru(NNN)(NN) dimers with rigid polypyridyl-based backbone ligands. Following the studies on the BD, an obvious step forward is the development of Ru dimer catalysts with a rigid polypyridyl-based backbone ligand. To prevent the deactivation of μ-O-linked Ru dimer catalysts, in 2004, Llobet and coworkers reported the first ruthenium dimer WOC (complex **6**) without a μ-O bridge ligand by using a rigid backbone ligand, 2,6-bis(pyridyl)pyrazole (Hbpp).[105] Under similar experimental conditions, the oxygen evolution catalyzed by **6** is more than three times faster than that by the BD. Moreover, since the turnover and the variation of the intermediates are slow, the mechanistic studies of this catalyst have been validated with details.[106] The O–O bond formation catalyzed by **6** occurs *via* the I2M pathway. The Llobet group further investigated the performances of Ru-bpp analogues[107–111] and the Ru-bpp catalysts anchored onto solid supports.[112,113]

Ru(NNN)(N)$_2$ dimers with rigid polypyridyl-based backbone ligands. Later, the Thummel group designed and synthesized a series of Ru dimer catalysts, containing a rigid polypyridyl-based backbone ligand and two pyridine axial ligands, *e.g.* complex **7**.[114,115] One advance made by the Thummel group is the introduction of monodentate axial ligands, instead of another polypyridyl ligand, into the catalyst structure. It produced a new family of Ru WOCs, the backbone-ligand-linked Ru(NNN)(N)$_2$ type. Thanks to the steric structure of the Ru(NNN)(N)$_2$-type catalysts, the open sites of catalysts became larger, facilitating the binding of the substrate H_2O molecule as an equatorial ligand and optimization of the catalysts. The Ru(NNN)(N)$_2$-type catalysts developed by Thummel showed significantly higher TONs (up to 600) than the BD catalysts and Ru-bpp catalysts.

Ru-Dimers with rigid bridge ligands. Another strategy to obtain a dimer catalyst with *cis* geometry between the two Ru centers is to use a rigid bridge to link two Ru monomers.[116,117] One typical example is the Ru dimer $[Ru_2(OH)_2(3,6\text{-}tBu_2qui)_2(btpyan)]^{2+}$ (**8**, 3,6-*t*Bu$_2$qui = 3,6-di-*t*-butyl-1,2-benzoquinone; btpyan = 1,8-bis(2,2′:6′,2′-terpyridyl)anthracene) reported by the Tanaka group.[116] Interestingly, complex **8** is a unique water oxidation catalyst because it contains a redox-active ligand, which plays a fundamental role in the catalytic activity of **8**.[118–120] Molecular WOCs involving redox-active ligands have recently attracted increasing attention.[121,122] The Berlinguette group has developed three Ru dimer catalysts with various distances between the Ru centers by linking two Ru(tpy)(bpy) units using different rigid bridge ligands (**9**).[123] However, no remarkable improvement in activity was obtained for the rigid-bridge-ligand-linked dimer catalysts.

From binuclear to mononuclear. Considering the multi-metallic Mn_4CaO_5 core of the OEC, it was long believed that synthetic molecular WOCs must also have multiple metal centers (at least two) to allow the accumulation of four oxidizing equivalents needed for catalytic water oxidation. In 2005, the Thummel group reported the first series of mononuclear Ru WOCs, *e.g.*, complex **10**, suggesting that the single metal center is active enough for catalyzing water oxidation.[115] Later, Meyer and co-workers emphasized that one site is enough for water oxidation by revealing a well-defined mechanism involving the Ru(v) centers of two monomeric Ru-based WOCs, $[Ru(tpy)(bpm)(OH_2)]^{2+}$ (bpm = 2,2′-bipyrimidine) and $[Ru(tpy)(bpz)(OH_2)]^{2+}$ (bpz = 2,2′-bipyrazine).[124,125] The concept of a single metal site catalyzing water oxidation represented a paradigm shift for the field and opened the door for developing a new series of catalyst systems with synthetic flexibility. With only one metal site, reaction mechanisms could also be deeply studied using much simpler platforms. Thus, the catalog of WOCs based on transition metal complexes has been significantly expanded. The paradigm shift from binuclear molecular WOCs to mononuclear ones is an essential step forward for developing efficient molecular WOCs.

The Ru(NNN)(N)$_2$ and Ru(NNN)(NN) type mononuclear catalysts. Mononuclear catalysts like complexes **10** and **11** can be classified as the Ru(NNN)(N)$_2$- and Ru(NNN)(NN)-type mononuclear catalysts.[115,126] One of the important differences between these two different types of catalysts is the binding of the substrate H_2O. The substrate H_2O molecule binds on the Ru site as an equatorial ligand and as an axial ligand in the Ru(NNN)(N)$_2$-type and the Ru(NNN)(NN)-type catalysts, respectively. The Ru(NNN)(N)$_2$-type catalysts were extensively investigated by the Thummel group.[115,127–129] They studied the effect of the axial ligands on the properties and catalytic performances of these catalysts.[127] Moreover, a great variety of equatorial ligands were designed and synthesized for these Ru catalysts. These studies inspired the design of ligands for Ru-based WOCs.

Ru(NNN)(NN)-type complexes constitute a major family of promising mononuclear WOCs. A typical representative of Ru(NNN)(NN)-type WOCs is the $[Ru(tpy)(bpy)(X)]^{n+}$ (X = H_2O or halogen atom), which, together with various derivatives, has been extensively researched.[126,130–134] The effect of the electronic properties on the activity of the $[Ru(tpy)(bpy)(X)]^{n+}$ catalysts was carefully studied by the groups of Berlinguette,[133–135] Thummel,[126,127] Sakai[130,131] and Yagi[136] by introducing a range of substituents to the periphery of both the tpy and bpy ligand frameworks. Instead of bpy or tpy, Meyer and co-workers have incorporated several strong σ-donating bidentate or tridentate

ligands into complexes of the $[Ru(tpy)(bpy)(X)]^{n+}$ motif.[132] The electrochemistry and spectroelectrochemistry of these catalysts have been studied extensively to elucidate the reaction kinetics and mechanism.[124,125,137,138] Based on these studies, Meyer and co-workers proposed an important strategy to accelerate the O–O bond formation, *i.e.*, the concerted atom-proton transfer (APT).[137,138]

Introduction of carboxylate-containing ligands. The Ru catalysts developed before 2009 are mainly based on neutral polypyridyl ligands. The studies on these complexes as WOCs have provided us considerable knowledge about how to design a WOC and how to evaluate the catalytic performance and catalytic mechanism. However, significant improvement in the catalytic activity for water oxidation was not achieved until the introduction of carboxylate-containing ligands into the catalyst structure.[87]

Inspired by the OEC in PSII containing several carboxylate ligands, the Sun group employed carboxylate ligands to synthesize Ru-based complexes that can efficiently catalyze water oxidation. The first carboxylate-containing Ru WOC reported by the Sun group was an unexpected *trans*-dimeric complex **12** with TON 4700 and TOF 0.28 s^{-1} (Ce^{4+} was used as the oxidant).[139,140] Later, a modified ligand 1,4-bis(6′-COOH-pyrid-2′-yl)phthalazine was synthesized to obtain a *cis* dimeric Ru complex **13**. By using Ce^{4+} as the oxidant, the *cis* complex **13** showed a catalytic TON of 10 400 and a TOF of 1.2 s^{-1}, far superior to those of the *trans* complex **12** and other reported catalysts at the time.[141] Moreover, the *cis* complex **13** showed a low onset potential of 1.15 V *vs.* NHE for water oxidation; therefore, light-driven water oxidation was also successfully achieved in the presence of $[Ru(bpy)_3]^{2+}$ as the photosensitizer. The outstanding activities of complexes **12** and **13** obviously indicate that introduction of carboxylate groups is an effective and essential strategy to obtain promising WOCs with low overpotentials, because the carboxylate groups could make the higher oxidation states more accessible and more stable.

Ru(bda)(pic)$_2$, founder of a new era for efficient molecular WOCs. Based on the concept of introducing carboxylate groups into the catalyst structure, the Sun group also designed a dianionic ligand, the 2,2′-bipyridine-6,6′-dicarboxylate (bda), to coordinate with Ru, producing a mononuclear Ru-bda complex, which is one of the most efficient catalytic center units known thus far.[80,83,87,142,143] Using Ce^{4+} as the driving force at pH 1, the parent $[Ru(bda)(pic)_2]$ complex (complex **5**) catalyzes water oxidation *via* a bimolecular I2M pathway with a TON of 2000 and a TOF of 41 s^{-1}.[144] An electrochemical study of **5** indicates that it needs an overpotential of only 180 mV to initiate water oxidation.[145]

Because of the outstanding activity, Ru-bda-type WOCs have received extensive research attention worldwide and have been widely investigated by the Sun group among many other groups; researchers have studied the effect of axial ligands,[146–149] catalytic mechanisms,[80,81,150–156] development of Ru-bda analogues[157–160] and applications of Ru-bda in AP devices.[161–166] The studies on the effect of axial ligands of Ru-bda-type WOCs were very fruitful. Electron-withdrawing and hydrophobic substituents on the axial ligands had positive influence on the water oxidation activity, *e.g.* Ru-bda catalysts with both 4-(EtOOC)-pyridine (TON = 4800 and TOF = 120 s^{-1}) and 4-bromopyridine (TON = 4500 and TOF = 115 s^{-1}) showed excellent water oxidation activities.[148] Ru-bda catalysts (*e.g.* complexes **14** and **15**) with π-extended axial ligands, such as isoquinoline and phthalazine, showed dramatically enhanced activities because the π–π stacking and hydrophobic effects between the axial ligands reduce the energy barrier for O–O bond formation *via* radical coupling.[143] Introduction of halogen substituents into the π-extended axial ligand further improved the catalytic activity of the Ru-bda catalysts, complex **16** with record TOF > 1000 s^{-1} and complex **17** with record TON > 100 000. To obtain higher catalytic activity, based on the bimolecular I2M mechanism of Ru-bda catalysts, various strategies have been tested to enhance the intermolecular interaction[167–170] or to create facile intramolecular reactions by linking two or more Ru-bda units,[171,172] *e.g.*, complex **18**.

Revealing the reason behind the outstanding catalytic performance of Ru-bda catalysts is essential to inspire further design of more efficient WOCs. The question has not been satisfactorily answered thus far; however, at least two dominant factors have been proved essential to the breakthrough activity of these catalysts. First, the carboxylate groups in the structure lower the potential needed to generate active Ru-oxo species for O–O bond formation. Second, the equatorial bda ligand accesses a strongly distorted octahedral geometry of $[Ru(bda)(L)_2]$ with a unique O–Ru–O angle of ∼124° for $Ru(bda)(pic)_2$, which is 34° larger than an ideal rectangular arrangement; consequently, it opens up a crucial seventh coordination site for the substrate water molecule to bind.[80,83,143] Further theoretical investigations concluded that the $Ru^{V}{=}O$ intermediate is hydrophobic and shows a distinct oxyl radical character, *e.g.* $Ru^{IV}–O^{\bullet}$, facilitating the bimolecular I2M pathway.[153,173] In complex **19**, one of the carboxylate groups was replaced by pyridine. Although the distorted octahedral geometry of the complexes was retained, the catalytic performance became several orders of magnitude lower and O–O bond formation proceeded *via* the WNA pathway.[174] The Ru complexes **20** and **21**, with a tridentate dianionic ligand 2,6-pyridine dicarboxylate (pdc)[175,176] and a pentadentate dianionic ligand [2,2′:6′,2′-terpyridine]-6,6″-dicarboxylate (tda),[159,177,178] respectively, also showed greater catalytic activities than the relatively neutral complex. Without the open site for hepta-coordination, these catalysts adopt the WNA pathway and the overpotentials are much higher than those of the Ru-bda catalysts, indicating that hepta-coordination is crucial for the I2M mechanism.

In addition to the above-mentioned ones, there must be other factors governing the special catalytic performance of Ru-bda catalysts. For instance, the $[Ru(pda)(pic)_2]$ (complex **22**, pda = phenanthroline dicarboxylate) complex possesses a coordination environment highly similar to that of $[Ru(pda)(pic)_2]$, including both dianionic groups and the large open site for hepta-coordination. However, the activity of **22** is much lower

than that of **5** (TON = 310; TOF = 0.1 s^{-1}), and the kinetics of catalytic water oxidation switches to first order.[179] DFT calculations suggest that the WNA pathway is more favored over the I2M pathway for **22**. The flexibility of the bda ligand may be one reason for this change. Further investigations are necessary to obtain a better understanding as to why Ru-bda WOCs are highly active and why they go through the uniquely effective I2M pathway; consequently, it will guide the design of more efficient WOCs.

Fast water oxidation has also been achieved by Ru WOCs bearing dianionic ligands *via* the WNA pathway. Electrochemical assessment by Llobet and co-workers yielded a TOF as high as 8000 s^{-1} at pH 7.0 for the $[Ru(tda)(pic)_2]$ (complex **21**).[159] Concepcion and co-workers investigated water oxidation catalyzed by Ru WOCs obtained by replacing one or two carboxylate groups of the Ru-bda catalysts with phosphate groups.[158,160] Both catalysts adopt the WNA pathway. The diphosphate catalyst showed very low activity (TOF = 0.3 s^{-1}).[158] Due to the lability and basicity of the bipyridine-carboxylate-phosphonate ligands, complex **23** exhibited remarkable catalytic activity *via* the WNA pathway (TOF = 100 s^{-1}).[160] Kunz *et al.* prepared the trinuclear macrocycle complex **24** by linking three Ru-bda units with ditopic axial bridging ligands.[157,180–182] The rigid cyclic structure prevents the coupling of the two Ru-bda units. Thus complex **24** efficiently catalyzes water oxidation (TON = 7400 and TOF = 150 s^{-1}) *via* the WNA mechanism, having benefited from an ordered hydrogen bonding network inside the macrocyclic cavity, demonstrating that the negatively charged ligand and the open coordination site can also enhance the oxygen evolution rate *via* the WNA pathway.[157]

After over 35 years of research, scientists nowadays have very detailed understanding of Ru-based molecular WOCs. Moreover, the catalytic activities have been dramatically improved with a low overpotential of 200 mV and TOF over 1000 s^{-1}, which is highly promising for fabricating efficient AP devices.

4.1.4 Ir-Based molecular WOCs. In the development of molecular WOCs, Ir-based complexes constitute another type of classic WOCs (Fig. 8).[183] In 2008, the Bernhard group for the first time reported a series of cyclometalated iridium complexes (complex **25**) with two substituted 2-phenylpyridine ligands and two water ligands that could catalyze water oxidation with the highest TON of 2760 by using Ce^{4+} as the oxidant.[184] These results facilitated the development of numerous Ir-based molecular WOCs. The second family of Ir-based WOCs, which has been widely studied, is composed of Ir complexes (complexes **26**, **27**, and **28**) bearing cyclopentadiene (Cp) or pentamethylcyclopentadiene (Cp*) ligands, as reported by Crabtree, Brudvig, and co-workers.[185,186] This type of Ir WOC affords faster catalysis than the catalysts reported by Bernhard and colleagues; however, these half-sandwich catalysts are less stable.

To improve their stability, a Cp*Ir complex bearing a strongly σ-donating N-heterocyclic carbine (NHC) ligand was developed, which effectively stabilizes the Ir^{IV} intermediates.[187] By the same strategy, Bernhard and Albrecht employed an abnormal pyridinium-carbene ligand to coordinate with the half-sandwich Cp*Ir (complex **29**), achieving a new benchmark for TON: 10 000 after 5 days. Very recently, they investigated

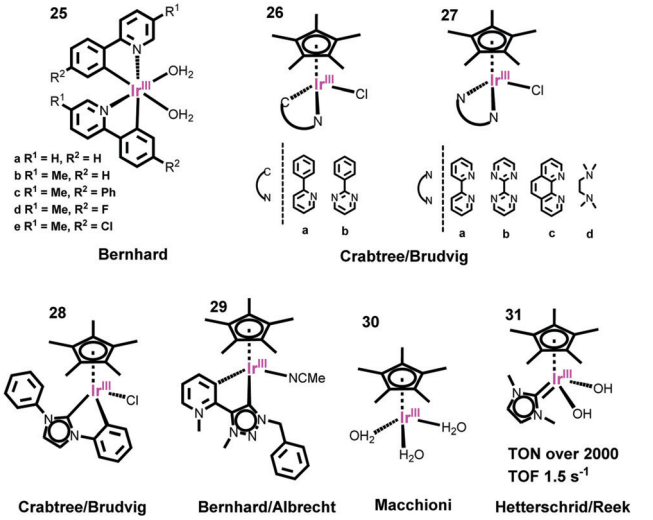

Fig. 8 Representative structures of Ir-based WOCs.

the promoting effect of incorporating MeO– groups.[188,189] Macchioni and co-workers found that the simple Cp*Ir complex $[Ir(Cp^*)(H_2O)_3]^{2+}$ (**30**) showed faster catalysis than those bearing auxiliary chelating ligands.[190] Hetterscheid and Reek reported a series of NHC-ligand-coordinated half-sandwich Cp*Ir complexes (**31**) with both high TOF (1.5 s^{-1}) and high TON (>2000) by using Ce^{4+} as the oxidant.[191] For the half-sandwich Cp*Ir WOCs, it should be noted that many initially obtained structures are precatalysts, with the actual catalyst losing the Cp* ligand to form a mono-μ-oxo dimer that is quite robust and active.[183,192,193]

4.1.5 Earth-abundant transition-metal-based molecular WOCs. Manganese-based complexes have been considered promising candidates for WOCs because manganese is the third-most-abundant transition metal on earth,[194] is a low-cost material, and has been used in nature in the form of a Mn_4CaO_5 cluster in the OEC of PSII. Moreover, manganese has a rich redox chemistry, and can bear multiple charges to generate reactive high-valent intermediates for water oxidation.

Naruta and co-workers repoted the first family of Mn-based molecular WOCs: three analogous dimeric manganese triphenylporphyrin complexes linked by an *o*-phenylene bridge (Fig. 9, complex **32**).[195] They found that these catalysts catalyze water oxidation with a TON of 9.2 and a TOF of 0.0018 s^{-1} under electrochemical conditions. In a further mechanistic study, the dimeric $Mn^{V}{=}O$ species was identified as a key intermediate by using *meta*-chloroperoxybenzoic acid (*m*CPBA) as an oxidant.[196] In 1999, Crabtree and Brudvig reported another important Mn-based molecular WOC, $[(H_2O)(tpy)Mn^{III}(\mu\text{-}O)_2Mn^{IV}(tpy)(OH_2)]^{3+}$ (complex **33**). When the catalytic performance of **33** was researched by using NaClO (0.07 M) as an oxidant, it gave a TON of 4 and an initial TOF of 0.0038 s^{-1}.[57] By using another chemical oxidant oxone ($KHSO_5$), the catalytic performance was further promoted to TON > 50 and TOF of 0.034 s^{-1}.[197,198] A $Mn^{V}{-}Mn^{V}{=}O$ species was proposed as a key intermediate for O–O bond formation by **33**, and the formation of MnO_4^- *via* oxidation of **33** was suggested as the deactivation pathway.[57]

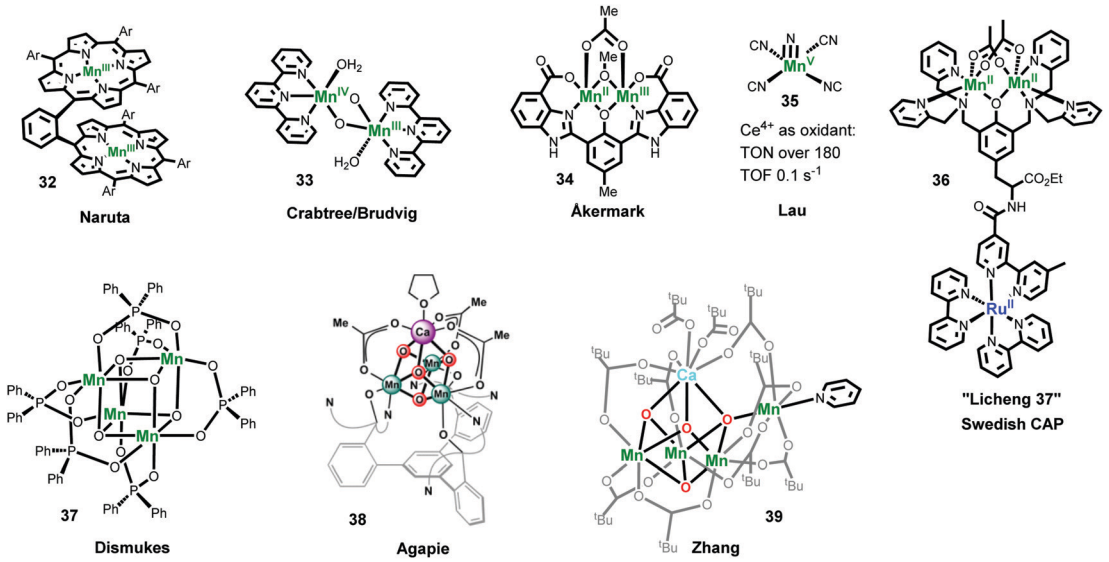

Fig. 9 Representative structures of Mn-based WOCs.

Complex **33** showed no catalytic oxygen evolution with the classical oxidant Ce^{4+} or with electrochemical oxidation.[199] However, complex **33** adsorbed on heterogeneous materials, such as clay compounds,[200–202] TiO_2,[203,204] or even metal–organic frameworks (MOFs) showed obvious water oxidation activity using Ce^{4+} as the oxidant.[205] Since the reports of the two above examples, many Mn-based catalysts have been explored for oxygen evolution.[4,58,206,207] However, a Mn-based molecular WOC, which can catalyze water oxidation without involving oxygen transfer reagents, was first reported by Åkermark and co-workers in 2011.[208] Complex **34** showed acceptable catalytic water oxidation activity by using $[Ru(bpy)_3](PF_6)_3$ oxidant, with a TON of 25 and an initial TOF of 0.027 s^{-1}. In 2015, a different class of Mn-based catalysts, *viz.* manganese(v)–nitrido complexes, were explored by Lau and co-workers. Complex **35**, $[Mn^{V}(N)(CN)_4]^{2-}$, turned out to be an active molecular WOC using Ce^{4+} as the oxidant, with a TON exceeding 180 and a maximum TOF of 0.1 s^{-1}, suggesting that active Mn-based WOCs may be constructed based on the $Mn^{V}(N)$ platform.[209]

Mn complexes have also been designed and synthesized to mimic the electron transfer reactions in PSII and the structures of the OEC.[210,211] Groups of the Swedish Consortium for Artificial Photosynthesis (CAP) did some pioneering research and have prepared several Mn complexes covalently coupled to $[Ru(bpy)_3]^{2+}$-type chromophores as functional models of PSII to investigate photoinduced electron transfer of binuclear Ru–Mn assemblies.[212–215] For example, complex **36** (also named as Licheng-37 synthesized by professor Sun in CAP) showed excellent photoinduced redox properties because it could transfer three electrons from the Mn centers *via* the Ru photosensitizer to the acceptor, resulting in a $Mn^{III}Mn^{IV}$ state with accumulation of three charges.[214] The studies on mimicking the key structural motif of the Mn_4CaO_5 cluster have yielded fruitful results in recent years.[211] The Dismukes group synthesized the first example the Mn_4O_4 cubane core (complex **37**). They found that under UV light irradiation, complex **37** efficiently released an O_2 molecule by coupling two of the corner oxos in the Mn_4O_4 cubane. An artificial Mn_3CaO_4 cluster coordinated by a multi-pyridylalkoxide ligand (complex **38**) was reported by Agapie and co-workers as the first representative model of the Mn_4CaO_5 cluster in PSII.[216,217] Although this cluster closely mimicked most of the key structural features of the Mn_4CaO_5 cluster of the OEC, the unique dangling Mn4 in the Mn_4CaO_5 cluster was missed. A breakthrough to overcoming this challenge was made by the Zhang group.[218] They reported the first artificial Mn_4Ca cluster (complex **39**) that entirely mimicked the structural features of the OEC. Although complex **39** is similar in many ways to native OEC, it did not display efficient water oxidation catalytic activity, indicating that the secondary coordination environment surrounding the Mn_4CaO_5 cluster in the OEC is also significant. These mimicking studies can enhance our understanding of the OEC, thereby facilitating the development of artificial systems. For instance, Maayan and co-workers recently reported a soluble manganese-oxo cluster with an exceptionally low overpotential of only 334 mV for electrochemical water oxidation operating at pH 6.[219]

Cobalt ions have been known to catalyze water oxidation since the 1960s;[220] however, cobalt complexes were not developed as molecular WOCs, until the Berlinguette group reported the first Co-based WOC (Fig. 10, complex **40**) in 2011, using the well-known oxidatively stable pentadentate ligand 2,6-(bis(bis-2-pyridyl)-methoxymethane)-pyridine (PY5).[221] Complex **40** showed remarkable activity for electrochemical water oxidation and was also a pioneer example of well-defined PCET at a first-row transition metal aqua site, *i.e.* $M–OH_2$. Subsequently, Nocera and co-workers reported that a perflurorinated "hangman" porphyrin complex (complex **41**) could electrochemically catalyze water oxidation and the hangman carboxylic group was essential in that it functioned as a secondary coordination site.[222] Since these two studies, developing Co-based molecular catalysts has

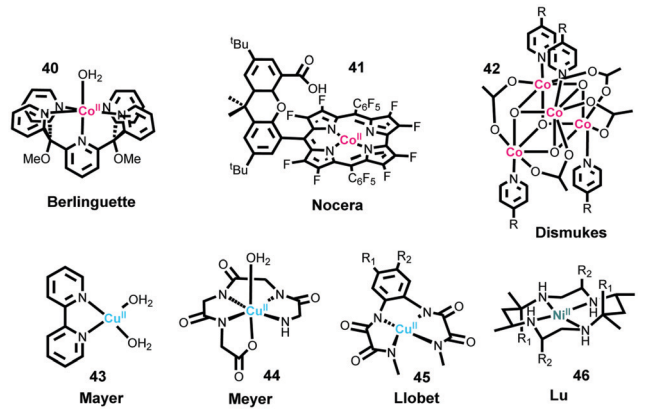

Fig. 10 Representative structures of Co-based, Cu-based and Ni-based WOCs.

attracted great research interest. Many different Co complexes, *e.g.*, Co porphyrins and Co salophens, have been studied as catalysts or precatalysts for water oxidation.[121,223–229]

One extensively studied family of noble-metal-free molecular catalysts comprises tetranuclear Co_4O_4 cubane compounds, such as complex **42**. Dismukes and co-workers were the first to report photocatalytic water oxidation by these Co_4O_4 cubane catalysts.[230] Later Bonchio and co-workers investigated the photocatalytic activities of a series of isostructural analogs of Co_4O_4 cubane complexes.[231,232] They revealed that the primary step of photoinduced electron transfer obeys the Hammett linear free energy relationship. To improve photocatalytic performance, several supramolecular assemblies were produced by coupling Co_4O_4 cubane cores with transition metal photosensitizers.[233,234] The Sun group studied the electrocatalytic properties of Co_4O_4 cubane catalysts by immobilizing them on ITO electrodes, and for the first time proved that Co_4O_4 cubane catalysts coupled well with visible-light-absorbing semiconductor α-Fe_2O_3 to form molecule–semiconductor hybrid photoanodes.[235] Based on this work, Co_4O_4 cubane catalysts have been widely employed as cocatalysts for semiconductor photoanodes, *e.g.*, $BiVO_4$.[236–238] Since the Co_4O_4 cubane complexes are coordinatively saturated, identifying the catalytic site and elucidating the mechanism of O–O bond formation are interesting. Dismukes and co-workers reported that water oxidation by the Co_4O_4 cubane complex is initiated by OH^- addition.[239] Mechanistic investigations by the Tilley group indicated the formation of highly oxidized intermediate Co^{IV}–oxo or Co^{V}–oxo complexes and the exclusive terminal oxo participation.[240] Although the Nocera group proposed that the activity of Co_4O_4 cubane catalysts may be derived from the Co^{II} impurities in the synthesized Co_4O_4 cubane samples, they revealed in their further studies the involvement of the high-valent intermediate Co^{IV}–oxo species in the catalytic mechanism.[241,242] In addition to the above fruitful results on the Co_4O_4 cubane catalysts, several other types of cobalt cubanes have also been investigated as WOCs.[243]

It is well known that copper-based metalloenzymes, where copper is the essential metal core, can activate oxygen by forming various Cu–oxo intermediate species, which can function as intermediates for O–O bond formation, indicating that Cu-based complexes can be used as WOCs.[244] The first molecular Cu-based WOC [Cu(bpy)$(OH)_2$] (complex **43**) was reported by the Mayer group in 2012.[245] Complex **43** displayed remarkable TOF ($\sim$100 s^{-1}, value calculated from electrocatalytic plot) for electrocatalytic water oxidation; however, this catalyst requires strong basic conditions and high overpotentials ($\sim$750 mV). To overcome these drawbacks, Lin *et al.* and Papish *et al.* designed and prepared several analogs of [Cu(bpy)$(OH)_2$] using a 6,6′-dihydroxy-2,2′-bipyridine (6,6′-dhbpy) ligand to assist proton transfer by the intramolecular base group.[246,247] Meyer and co-workers reported a Cu-based WOC bearing a polypeptide-type ligand (complex **44**).[82] The onset potential of complex **44** for water oxidation was 1.10 V at pH 11, corresponding to an overpotential of 520 mV. Cu-Based WOCs similar to complex **44**, bearing a polypeptide-type ligand, were also reported by Pap and Szyrwiel *et al.*[248] Recently, the Llobet group synthesized a series of copper complexes (complex **45**) containing redox-active tetradentate amidate acyclic ligands with various electron-donating substituents.[122] They found that the overpotentials of these catalysts for water oxidation dramatically decreased with increasing electron-donating ability of the substituent on the backbone ligand. An extremely low overpotential of 170 mV was achieved for the complex with two methoxy groups. They also proposed a catalytic mechanism involving oxidation of the ligand. Brudvig and co-workers investigated the water oxidation property and mechanism of a robust copper complex $Cu^{II}(pyalk)_2$ (pyalk = 2-pyridyl-2-propanoate).[249,250] In addition to the above-mentioned Cu-based catalysts, all of which required strong basic conditions, Zhang and co-workers reported the first Cu-based WOC that can operate under neutral pH conditions.[251] These previous results demonstrate that efficient and stable electrochemical Cu-based WOCs can be developed.

Developing Ni-based molecular WOC was initiated by the Lu group with a Ni macrocyclic catalyst (complex **46**) in 2014.[252,253] Complex **46** showed an electrocatalytic current of 0.9 mA cm^{-2} at an overpotential of 750 mV in a neutral sodium phosphate buffer (NaPi). They further investigated the catalytic mechanism of this catalyst.[253,254] Cao and co-workers reported the use of a water-soluble nickel porphyrin complex as a molecular electrocatalyst for water oxidation under neutral conditions.[255] The Sun group studied the water oxidation property of the well-known Ni–PY5 complex, and molecular catalysis was well proved.[256] Several Ni complexes based on well-known non-heme-iron ligands, such as *N*,*N*′-dimethyl-*N*,*N*′-bis(pyridin-2-ylmethyl)-1,2-diaminoethane (mep), *N*,*N*′-dimethyl-*N*,*N*′-bis(pyridin-2-ylmethyl)-1,2-diaminocyclohexane (mcp), and 2-((bis(pyridin-2-ylmethyl)amino)methyl)phenol, have been synthesized and used to assess the performance of catalytic water oxidation.[254,257–259] Some other Ni-based complexes were reported as precursors to generate active Ni oxide films for water oxidation.[260–262] Because of the fewer redox states of Ni ions, development of Ni-based WOCs with low overpotentials remains challenging.

Iron is the most abundant, non-toxic, and inexpensive transition metal. Additionally, it has a rich redox chemistry, and thus many iron-based complexes can generate reactive

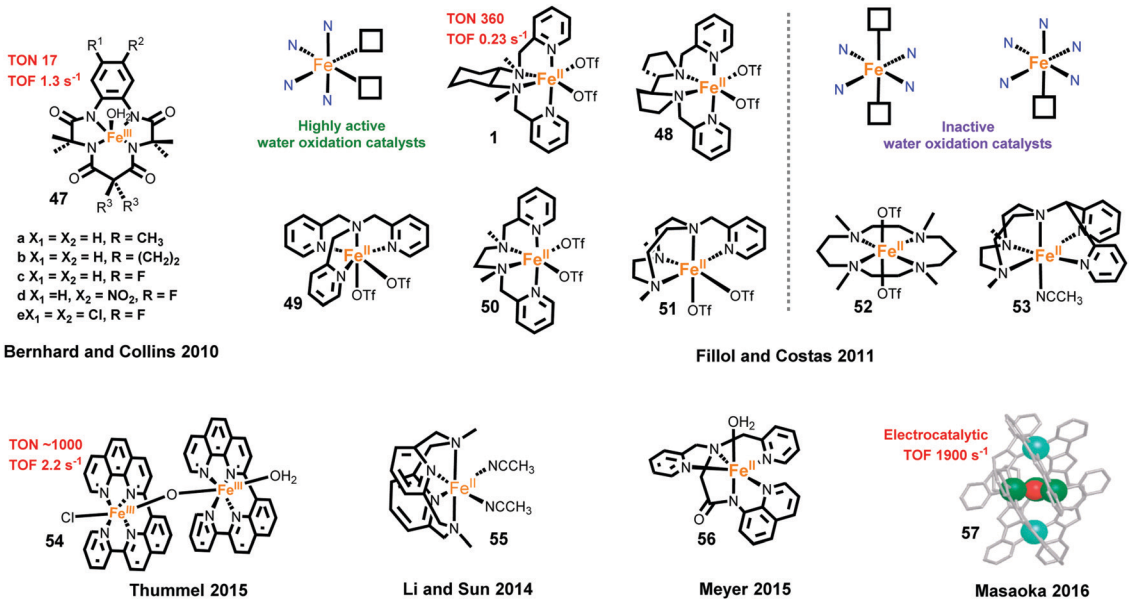

Fig. 11 Representative structures of Fe-based WOCs.

valent states for oxidation reactions in both natural[263,264] and artificial systems.[265] Due to these advantages, we strongly agree that iron complexes are ideal and promising candidates for WOCs.[266]

The first family of Fe-based molecular WOCs, iron(III)–tetraamido macrocyclic ligand complexes (Fe^{III}–TAMLs, complex **47**) (Fig. 11), was reported by the Bernhard and Collins groups in 2010.[267] Using Ce^{4+} as the oxidant, fast O_2 evolution was observed for these Fe^{III}–TAMLs. The catalytic performances of the Fe^{III}–TAMLs were dominated by the substituent groups on the macrocyclic ligands. The highest TOF of 1.3 s^{-1} was achieved for a Fe^{III}–TAML with a strong electron-withdrawing group; however, these Fe^{III}–TAMLs have low stabilities under the testing conditions, and remain active for only 20 s. Subsequently, this family of Fe-based WOCs was further investigated for electrochemical water oxidation,[268] photocatalytic water oxidation[268] and catalytic mechanisms.[268–270]

One year later, a second class of Fe-based WOCs was reported by Fillol, Costas and co-workers. The authors studied catalytic water-oxidation properties of several classical non-heme iron complexes (complexes **1** and **48–53**).[40] They reported that non-heme iron complexes with two *cis* labile sites may have catalytic activity for water oxidation, whereas the complexes bearing two *trans* labile sites or only one labile site are not active for water oxidation. Complex **1** is the most efficient WOC reported by them with a TON of 360 and a TOF of 0.23 s^{-1} using Ce^{4+} as the oxidant. This type of Fe-based WOC has attracted widespread research attention, making it one of the most studied molecular noble-metal-free WOCs. Effects of electronic modification and of pendant bases have also been explored.[271–273] Several studies have been conducted to elucidate the catalytic mechanism.[269,274–277] Recently, a $Fe^{IV}(O)(OCe^{4+})$ motif is proved to be a key intermediate in catalyzed water oxidation by **1** under acidic conditions.[276]

Recently, a highly active binuclear Fe-based WOC $[(ppq)(H_2O)Fe(\mu\text{-}O)(Cl)(ppq)]^{3+}$ (complex **54**, ppq = 2-(pyrid-2′-yl)-8-(1″,10″-phenanthrolin-2″-yl)-quinoline) was reported by Thummel and co-workers.[278] Using Ce^{4+} as the oxidant, complex **54** showed much higher activity than a mononuclear analog, affording a TON of ~1000 and a TOF of 2.2 s^{-1}, which are the corresponding records for molecular noble-metal-free WOCs under similar conditions. The excellent catalytic performance may be attributed to the easy disproportionation of the intermediate $[Fe^{IV}Fe^{IV}\text{–}OH_2]$ to a key intermediate $[Fe^{III}Fe^{V}{=}O]$. Moreover, binuclear Fe-based complexes $[(tpa)(H_2O)Fe(\mu\text{-}O)(H_2O)(tpa)]^{4+}$,[279] $[(tpa)Fe(\mu\text{-}O)(\mu\text{-}SO_4)\text{-}(H_2O)(tpa)]^{2+}$ and $[(tpa)(Cl)Fe(\mu\text{-}O)(Cl)\ (tpa)]^{2+}$ were also reported to have higher activities than the mononuclear analog.[280,281] These results suggest that binuclear Fe-based complexes can generate more efficient molecular catalysts for water oxidation. To explore a better coordination environment for efficient Fe-based WOCs, the Sun group examined the activities of eleven separated iron complexes and nine *in situ*-generated iron complexes towards catalytic water oxidation using Ce^{4+} as the oxidant.[282] Complex **55** was obtained as a promising catalyst for water oxidation, and its catalytic mechanism was further investigated by the Che group.[283]

Fe-Based molecular electrocatalysts for water oxidation have also been developed in recent years. Meyer and co-workers reported the electrocatalytic properties of an iron complex bearing a pentadentate ligand, $[Fe^{III}(dpaq)(H_2O)]^{2+}$ (complex **56**, dpaq = 2-[bis(pyridine-2-ylmethyl)]amino-*N*-quinolin-8-yl-acetamido) in 2015. Complex **56** showed only moderate performance with a low faradaic efficiency of 45% and a low TOF of 0.15 s^{-1}.[284] One year later, Masaoka and co-workers reported the most active Fe-based electrocatalyst, a pentanuclear iron complex surrounded by six 3,5-bis(2-pyridyl)pyrazole ligands and linked by one μ_3-O bridging ligand (complex **57**).[285] The calculated electrocatalytic TOF is as high as 1900 s^{-1}, and the

Faradaic efficiency obtained from the controlled potential electrolysis is 96%. A plausible catalytic cycle was constructed based on the promising characterization of intermediate species and quantum chemical calculations. However, it should be noted that the two above-mentioned catalysts work only in special organic solvent systems, due to the instability of the high-valent iron intermediate in aqueous solution.

4.1.6 Polyoxometalate water oxidation catalysts (POM WOCs). In addition to molecular WOCs based on conventional organic ligands, metal complexes coordinated with polyoxometalates (POM), which combine the advantages of homogeneous and heterogeneous catalysts, have been thoroughly investigated as promising catalysts for water oxidation.[56] The first breakthrough in POM WOC development was made in 2008 independently by two groups.[286,287] The synthesis and homogeneous catalytic water oxidation of the same tetranuclear Ru-based polytungstate, $[Ru_4(\mu\text{-}O)_4\text{-}(\mu\text{-}OH)_2(H_2O)_4(\gamma\text{-}SiW_{10}O_{36})_2]^{10-}$ (complex **58**, Ru_4SiPOM), were reported (Fig. 12). A TON of 18 and a TOF of 0.45–0.6 s^{-1} were obtained using $[Ru(bpy)_3]^{3+}$ as the oxidant by the Hill group, and a TON of 500 and an initial TOF of 0.125 s^{-1} using Ce^{4+} oxidant were reported by the Bonchio group.

Another important improvement in developing POM WOCs was the report of a tetracobalt-substituted polytungstate, $[Co_4(H_2O)_2(PW_9O_{34})_2]^{10-}$ (complex **59**, Co_4PPOM), which catalyzed water oxidation with a high TON per active site metal of 1000 and a TOF of 5 s^{-1} using $[Ru(bpy)_3]^{3+}$ as a chemical oxidant in an aqueous Pi buffer solution at pH 8.0.[288] Following these two pioneering works, extensive research has been conducted in recent years, on the variation in POM structures[289,290] and different metals,[291–293] mechanistic evaluation,[294–296] application on electrodes,[297,298] and the stability of POM WOCs.[221,299–303] There are also several recent reports of POM WOCs; for example, the report on the development of Mn-based POM WOCs.[304,305] Very recently, the excellent catalytic activity of a water-insoluble Co-POM (complex **60**) under acidic conditions was reported by the Galan-Mascaros group in 2018.[306] POM WOCs, as a unique molecular system, exhibit considerable promise in the development of AP devices.

WOCs based on noble metals Ru and Ir have been well developed in the past thirty years, and catalysts with promising activity have been achieved. However, from the viewpoint of practical application, an earth-abundant transition-metal-based catalyst will be necessary for AP devices. Although some progress has been made toward the development of WOCs based on earth-abundant transition metals,[4,55,244,307] including Mn, Co, Ni, Cu, and Fe, the activity of available earth-abundant transition-metal-based catalysts is still very low. A high overpotential and strong basic condition are required, under which conditions some of the catalysts decompose into metal oxides to serve as the true catalysts.[308–310] The unsatisfactory progress in the development of earth-abundant transition-metal-based WOCs signifies the magnitude of the challenge and the efforts needed to overcome it. Research on the development of earth-abundant transition-metal-based molecular WOCs commenced in the 2010s;[4,55,244,307] this is much later than the initial development of Ru and Ir based WOCs. To obtain efficient and inexpensive metal-based WOCs for future AP application, more designs and research are required.

4.2 Overview of molecular catalysts for reduction reactions

To efficiently produce valuable fuels using the protons and electrons obtained from the oxidation of water, highly active and selective catalysts are essential for the reduction reactions (hydrogen evolution and CO_2 reduction reaction).[10] Molecular catalysts with the above-mentioned advantages have attracted immense attention in the field of reduction half reactions. It is necessary to note that, in the development of molecular WOCs, a number of suitable chemical oxidants allow evaluation of the catalytic activity in a simple chemical-driven water-oxidation system to thereby reveal the mechanism. On the other hand, studies on the molecular catalysis of the hydrogen evolution and CO_2 reduction reactions are mainly conducted in photochemical and electrochemical systems. In this part, we present an overview of the most typical and well-studied catalysts for hydrogen evolution and CO_2 reduction.

4.2.1 Molecular hydrogen-evolution catalysts (HECs). Hydrogen evolution in nature is accomplished by two main classes of hydrogenases – [FeFe] and [NiFe] – which are highly active with a TOF of 9000 s^{-1} at 100 mV overpotential and 500 s^{-1} near the thermodynamic potential, respectively.[311–313] The structures of these two hydrogenases were revealed during the 1990s.[51,314,315] As shown in Fig. 13, the catalytic core of [FeFe]-hydrogenase is a Fe–Fe dinuclear complex coordinating

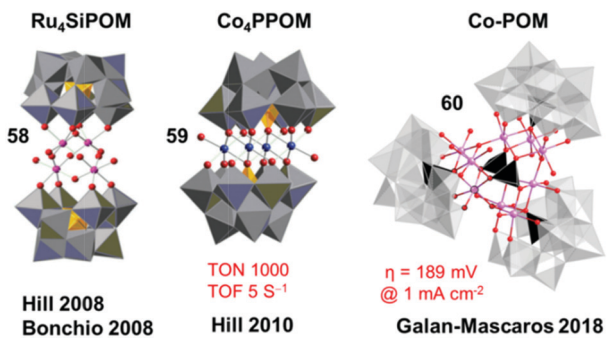

Fig. 12 Representative structures of POM WOCs. Reproduced from ref. 56 with permission from The Royal Society of Chemistry.

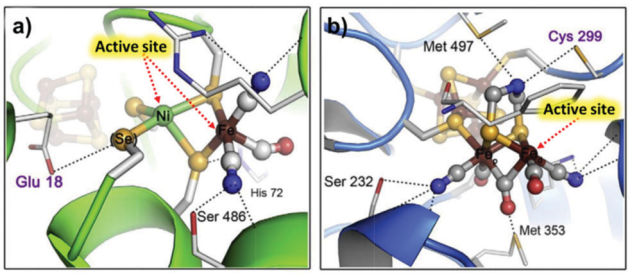

Fig. 13 X-ray structures of (a) NiFe cluster of [NiFe(Se)]-hydrogenases; (b) 2Fe sub-cluster of the [FeFe]-hydrogenase H cluster. Adapted with permission from ref. 314. Copyright 2015 Elsevier.

with CN^-, CO ligands as well as an azadithiolate (adt^{2-}) double-bridge ligand. One Fe ion is in a six-coordinated ideal octahedral configuration, whereas the other Fe ion has only five-coordination, leaving one coordinating vacancy as an active site. The active center of [NiFe]-hydrogenase is an asymmetric Ni–Fe hetero-dinuclear cluster. The CN^- and CO ligands coordinate with the Fe ion, and the Ni ion is in a highly distorted square-planar configuration formed by four cysteinate ligands, two of which bridge with the Fe site. Both the Fe and Ni sites provide coordinating vacancies as active sites.

A reasonable design for an artificial catalyst can be facilitated by unveiling the structure and catalytic mechanism of the natural system. A general catalytic mechanism for hydrogen evolution is shown in Fig. 14.[316–319] The active metal center undergoes either consecutive or coupled electron and proton transfers to generate a reactive metal-hydride intermediate, which can react in two possible ways to evolve hydrogen. In the left cycle, the metal-hydride reacts with another metal-hydride to generate H_2 *via* reductive elimination, *i.e.*, the homolytic pathway. Alternatively, in the right cycle, the metal-hydride is further reduced and protonated to form H_2, *i.e.*, the heterolytic pathway. Taken together, to obtain a high activity for hydrogen evolution, a metal complex should have wide open coordination sites for binding the substrate and an appropriate electronic structure for generating and stabilizing a reactive metal-hydride intermediate. With these criteria in mind, hundreds of molecular HECs have been developed thus far (Fig. 15).

In the first fully molecular example of photocatalytic hydrogen evolution, the catalyst was a Rh-based complex bearing a polypyridyl ligand.[320] Several Rh-based HECs have been developed for photocatalytic hydrogen evolution since then.[321–323] The Bernhard group reported the most efficient Rh-based HEC by modification of the polypyridyl Rh-complex (complex **61**).[323] In their photocatalytic system, the catalytic TON of **61** exceeded 5000. Another large family of noble-metal-based HECs is the platinum complexes.[324] Sakai *et al.* have developed numerous platinum complexes for photocatalytic hydrogen evolution. As a representative example, complex **62** showed outstanding catalytic performance with a TON of 100 and a high quantum efficiency of 31% in an optimized three-component photocatalytic system.

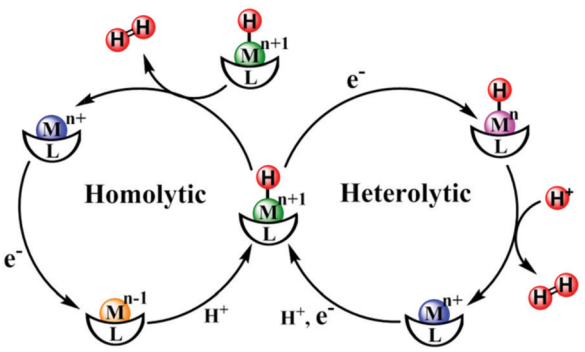

Fig. 14 Proposed mechanistic pathways for H_2 evolution by a metallic catalytic center.

Over the last decade, studies have mainly concentrated on developing earth-abundant metal-based HECs.[54,313,325–327] Chemists are engaged in the synthesis of structural and functional mimics of [FeFe]- and [NiFe]-hydrogenases to understand the mechanisms of H_2 evolution by natural hydrogenases, which is key to the design of artificial HECs.[39,328–332] Complexes **2** and **63** are two early available models reported by Rauchfuss *et al.* for [FeFe]- and [NiFe]-hydrogenase, respectively.[39,330,332] More than hundred synthetic mimics have been reported thus far.[333] These complexes faithfully reproduce the structure of the active center of the hydrogenases, and the related investigations provide in-depth information on the H_2 evolution mechanisms. However, the complexes exhibit poor catalytic performances, *i.e.*, low stability and larger overpotential requirements.

To obtain more advanced and cost-effective synthetic HECs, researchers have designed and synthesized various ligand platforms for earth-abundant metals, *e.g.*, Ni, Co, Fe, and Mo.[313,325,326] Thus far, the most efficient and stable molecular HECs are Ni-complexes (*e.g.*, complex **64** and **65**) bearing base-containing diphosphine ligands, which were first reported by DuBois and co-workers in 2002, and are therefore well known as ''DuBois catalysts''.[334–338] In an acetonitrile solution with 1.2 M H_2O, the catalytic TOF of H_2 production by **64** could exceed 100 000 s^{-1} at a high overpotential.[312] On the other hand, the lowest overpotential among the DuBois catalysts was exhibited by **65**.[339] Further studies on these catalysts proved the importance of pendant amines for proton transfer.

Another series of HECs, which are among the most efficient catalysts, is the cobaltoximes formed from the coordination of two glyoximato equatorial ligands with a cobalt ion. These complexes were originally reported in the 20th century, and their early use as a HEC was reported by Lehn in 1983[340] and Espenson in 1986.[341] The Peters group[342] and Fontecave group[343] in 2005 simultaneously revisited cobaltoximes (complex **66**) and studied their electrocatalytic properties for hydrogen evolution. Following these works, cobaltoxime-based HECs have been extensively studied over the last 10 years, and have achieved the high-efficiency and low-overpotential requirement.[344] Cobaltoximes can catalyze hydrogen evolution from protic solutions requiring overpotentials as low as 40 mV.[325] The second generation of cobaltoxime-based HECs, cobalt diamine–dioxime complexes, was studied by the Fontecave group (complex **67**).[345] These diamine–dioxime complexes catalyze H_2 evolution from acidic solutions with similar overpotentials to conventional cobaltoximes, but display better stability owing to the propylene bridge. The structural modification, catalytic mechanisms, and decomposition pathway of cobaltoxime catalysts have been studied in detail.[346–349]

Mo-Based HECs are mainly the contribution of Chang *et al.*[350–353] The Mo^{IV}–oxo complex [Mo(PY5Me)(O)] (complex **68**) is among the most efficient electrocatalysts ever reported for H_2 evolution from an aqueous solution at neutral pH with good durability, and high catalytic TOF but high overpotential. After CPE on a Hg pool electrode at an overpotential of 1.0 V in a phosphate buffer at pH 7 for 71 h, **68** displayed 100% Faradaic efficiency, a TON of 6.1×10^5, and a TOF of 2.4 s^{-1}.[351] Using the same ligand

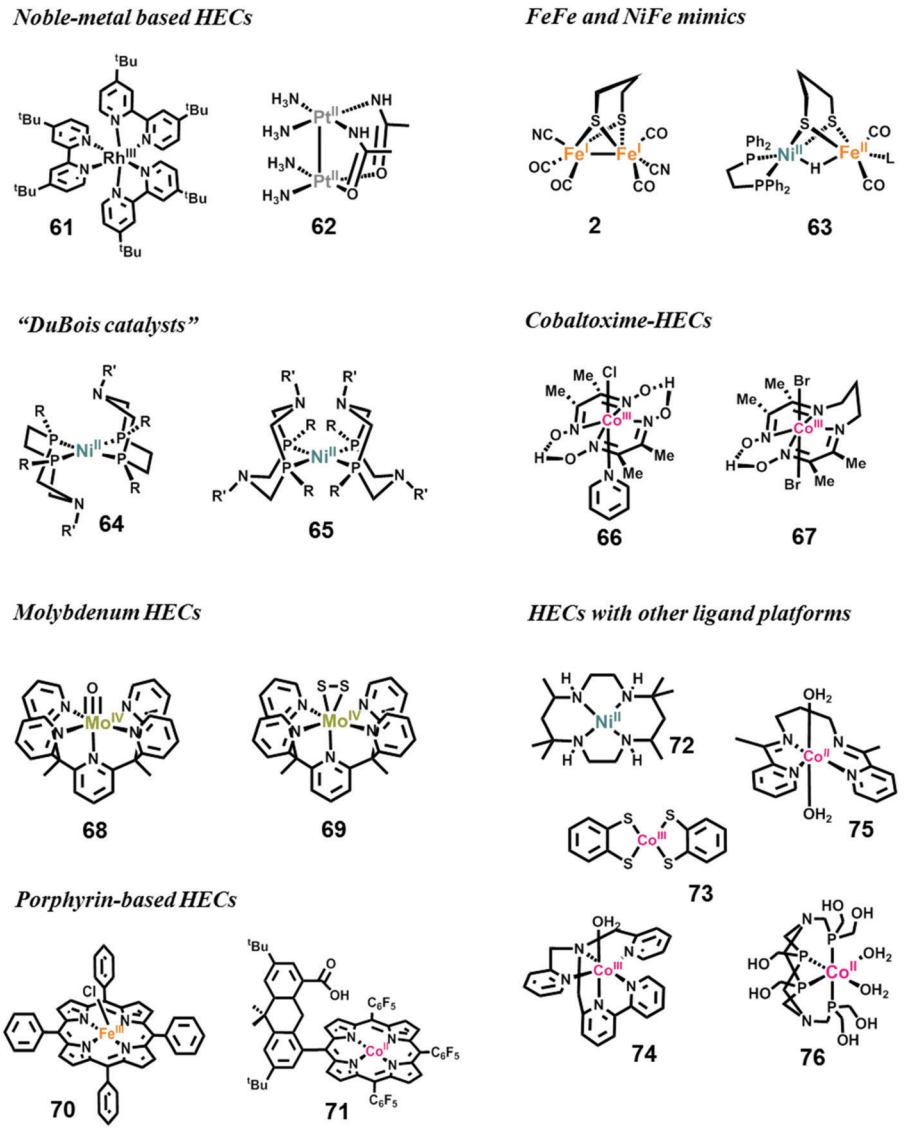

Fig. 15 Representative structures of HECs.

framework, Chang *et al.* synthesized complex **69** to mimic the reactive edge site of the MoS_2 material,[354] which is a well-known heterogeneous HEC. Like **68**, upon electrochemical reduction, **69** also showed impressive performance with 100% Faradaic efficiency, a lower-limit TON value of 3.5×10^3 calculated from the bulk solution, and an upper limit of 1.9×10^7, assuming a constant monolayer on the electrode. In subsequent work, it was proved that the PY5-based ligand also works well when cobalt is placed as the catalytic center.[350] Mo complexes with Schiff base ligands have been studied recently as a catalyst for electrochemical hydrogen evolution.[355,356]

Porphyrin-based transition metal complexes have been widely employed for the catalysis of energy-conversion-related small-molecule activation.[357] Many transition metal porphyrin complexes have been investigated as HECs, including Fe-,[358,359] Co-,[357,360–362] and Ni-porphyrins.[363] The Fe-porphyrin complex **70** reported by Savéant and co-workers can produce H_2 from an acidic DMF solution at a TOF of 10^5–10^6 s^{-1}.[358,364] The Nocera group invented a series of ''hangman porphyrins'', featuring dangling proton-transfer groups, such as carboxylic acid (complex **71**),[359,362,363,365] sulfonic acid[359] or amine,[359] fixed on top of the active metal center. Due to the promoted PCET processes, these catalysts exhibited decreasing overpotential and increasing TOFs for H_2 evolution.

In addition to the above main series of HECs, many other well designed ligand platforms have been applied for housing transition metals as HECs.[313,326,366–369] For example, the macrocyclic Ni complex **72** and its analogues were good electrochemical HECs under organic-aqueous solutions[370] and fully aqueous solutions.[371] Recent studies demonstrated that dithiolene complexes **73** and the nitrogen donor ligand stabilized complex **74** could efficiently catalyze both electrochemical and photochemical H_2 evolution from water reduction,[372–374] and a cobalt bis(iminopyridine) complex **75** could also act as an efficient electrocatalyst for H_2 production from an aqueous solution.[375] Using a multihydroxy-functionalized tetraphosphine ligand, Sun

and Wang obtained a self-assembled cobalt complex **76** in 2014. Although the crystal structure of **76** is not available, the complex exhibits highly-efficient activity. Electrocatalytic H_2 generation from neutral water by **76** on a mercury electrode requires an overpotential of only 80 mV. The bulk electrolysis of **76** in a neutral phosphate buffer solution at −1.0 V *vs.* NHE generated 9.24×10^4 mol H_2 per mol **76** over 20 h, with a Faradaic efficiency close to 100% and without obvious deactivation.[376]

4.2.2 Molecular catalysts for CO_2-reduction. In addition to the reduction of protons into H_2, another promising route to obtain fuels is the reduction of CO_2 into valuable chemicals using electrons and protons extracted from H_2O.[53] As shown in eqn (1)–(7) (E^0 *vs.* NHE at pH 7), the reduction of CO_2 can not only produce gaseous fuels such as CO and CH_4, but also energy-dense liquid fuels such as CH_3OH and HCOOH.[377] However, effective CO_2 reduction catalysts (CO_2RCs) are urgently required to reduce the energy barriers of these reactions involving multiple electrons and protons, to compete with the proton reduction reaction, and control the selectivity of the products from reducing CO_2.[44] Development of d-block metal based molecular catalysts can be traced back between the 1970s and 1980s, mainly involving Co^{II} and Ni^{II} complexes with macrocyclic ligands, such as phthalocyanines and tetraazamacrocycles.[370,378,379] Many articles were published on Re,[380–383] Ru[384–389] and Rh[390–393] based catalysts in the 1980s and 1990s. After a short gap, the field gained resurgence in the 2010s with the development of catalysts based on first-row transition metals, and reports of supramolecular assemblies and hybrid devices for CO_2 reduction.[43,377,394]

$$CO_2 + 1e^- \rightarrow CO_2^{\bullet -} \quad -1.90\ V \tag{1}$$

$$CO_2 + 2H^+ + 2e^- \rightarrow HCOOH \quad -0.61\ V \tag{2}$$

$$CO_2 + 2H^+ + 2e^- \rightarrow CO + H_2O \quad -0.53\ V \tag{3}$$

$$2CO_2 + 2H^+ + 2e^- \rightarrow H_2C_2O_4 \quad -0.49\ V \tag{4}$$

$$CO_2 + 4H^+ + 4e^- \rightarrow HCHO + H_2O \quad -0.48\ V \tag{5}$$

$$CO_2 + 6H^+ + 6e^- \rightarrow CH_3OH + H_2O \quad -0.38\ V \tag{6}$$

$$CO_2 + 8H^+ + 8e^- \rightarrow CH_4 + H_2O \quad -0.24\ V \tag{7}$$

One of the most important catalysts for CO_2 reduction is the Re^I bipyridyl complex (complex **77**; $Re^I(bpy)(CO)_3Cl$), which was reported in the early 1980s by Lehn, Ziessel and Hawecker.[381,382,395] CV studies of the electrochemical reduction of CO_2 by **77** showed a reversible peak first at −1.68 V *vs.* Fc^+/Fc corresponding to the one-electron reduction of the bpy ligand, and a catalytic peak at −1.98 V *vs.* Fc^+/Fc which also involved the generation of Re^0 species.[381,383] This type of catalyst has a high Faradaic efficiency and excellent selectivity for the reduction of CO_2 to CO. Electronic effects on the bpy ligand were investigated by the group of Johnson *et al.* in 1996[396] and Kubiak *et al.* in 2010.[397] Their results indicated that the catalytic performance increased with increasing electron density on the bpy ligand. Kubiak and co-workers further studied the steric effects on the bpy ligand and the deactivation pathway of this type of catalyst.[398,399] Dimerization of two Re complexes results in the deactivation of **77**. The effect of ligand X on $Re^I(bpy)(CO)_3X$ was researched by Ishitani and co-workers, including Cl^-, Br^-, CN^-, NCS^-, P-based ligand, and pyridyl-based ligand.[400] They also investigated numerous photocatalytic systems for CO_2 reduction using these $Re^I(bpy)(CO)X$ type catalysts.[401,402]

Owing to the success of $Re^I(bpy)(CO)_3X$ type catalysts, polypyridyl complexes of Ru,[385,403–406] Os,[407–409] and Ir[410] have also been further developed as catalysts for CO_2 reduction in recent years. As the types of Ru(tpy)(bpy)X shown in Fig. 16 (complex **78**),[403,404,406] $Ru(bpy)_2(CO)_2$[385,411,412] and $Ru(bpy)(CO)_2X_2$[405,413] have been extensively studied by different groups. For Pd-based catalysts, Dubois and co-workers reported Pd complexes using multidentate phosphine ligands (complex **79**).[414,415]

In contrast to WOCs, the development of earth-abundant metal-based CO_2 reduction molecular catalysts has been much more successful.[43,377,394] For Co- and Ni-based catalysts, besides complexes with common polypyridyl ligands,[416–418] tetraaza-macrocycle Co and Ni complexes, Co^{II}(macrocycle) and Ni^{II}(macrocycle), *e.g.*, complexes **80** and **81**, have been reported as efficient catalysts for CO_2 reduction.[370,379,419–423] Although Ni^{II}(macrocycle) has been reported with Faradaic efficiencies over 95% in the production of CO, its good selectivity is strongly dependent on the pH of the reaction solution, and the low TOF is its drawback.[421] In complex **82**, the macrocycle includes four pyridines linked by pendant amine groups, which can contribute toward stabilizing the Co^I-CO_2 intermediate during catalysis, making **82** an efficient Co catalyst with high selectivity for CO formation.[422]

Replacing the Re metal in the $Re^I(bpy)(CO)_3X$ catalysts with Mn metal, Deronzier and co-workers discovered a new class of highly active CO_2 reduction catalysts in 2011, an example of which is complex **83**, $Mn(bpy)(CO)_3Br$.[424] Subsequently, a wide variety of analogues of $Mn(bpy)(CO)_3Br$ were designed and investigated.[394] To prevent deactivation due to the dimerization of Mn^0 intermediates, bulky substituents with two phenyl rings were introduced into the bpy ligand (complex **84**).[425] By further introduction of four methoxy groups on the two phenyl rings, the proton transfer steps were promoted; consequently, the CO_2 conversion overpotential was reduced by 0.55 V (complex **85**).[426]

Another important series of noble-metal-free catalysts for CO_2 conversion is iron porphyrins (*e.g.*, complexes **3**, **86**, and **87**), which are among the most efficient molecular catalysts for the electrochemical reduction of CO_2 into CO.[43,427,428] In 1991, Savéant and co-workers found that Fe^0 porphyrins can reduce CO_2 to CO at −1.8 V *vs.* SCE in DMF.[429] However, the iron-porphyrin catalysts were not stable after several catalytic cycles. In further studies, they found that the addition of a hard electrophile (*e.g.* Mg^{2+}) or Brønsted acids (*e.g.* 1-propanol, 2-pyrrolidine, and CF_3CH_2OH) could improve the catalytic efficiency and stability.[430] In 2012, the Savéant group made a breakthrough in reducing CO_2 to CO by iron porphyrins. They introduced phenolic groups in all *ortho* and *ortho′* positions of the phenyl groups in the structure of iron porphyrin to increase the local proton effect to stabilize the Fe^0 intermediate. At a low overpotential of 0.47 V, the catalyst

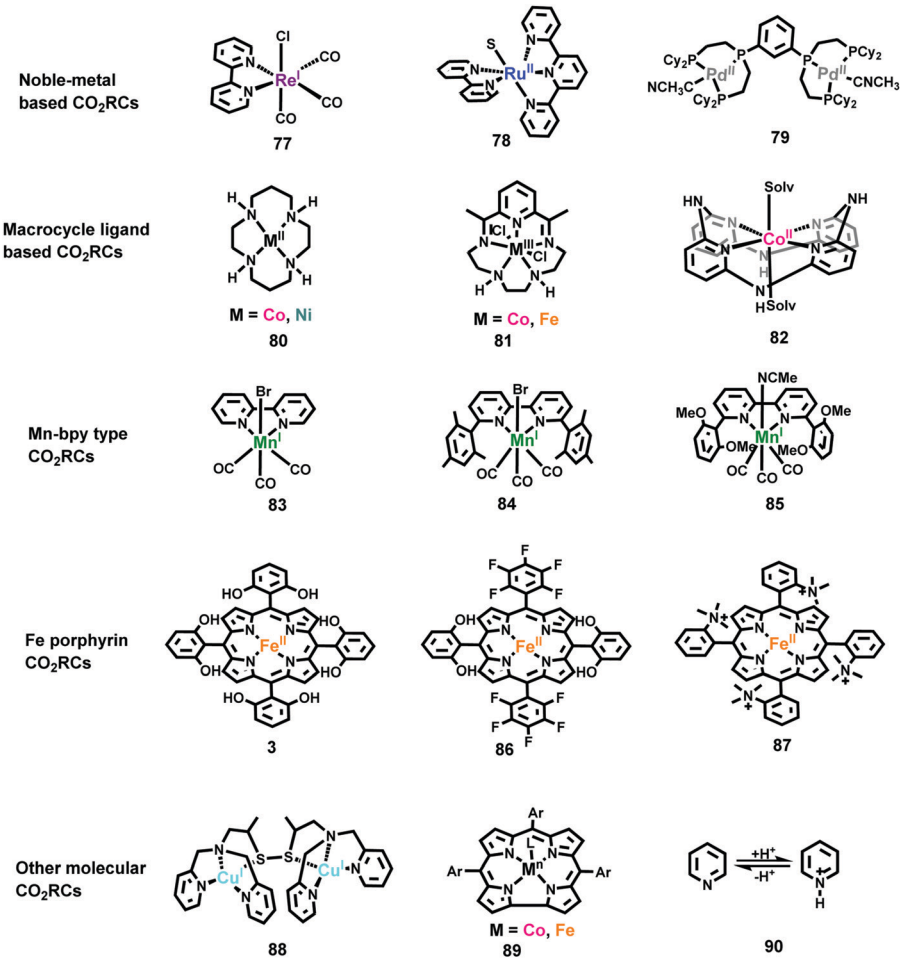

Fig. 16 Representative structures of CO_2RCs.

displayed a CO Faradaic efficiency above 90% through TONs of 50 million over 4 h electrolysis without obvious degradation.[41,431] Very recently, the performance of iron porphyrins for reducing CO_2 to CO was dramatically boosted again by Savéant and co-workers. By introducing four charged trimethylanilinium groups in the para- or *ortho*-position of the phenyls in the iron porphyrin structure, complex **87** could selectively produce CO from CO_2 under the test conditions with a TOF of 10^6 s^{-1} at an overpotential of only 220 mV for 80 h with no degradation observed.[432]

In addition to iron porphyrin complexes, porphyrin complexes with many other transition metals have been investigated for catalytic CO_2 reduction.[43,433–435] Interestingly, a Zn–porphyrin complex with a redox-innocent metal center was reported with a TOF as high as 14.4 s^{-1} and a Faradaic efficiency as high as 95% for CO_2 electroreduction to CO at −1.7 V *vs.* NHE.[433] The observation in this work that the ligand acts as the redox center during CO_2 electroreduction calls for further mechanistic studies. Furthermore, Brudvig and co-workers reported a novel zinc(II)–bacteriochlorin complex to improve the stability of CO_2RCs by taking advantage of the superior stability of the bioinspired bacteriochlorin ligand.[436]

Besides the above main class of CO_2 reduction catalysts, there are many other notable reports of CO_2RCs.[437] For example, Bouwman and co-workers reported in 2010 a binuclear copper catalyst (complex **88**) that could produce oxalate by catalyzing the one-electron reduction of CO_2 at a very low overpotential.[438] Metal corroles have also been reported with activity for CO_2 reduction (complex **89**).[439] Interestingly, the pyridinium ion without the involvement of any metals has been proven to be a suitable electrocatalyst for the six-electron reduction of CO_2 to methanol (complex **90**).[440–442] Except for pyridinium ion catalysts, molecular catalysts could only realize the one-electron and two-electron reduction of CO_2, until the recent reports of a Cu-based porphyrin[434] and a carbine-coordinated Ni complex,[443] which are able to produce methane/ethylene and methanol, respectively. The development of efficient molecular catalysts for CO_2 reduction still faces numerous challenges. Most CO_2 reduction molecular catalysts still need to be able to work under organic conditions; however, the catalysts are not suitable under water oxidation conditions for future device fabrication.

4.3 Promotion of intrinsic activity by precise structural control

As is known, one of the basic principles of chemistry is that the structure determines the property. The activity of a catalyst closely depends on its structure. Therefore, fine adjustment of

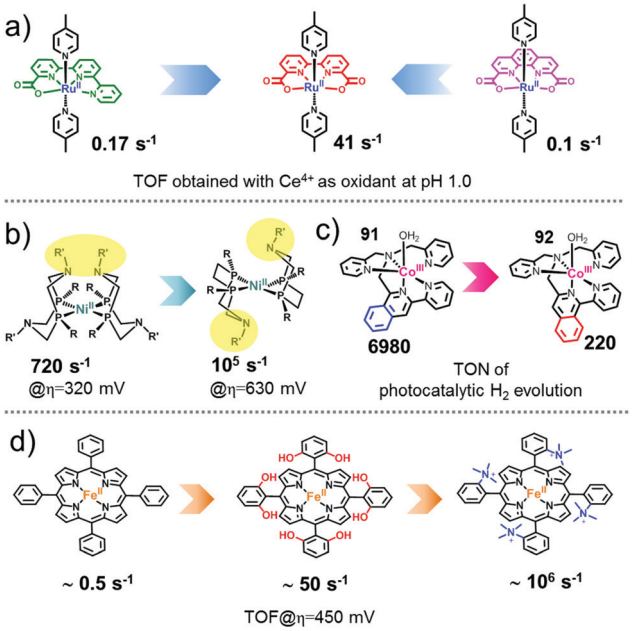

Fig. 17 Fine structural adjustments and dramatic performance (*e.g.* catalytic TON or TOF under comparable conditions) promotion of (a) Ru-bda WOCs; (b) Ni-diphosphine HECs; (c) pentadentate polypyridyl-amine Co HECs; and (d) Fe-porphyrin CO_2RCs.

the catalyst structure is essential for the promotion of its activity. The most prominent advantage of a molecular catalyst is that it is possible to precisely regulate the electronic and steric structure to obtain extremely high catalytic performance.

There are numerous examples of WOCs, HECs, and CO_2RCs that highlight the importance of precise structural control for achieving new catalysts with high intrinsic activities. As shown in Fig. 17, the intrinsic activities of representative successful WOCs,[174,179] HECs[312,444] and CO_2RCs[41,432] have been improved by several orders of magnitude after precise structural adjustments. Small changes in the structure of the molecular catalyst may result in a new catalyst with higher intrinsic activity. Therefore, the development of an efficient molecular catalyst is highly feasible with a clear understanding of the catalytic mechanism and reasonable design of the structure. This is the significant advantage of developing molecular catalysts.

5. Heterogenization of molecular catalysts – challenges of molecular catalysis

As discussed in the previous sections, there is a large gap between existing molecular catalysts and the development of effective AP devices. The heterogenization of molecular catalysts is essential to achieve simultaneous progress in the development of molecular catalysts and effective AP devices. Using the proposed model of the AP devices (Fig. 2), chemists have designed and reported many molecular catalyst-modified electrodes for AP devices during the past 10 years.[445] Efficient molecular catalysts developed in the first stage, especially catalysts with low overpotential, are essential to achieve efficient AP devices. In this part, we summarize the research status of molecular-catalyst-based AP devices. These works have successfully demonstrated model design and the behavior of catalysts on the surface of electrodes. However, few studies have focused on exploring strategies and principles for the heterogenization of molecular catalysts by considering practical problems, such as the density of catalysts, exposure of the catalyst active sites, conductivity issues, enhancement of mass transport, and improvement in the stability of the molecule-catalyst-derived material or electrode. Setting aside the research on the development of more efficient and cheaper molecular catalysts, the heterogenization of molecular catalysts constitutes the main challenge toward their application in AP devices.

5.1 Molecular-catalyst-modified dye-sensitized PEC cells (DSPEC cells)

The concept of a DSPEC cell has evolved from the dye-sensitized solar cell (DSSC), which was first proposed by O'Regan and Grätzel in 1991 (Fig. 18a).[446] A new type of solar cell was invented by sensitizing nanocrystalline films of TiO_2 with Ru^{II} dyes for molecular-level light absorption. An essential feature in these devices is that photo-excited electrons of Ru^{II} are irreversibly injected into the conduction band of TiO_2, yielding the oxidized dye Ru^{III}. Ru^{III} is reduced to regenerate Ru^{II} dye by electron transfer from a redox species in the electrolyte solution, which is then reduced at the counter electrode.

Instead of simply generating electricity, the cell can be modified with a molecular assembly of chromophore-catalysts (*e.g.*, WOC, HER or CO_2RR) to use the electron flow to drive reactions that produce chemical fuels.[79] As shown in Fig. 18b, the light excitation of chromophore (C) leads to the generation

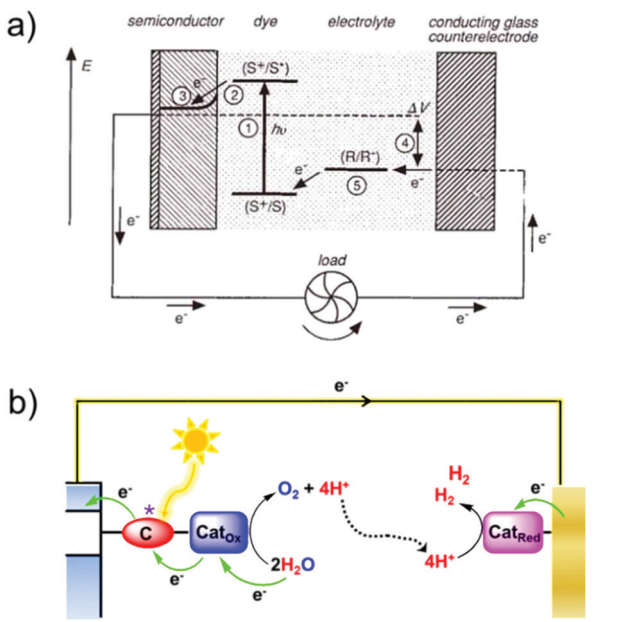

Fig. 18 Schematic representation of (a) principle of dye-sensitized solar cells. Reprinted with permission from ref. 446. Copyright 1991 Nature publications. (b) Photoelectrochemical cells for water splitting.

of its excited state C*, which subsequently transfers electrons to the conduction band of TiO_2 to form the oxidative state C^+. C^+ is reduced by the electrons from the catalytic oxidation of H_2O to O_2. Electrons diffuse through the TiO_2 film to the conductive contactor, and then to the cathode, where the electrons are finally used to catalytically reduce protons into H_2. This provides a straightforward theoretical basis for water splitting and CO_2 reduction based on the molecular chromophore and molecular catalyst.

5.1.1 DSPEC cells with molecular-catalyst-modified photoanodes. In 1999, Meyer and co-workers reported the first DSPEC cell with a TiO_2 photoanode modified by a Ru–Ru chromophore-catalyst molecular assembly (complex **93**) and a platinized cathode (Fig. 19a).[447] Although this two-compartment cell displayed only extremely low photocurrent and produced no oxygen, it demonstrated the construction of a DSPEC cell with chromophore-catalyst molecular assembly, thereby providing the basis for further studies on electron transfer, multiple oxidation on the surface of the electrode, and the development of more advanced DSPEC cells. However, in the following ten years, the development of DSPEC cells stagnated due to the lack of promising molecular WOCs. The rate of solar insolation for a chromophore-catalyst molecular assembly is only less than 2 s^{-1}.[448] An efficient catalyst with a high catalytic rate is needed to exceed this rate.

In 2009, Mallouk and co-workers rekindled research on the development of DSPEC cells by reporting the first example of a DSPEC cell with a photoanode for visible-light-driven water oxidation.[449–451] They reported a DSPEC cell with a photoanode consisting of a Ru-based molecular chromophore and the state-of-the-art WOC IrO_2 (Fig. 19b). A photocurrent of 30 μA for water oxidation was obtained by this DSPEC cell. The low photocurrent indicates that the electron transfer from IrO_2 to the Ru chromophore is poor. To overcome this inefficient electron transfer, the photoanode was improved by introducing an electron-transfer mediator.[450] This strategy enhanced the photocurrent three-fold. The works of the Mallouk group encouraged many following reports of DSPEC cells.

Because of the challenge in synthesizing a chromophore-catalyst molecular assembly, molecules entrapped in a Nafion polymer layer have been used to modify molecular catalysts onto the electrode in a simple method to build DSPEC cells (Fig. 20).[452,453] A bioinspired manganese molecular catalyst[452] and the state-of-the-art molecular WOC Ru-bda[453] were immobilized on a TiO_2 film sensitized by Ru^{II} molecular chromophores to fabricate DSPEC cells. The achieved photocurrents of water splitting by these DSPEC cells were still only tens of μA. The reason for this low efficiency may be the inefficient electron transfer from the polymer coated catalysts to the excited Ru dye adsorbed on the surface of TiO_2. Nevertheless, these works further demonstrated the success of water splitting by molecular catalyst-modified DSPEC cells.

In 2011, a seminal work reported the co-adsorption of a photoanode by a high-potential Zn-based porphyrin and a Cp*–iridium molecular WOC.[454] As shown in Fig. 21a, the photoanode provided a photocurrent density of 30 μA cm^{-2} for water oxidation. This work is the first example to prove that the self-assembled co-adsorption of a molecular chromophore

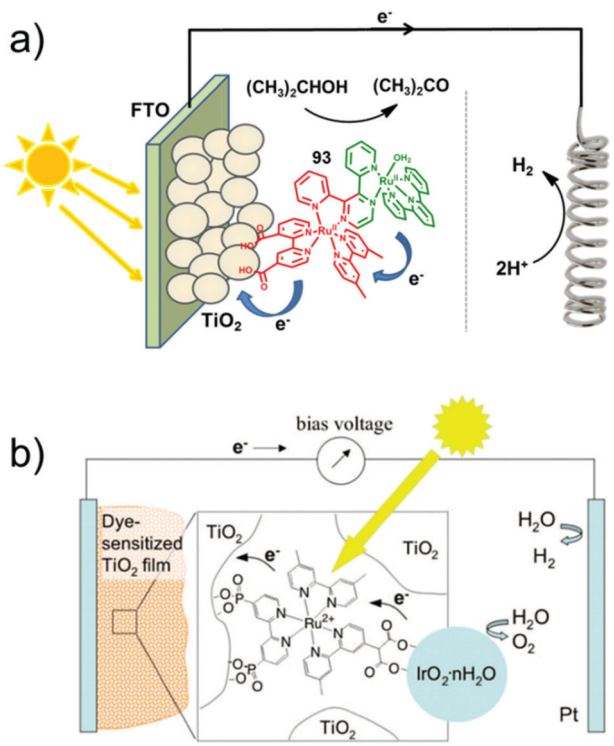

Fig. 19 Schematic of the water splitting dye sensitized solar cell, with (a) Ru–Ru chromophore-catalyst molecular assembly; (b) Ru-based molecular chromophore and IrO_2 WOC. Reprinted with permission from ref. 449. Copyright 2013 American Chemical Society.

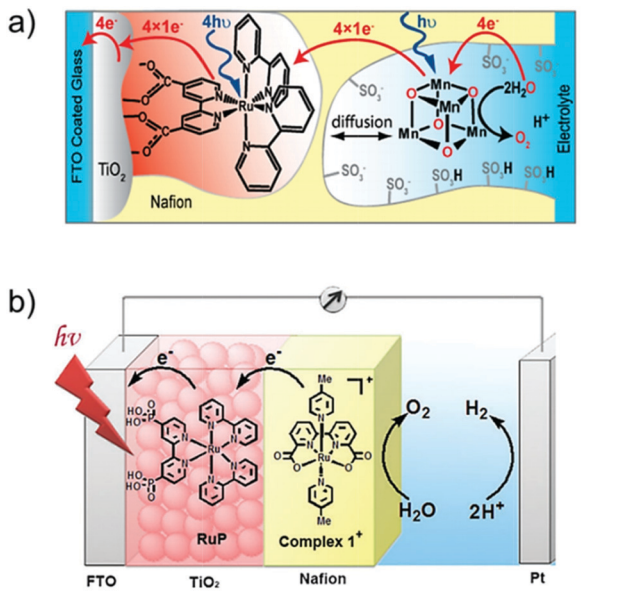

Fig. 20 Depiction of PEC devices consisting of photoanodes immobilized by molecular WOCs embedded in a Nafion film. (a) Ru–sensitized TiO_2 film coated with the "Mn_4O_4" WOC embedded in a Nafion film. Reprinted with permission from ref. 452. Copyright 2013 American Chemical Society. (b) Ru sensitized TiO_2 film coated with the Ru-bda WOC embedded in a Nafion film. Reproduced by permission of The Royal Society of Chemistry.

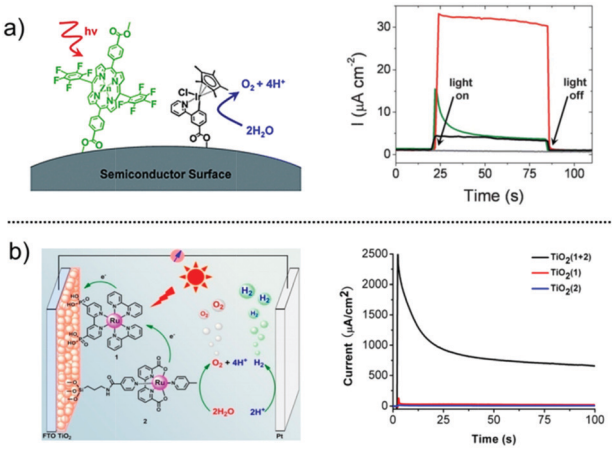

Fig. 21 Schematic of PEC devices consisting of photoanodes coadsorbed with molecular photosensitizers and WOCs. (a) Photoanodes immobilized with a zinc porphyrin photosensitizer and Cp*–Ir WOC. Adapted from ref. 454 with permission from The Royal Society of Chemistry. (b) Photoanodes immobilized with a Ru photosensitizer and Ru-bda WOC. Adapted with permission from ref. 163. Copyright 2013 American Chemical Society.

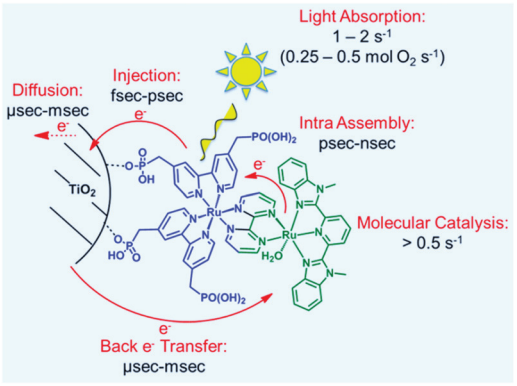

Fig. 22 Summary of relevant time scales for light absorption, electron injection, and intra-assembly electron transfer of a photoanode modified with Ru–Ru chromophore-catalyst molecular assembly. Adapted with permission from ref. 20. Copyright 2015 American Chemical Society.

and molecular catalyst on a TiO_2 film can also result in the formation of a photoanode capable of visible-light-driven water oxidation. Employing the same strategy, the Sun group in 2013 made a breakthrough in improving the performance of this family of DSPEC cells by employing the highly efficient Ru-bda WOC.[163] Under an external bias of 0.2 V *vs.* NHE, the DSPEC cell shown in Fig. 21b displayed a high initial photocurrent density of more than 1.7 mA cm^{-2} and a steady photocurrent density of 0.8 mA cm^{-2}. Oxygen evolution on the photoanode was distinct, and the determined Faradaic efficiency was also high. Apparently, the dramatically improved performance of the DSPEC cell could be attributed to the excellent catalytic activity of the Ru-bda WOC with a low overpotential and high catalytic rate. The simple but advanced method of self-assembled co-adsorption is also essential, if we consider the above photoanode with the Ru-bda WOC entrapped in the Nafion polymer layer.

On the basis of these proof-of-concept examples and the breakthrough work, an increasing number of photoanodes have been developed for efficient and stable DSPEC cells.[18,20,455,456] Considering the benefits of intra-assembly electron transfer, various strategies have been investigated to produce chromophore-catalyst molecular assemblies for DSPEC cells, including bpm ligand-linked assembly,[457] covalent bond linked assembly,[458–461] self-assembly *via* Zr "chemical glue"[462–464] and self-assembly *via* electro-polymerization.[465–467] For several of these DSPEC cells, the working mechanisms and dynamics have been elucidated.[78,461,468] As an example, a summary of the relevant time scales for light absorption, electron injection, intra-assembly electron transfer and other steps is shown in Fig. 22 for the related chromophore-catalyst molecular assembly-modified TiO_2 photoanode.[20,461,468] It is clear that the intra-molecule electron transfer is ultrafast, whereas the back electron transfer from TiO_2 to the Ru catalyst core is rather slow.

The stability of the adsorption of molecules on the metal oxide surface is always a challenge. To stabilize the attachment of functional molecules to the surface of the metal-oxide substrate, various methods have been attempted, such as electro-assembly,[465–467] the use of hydrophobic polymer overlayers,[471] silatrane surface bindings,[472–474] siloxane surface bindings[475,476] and hydrophobic environments.[477] As shown in Fig. 23a, the most effective stabilization was recently achieved by Meyer and co-workers *via* embedding the functional molecules into thin overlayers of Al_2O_3 or TiO_2 formed by atomic layer deposition (ALD). After the deposition of a protective layer, the long-term stability of the Ru molecular WOC-modified ITO electrodes for water oxidation was dramatically enhanced (Fig. 23b).[20,469,470,478,479]

A high catalytic rate for water oxidation is essential to prevent electron recombination and consequently achieve high photocatalytic performance. Owing to the remarkable activity, Ru-bda type WOCs have been extensively employed for the development of DSPEC cells in the last three years by not only the Sun group but also many other scientists.[161,458,480–486] A photocurrent density of approximately 1.0 mA cm^{-2} can be achieved for DSPEC cells with a Ru photosensitizer and Ru-bda type WOCs, with significantly improved stability.[165]

5.1.2 DSPEC cells with molecular-catalyst-modified photocathodes. Considering the limitation of the light absorption range and driving force by only one chromophore, as well as the high reaction barrier of water splitting and CO_2 reduction, it is important to use photocathodes to finally fabricate tandem cells with a powerful driving force for overall water splitting or water oxidation-coupled CO_2 reduction.[25,487] In 1999 Lindquist *et al.* found that dye-sensitized NiO can be used as a p-type photoelectrode to generate a cathodic photocurrent. They invented the first p/n tandem DSSCs.[488] Theoretically, with modification of a HEC catalyst, it is possible to use a dye-sensitized NiO photocathode to form a DSPEC cell for reducing protons or CO_2 instead of reducing a reversible iodine-based redox.[489] In 2012, the Sun group reported the first proof-of-concept example of a DSPEC cell with a NiO photocathode

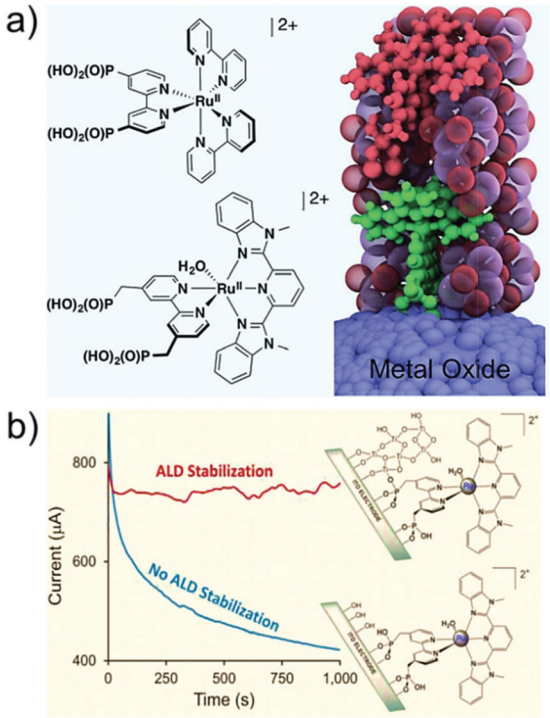

Fig. 23 (a) Depiction of the ALD layer-protected surface assembly with a Ru photosensitizer molecule (green molecule) and a Ru WOC molecule (red molecule) embedded in 3 nm of Al_2O_3. Adapted from ref. 469 with permission from The Royal Society of Chemistry. (b) Electrolysis curves for water oxidation catalysis by a Ru WOC surface bound to ITO with and without a 1 nm TiO_2 protective layer at pH 11 at 1.40 V *vs.* NHE. Adapted with permission from ref. 470. Copyright 2013 National Academy of Sciences.

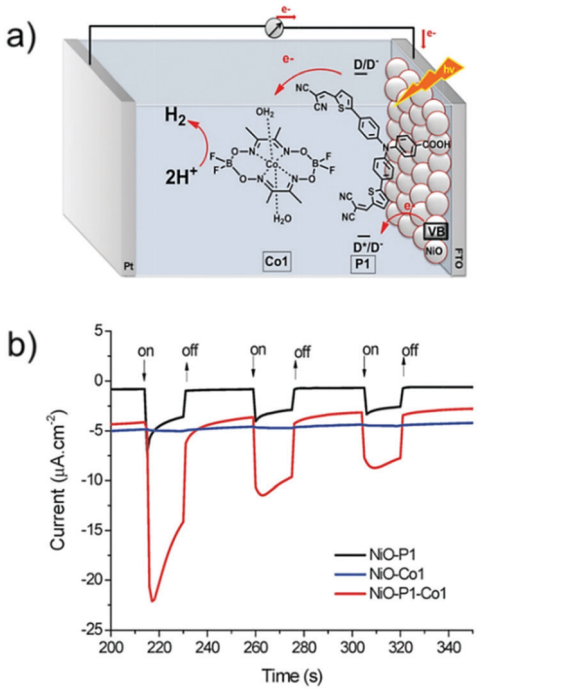

Fig. 24 (a) Depiction of PEC devices consisting of a photocathode based on an organic dye sensitized nanostructured NiO film coated with cobaltoxime HEC. (b) The photoelectrochemical performance. Adapted with permission of The Royal Society of Chemistry.

consisting of a molecular catalyst and organic dye (Fig. 24).[490] As the first attempt, they chose the simplest loading method, drop casting, to immobilize the cobaltoxime catalyst onto the photocathode. A photocurrent density of 15 μA cm^{-2} was achieved for H_2 evolution. This is the first noble-metal-free DSPEC cell that can produce hydrogen from water driven by sunlight.

Several strategies as shown above for fabricating molecular-catalyst-modified dye-sensitized photoanodes, including chromophore catalyst self-assembled co-adsorption,[491–494] adsorption of chromophore-catalyst assembly[495–497] and self-assembly of a system *via* Zr "chemical glue",[498,499] have been duplicated for the development of molecular-catalyst-modified dye-sensitized photocathodes. For example, Ott, Hammarström and their co-workers researched the light-driven electron transfer dynamics of a photocathode with the co-adsorption of a Coumarin-343 sensitizer and iron-dithiolate HECs (Fig. 25a).[491,494,500,501] By coordinating a cobaltoxime catalyst to the Ru^{II} dye molecule with a free pyridyl ligand already on a NiO electrode, Wu and co-workers obtained a chromophore-catalyst assembly-immobilized photocathode (Fig. 25b). One important benefit of this approach is that it does not require a readily synthesized chromophore-catalyst assembly.[496]

In very recent years, two covalently linked organic dye–cobaltoxime catalyst assemblies were separately reported by the Artero group[497] and Tian group (Fig. 25c).[495] Tian and co-workers deeply investigated the mechanism of their system to facilitate the better design and further promotion of more efficient organic dye–molecular catalyst assemblies. During the preparation of this review, Artero and co-workers reported insights into the mechanism and aging of a photocathode with the co-adsorption of an organic push–pull dye and a cobaltoxime catalyst.[493] They suggested decomposition pathways of the dye and a triazole linkage to immobilize the catalyst onto NiO, providing grounds for the development of more advanced molecular DS-PEC components. Instead of NiO, Reisner and co-workers recently employed a p-type semiconductor $CuCrO_2$ as a novel hole-collector substrate for fabricating a DSPEC cell upon the co-adsorption of a phosphonated diketopyrrolopyrrole dye with a Ni-bis(diphosphine) catalyst (Fig. 26a).[492] This work demonstrated the importance of developing new delafossite structures as p-type semiconductors for the production of solar fuels.

As the development of photocathode-based DSPEC cells is a relatively recent research area, in most of the above reported cases, the photocurrent densities were of the order of tens of microamperes per square centimeter. Nevertheless, the strategies aimed at building a device and the subsequent revealed mechanisms are promising for the future development of more efficient DSPEC cells. Recent work from the Wu group shows promise. Using an organic push-double-pull dye BH4-sensitized NiO photocathode and a $[Mo_3S_4]^{4+}$ cluster as a catalyst in an electrolyte solution (Fig. 26b), they achieved a proton-reducing photocurrent of approximately 183 μA cm^{-2} (0 V *vs.* NHE with 300 W Xe lamp) for an unprecedented 16 h without degradation.[502] Further improvement in the

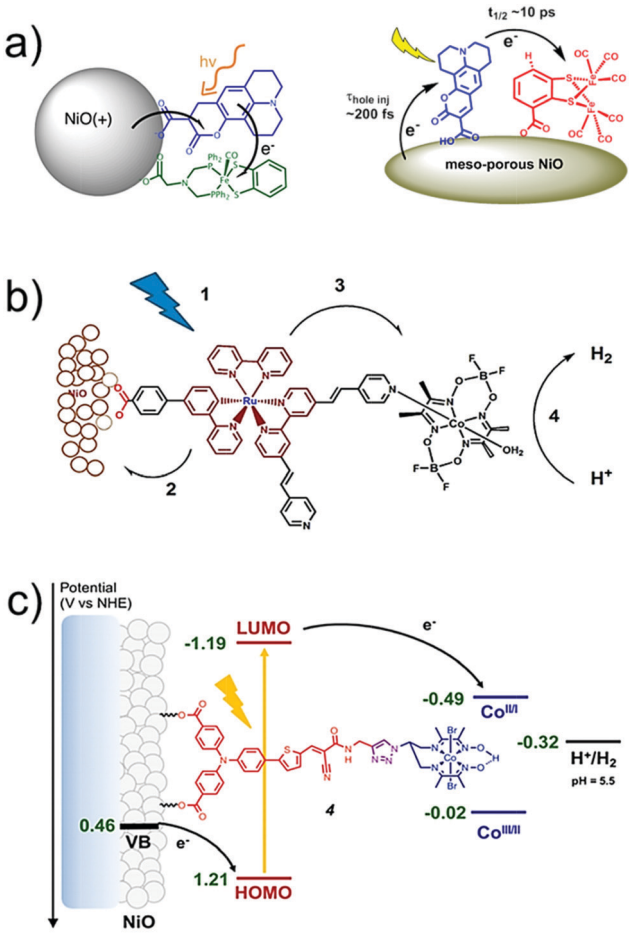

Fig. 25 Schematic representation of (a) the sequence of photoinduced electron transfer processes leading to iron catalyst reduction in coumarin dye and an iron catalyst co-sensitized NiO photocathode. (b) Ru^{II} dye cobaltoxime catalyst assembly-immobilized photocathode. Adapted with permission from ref. 496. Copyright 2013 American Chemical Society. (c) Organic dye cobaltoxime catalyst assembly-immobilized photocathode. Adapted with permission from ref. 497. Copyright 2016 American Chemical Society.

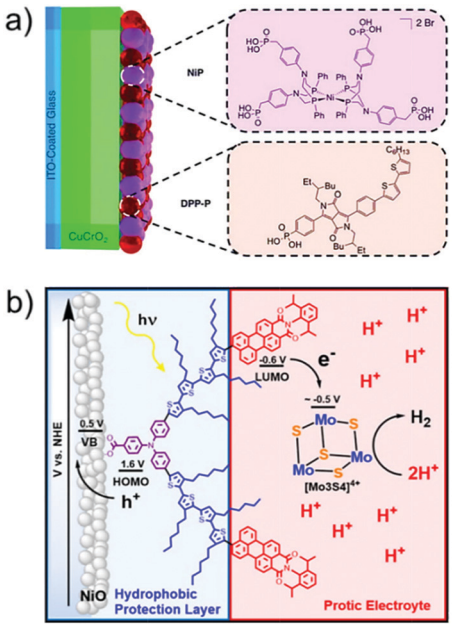

Fig. 26 Schematic representation of H_2-evolving photocathodes (a) co-immobilized by an organic dye (DPP-P) and Ni-bis(diphosphine) HEC on the $CuCrO_2$ electrode. Reproduced from ref. 492 with permission from The Royal Society of Chemistry. (b) Modified by a membrane mimicking organic dye working in an electrolyte solution with $[Mo_3S_4]^{4+}$ HEC. Reprinted with permission from ref. 502. Copyright 2016 American Chemical Society.

catalytic photocurrent is expected if the catalyst is modified on the electrode, as it will facilitate electron transfer between the dye and catalyst and also increase the local concentration of catalysts.

Encouraged by the development of DSPEC cells for water splitting, CO_2RC molecular-catalyst-modified DSPEC cells have also been reported in recent years. The first example of a DSPEC cell for the reduction of CO_2 was reported by Inoue and co-workers with a photocathode immobilized by a chromophore-catalyst assembly of a zinc porphyrin photosensitizer and a bipyridyl rhenium catalyst (Fig. 27a).[504] Due to the fast intramolecular electron transfer from zinc porphyrin to the rhenium catalyst, the hole-injection efficiency of this system was as high as 98.2%. A catalytic photocurrent of 20 μA was obtained with a low Faradaic efficiency of 6.2% for CO_2 reduction to CO, and the TON was determined to be 10. Decomposition of the sensitizer part is one reason for the moderate performance, as a TON of 122 was achieved when more separate zinc porphyrin was adsorbed onto the photocathode. This was further proved by a subsequent work from the group of Ishitani *et al.* The authors synthesized a Ru photosensitizer–Re catalyst assembly to sensitize a NiO film to form a photocathode for light-driven CO_2 reduction (Fig. 27b). With a bias potential of −1.25 V *vs.* $Ag/AgNO_3$ under light ($\lambda > 460$) illumination, a TON of 32 and a Faradaic efficiency of 71% were achieved for the reduction of CO_2 into CO by this DSPEC cell.[503] Furthermore, they reported a new hybrid photocathode, a Ru(II)–Re(I) supramolecular photocatalyst-modified $CuGaO_2$ p-type semiconductor (RuRe/$CuGaO_2$), instead of the NiO. By the RuRe/$CuGaO_2$ hybrid photocathode, a 400 mV more positive onset potential was achieved for the conversion of CO_2 to CO in an aqueous electrolyte solution.[505]

5.1.3 Molecular catalyst modified DSPEC tandem cells. The success of developing molecular-catalyst-modified DSPEC cells, with a single photoelectrode, photoanode, or photocathode, facilitates the engineering of tandem full DSPEC cells. A tandem full DSPEC cell improves the absorption of sunlight, increases the driven force of the whole device, and eliminates the usage of the Pt-based counter electrode. With a TiO_2/RuP/RuOEC photoanode and a NiO/RuP/CoHEC photocathode, the Sun group reported the first fully molecular tandem DSPEC cell (Fig. 28a).[507] For the DSPEC cell with a single photoanode of TiO_2/RuP/RuOEC, a photocurrent density of ~100 μA cm^{-2} was obtained with 0 V bias *vs.* Ag/AgCl. On the other hand, photocurrent achieved by the NiO/RuP/CoHEC–Pt cell under the bias of −0.4 V *vs.* Ag/AgCl was 13 μA cm^{-2}. After coupling them together, the average photocurrent density of the tandem DSPEC cell can achieve ~40 μA cm^{-2}, which is between the

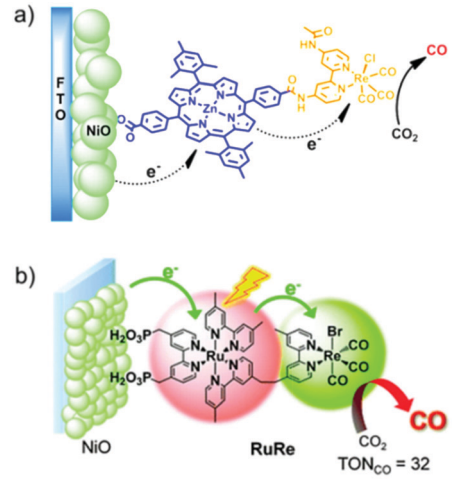

Fig. 27 Schematic representation of CO_2-reduction photocathodes (a) immobilized by a chromophore-catalyst assembly of a zinc porphyrin photosensitizer and Re-bpy CO_2RC; (b) modified with a Ru photosensitizer–Re catalyst assembly. Reproduced from ref. 503 with permission from The Royal Society of Chemistry.

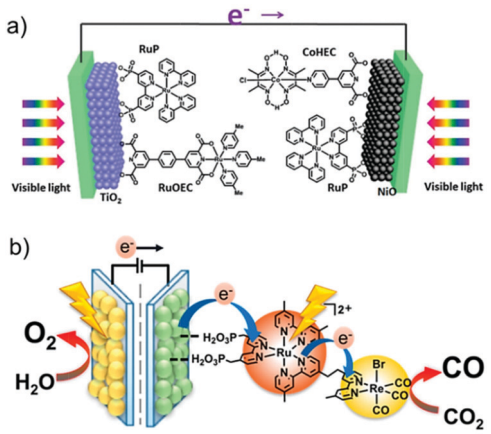

Fig. 28 Schematic representation of (a) a tandem DSPEC cell for water splitting based on molecular-WOC-modified TiO_2 as the photoanode and molecular-HEC-modified NiO as the photocathode. Reproduced by permission of The Royal Society of Chemistry. (b) A hybrid photoelectrochemical cell with TaON as the photoanode and chromophore-catalyst-assembly-sensitized NiO as the photocathode. Adapted with permission from ref. 506. Copyright 2018 American Chemical Society.

above two values obtained by the DSPEC cell with the single photoelectrode. These results imply two important points: the performance of the tandem PEC cell is dramatically limited by the low efficiency of the photocathode (40 μA cm^{-2} < 100 μA cm^{-2}) and the designed PEC system based on both photoanode and photocathode is effective with significant potential to develop more efficient devices (40 μA cm^{-2} > 13 μA cm^{-2}). Subsequently, the Sun group developed the second fully molecular tandem DSPEC cell by using two pure organic photosensitizers instead of the above-mentioned Ru photosensitizer to demonstrate the benefits and future of pure organic photosensitizers for DSPEC cells.[19,508] Ishitani and co-workers coupled their Ru photosensitizer–Re catalyst-assembly-modified NiO photocathode with a CoO_x/TaON photoanode to form a tandem cell for the production of CO from reducing CO_2 by using H_2O as an electron source (Fig. 28b).[506,509]

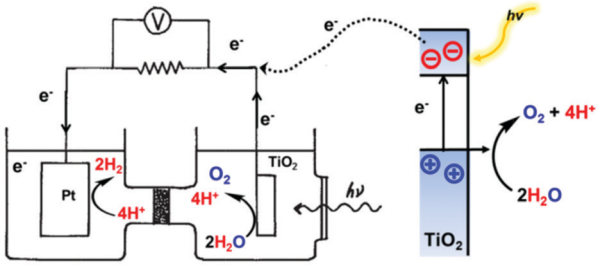

Fig. 29 Simple PEC cell reported by Fujishima and Honda in 1972 and the working mechanism. Adapted with permission from ref. 510. Copyright 1972 Nature publications.

5.2 PEC cells with molecular catalyst modified VLA-SC photoelectrodes

In the DSPEC cells, dyes are used to absorb light to generate charge separation, and transparent semiconductors, such as TiO_2 and NiO, are used to transport charge. Indeed, the earliest PEC cell was reported with a TiO_2 film under UV light in the 1972 paper of Fujishima and Honda (Fig. 29).[510] In contrast to the dye sensitized TiO_2 film working under visible light, the PEC cell with a bare TiO_2 film under UV-light illumination works according to a different mechanism. UV light is absorbed by TiO_2, and it consequently generates charge separation in the energy band of TiO_2. The electrons flow *via* the conduction band to the counter electrode for reduction reactions, and the holes diffuse to the TiO_2 film surface to oxidize water (Fig. 29).

However, bare TiO_2 cannot be used to produce an applicable PEC cell because a large band gap of 3.1 eV makes it unable to absorb visible light, which accounts for over 95% irradiation of the solar spectrum. In contrast, visible-light-absorbing semiconductors (VLA-SCs) with narrow band gaps and a suitable energy band for driving the reactions involved in AP can be directly employed to build PEC cells without the sensitization of dyes.[26] For example, a PEC cell with a p-GaAs–n-GaAs–p-$GaInP_2$ multijunction photoelectrode was reported in 1998 by Turner and co-workers for hydrogen evolution.[511] Under visible-light illumination, electrons flow toward the illuminated surface and holes flow toward the ohmic contact. The hydrogen production efficiency of this system is 12.4%.

In recent years, n-type VLA-SCs, *e.g.*, Fe_2O_3, WO_3, and $BiVO_4$, have been extensively studied as a photoanode for photoelectrochemical water oxidation, and p-type VLA-SCs, such as p-Si, InP, GaP, and InGaP, have been employed as a photocathode for proton and CO_2 reductions (Fig. 30).[34,512] Three basic properties of a VLA-SC for efficient photosynthesis are good light absorption ability, high efficiency of charge separation and migration, and a powerful energy band to drive the photosynthetic reaction, which can be dominated by adjusting the band gap and by tuning its physical features, such as crystal structure, crystallinity, and particle size.

However, for a bare VLA-SC, even if it possesses the above-mentioned basic properties, in most cases, it may show a very

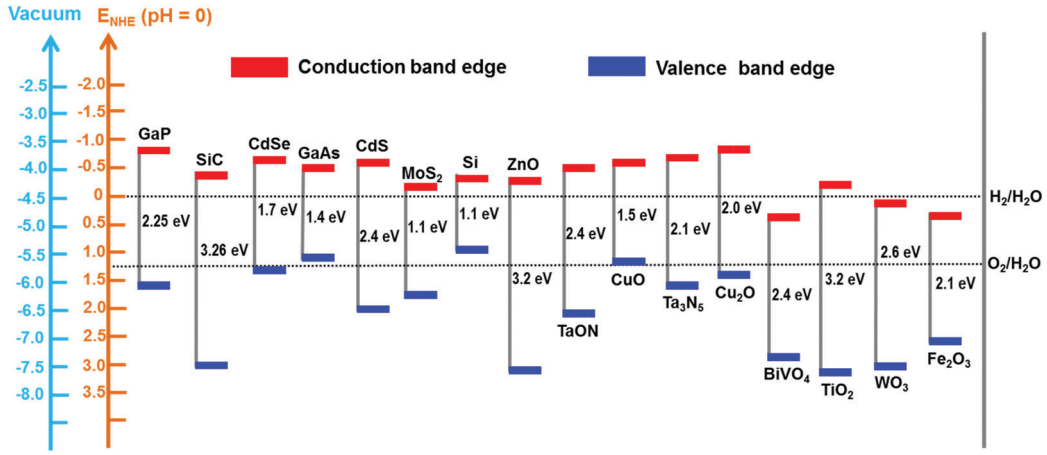

Fig. 30 Band gaps and band positions for common semiconductors.

low catalytic photocurrent because of the recombination of a vast majority of photo-generated electrons and holes on the surface before being used to drive reactions, which are uphill reactions with a slow reaction rate (Fig. 31a). Therefore, cocatalysts modified on the surface of the semiconductors to accelerate the reaction rates are considered to be the other essential components to fabricate efficient VLA-SC-based PEC cells.[513,514] The use of a molecular catalyst is one of the best approaches for the modification of photoelectrodes (Fig. 31b). With high TOFs, molecular catalysts can effectively restrain the combination of electrons and holes on the surface of photoelectrodes. The modification by molecular catalysts is homogeneous and at a molecular level, thereby facilitating direct transfer of charge to every catalytic site. In general, the cover of a molecular layer will not affect the light absorption of the semiconductor and the mass transfer.

The earliest example of molecular-catalyst-based VLA-SC hybrid devices was reported by Mueller-Westerhoff in 1984. Proton reduction catalyst 1-methyl-[1.1]ferrocenophane was immobilized onto a p-Si photocathode *via* the formation of a co-polymer film with poly(chloromethyl)styrene.[515] By this hybrid device, a photocurrent density of 194 mA cm^{-2} was achieved at $-0.54V_{SCE}$ in the HBF_3OH electrolyte under 870 mW cm^{-2}. Moreover, it maintained high performance for 5 days. However, the continuous reports of molecular-catalyst-based VLA-SC hybrid devices did not appear until the 2010s. Development of molecular-catalyst-based VLA-SC hybrid devices for artificial photosynthesis has attracted considerable research attention since the last 5 years.[26]

5.2.1 PEC cells with molecular-catalyst-modified VLA-SC photoanodes. The pioneer molecular catalysts on VLA-SC hybrid photoanodes were separately reported by the group of Zhuang and the group of Fujita in 2013.[516,517] Ru(tpy)(bpy)(Cl) WOC with a carboxylic anchoring group was immobilized on α-Fe_2O_3 by Zhuang *et al.*,[517] and two isomers of Ru(tpy)(pynap)(Cl) (pynap = 2-(pyrid-2′-yl)-1,8-naphthyridine) with a phosphate group were modified on WO_3 by Fujita *et al.*[516] Obvious cathodic shifts of the onset potential for water oxidation and increasing catalytic photocurrent were achieved for both hybrid photoanodes.

VLA-SC hybrid photoanodes modified by two pioneer noble-metal-free molecular catalysts were developed by the Bartlett group and the Sun group in 2014.[235,518] Bartlett and co-workers synthesized non-heme-iron WOC Fe(mcp)$(Cl)_2$ with two phosphate groups to modify the WO_3 electrode (Fig. 32a).[518] After modification of the iron catalyst, the catalytic photocurrent density of WO_3 under 100 mW cm^{-2} illumination increased from 0.7 mA cm^{-2} to 1.3 mA cm^{-2}. The combination of non-heme-iron WOC and WO_3 photoanode was further studied by the Reisner group.[519] The Sun group for the first time modified VLA-SCs α-Fe_2O_3 with the OEC mimic "Co_4O_4 cubane" catalyst (Fig. 32b).[235] Under the same conditions, α-Fe_2O_3 with the modification of the "Co_4O_4 cubane" catalyst exhibited a transient photocurrent that was eight times higher than that of the control α-Fe_2O_3 electrode, indicating that "Co_4O_4 cubane" is effective at accelerating the water-oxidation rate on the surface of the VLA-SC. On the basis of this work, "Co_4O_4 cubane" was employed as cocatalysts on other VLA-SCs, such as $BiVO_4$[237,238] and Ta_3N_5.[520] A stable photocurrent density of 5 mA cm^{-2} was obtained by the "Co_4O_4 cubane" modified $BiVO_4$ photoanode at 1.23 V_{RHE} in a pH 9.3 solution.[238] Ta_3N_5 integrated with hole storage layers of $Ni(OH)_x$/ferrihydrite and a layer of "Co_4O_4 cubane" and Ir-based catalysts displayed a high photocurrent density of 12.1 mA cm^{-2} at 1.23 V_{RHE} under 100 mW cm^{-2} illumination.[520]

The effect of modification of molecular catalysts on VLA-SCs has been further proved by more examples in recent years, including α-Fe_2O_3 modified with a Ru-pdc complex,[521] binuclear Ir complex,[183,522–524] and Co-phthalocyanines,[525] and $BiVO_4$ modified with Co-porphyrin,[526] Co-salophen[527] and Cu-porphyrin.[528]

5.2.2 PEC cells with molecular-catalyst-modified VLA-SC photocathodes. Following the work in 1984, Nann, Pickett and their co-workers developed the second molecular-catalyst-based VLA-SC hybrid device, a hybrid p-type InP photocathode with the modification of a Fe_2S_2 catalyst. However, this device showed a very low catalytic current.[27] The modification of open cubane-like Mo_3S_4 clusters on the p-Si photocathode results in a high photocurrent density of 8 mA cm^{-2} at 0 V_{RHE} and an anodic shift of 550 mV in the onset potential ($\lambda > 620$ nm, 28.3 mW cm^{-2}).[529]

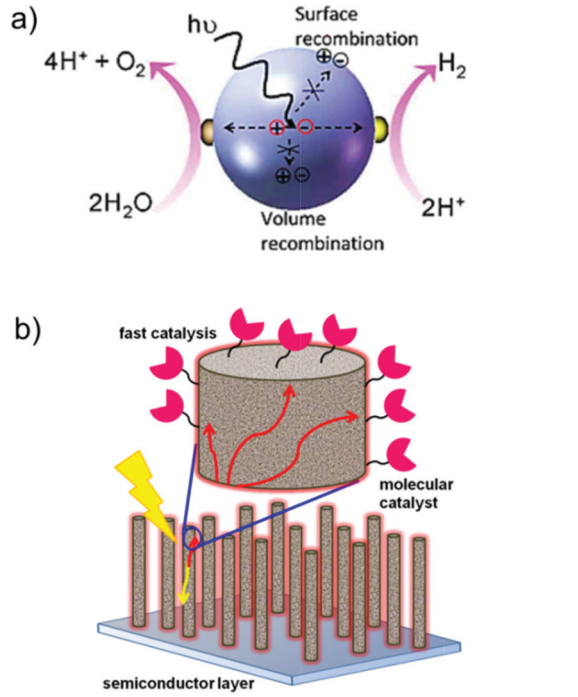

Fig. 31 Schematic representation of (a) catalytic reactions on the surface of VLA-SCs and pathway of charge recombination. Reprinted with permission from ref. 513. Copyright 2013 American Chemical Society. (b) Molecular-catalyst-modified semiconductor.

According to the loading amount of the Mo_3S_4 clusters, TOF of hydrogen evolution at the reversible potential increased to 960 s^{-1}. For the hybrid photocathode with a pillar Si substrate, a photocurrent density of 30 mA cm^{-2} was reached at 0 V_{RHE} ($\lambda > 620$ nm, 85.8 mW cm^{-2}). The performance of the Mo_3S_4-cluster-modified p-Si photocathode was dramatically enhanced by introducing a 100 nm protective coating of TiO_2 to the p-Si photocathode and using a covalent grafting method to immobilize Mo_3S_4 clusters as the surface HER catalyst.[530] The Reisner group has also developed several p-Si photocathodes with the modification of Ni-based HECs.[531–533] It is worth mentioning that one of those p-Si photocathodes is integrated with the [NiFeSe]-hydrogenase to form an enzyme–material hybrid device,[533] which is also known as a semi-artificial photosynthetic system.[534,535] In addition to pure artificial photosynthesis, it can overcome the limitations of natural and artificial photosynthesis.[534] Several successful examples of semi-artificial devices have been reported recently, especially studies by the Reisner group.[536–541]

The group of Moore reported a family of cobaltoxime/GaP hybrid photocathodes by coordinating cobaltoxime to the pyridyl or imidazolyl groups in the polymer coated on the GaP electrode (Fig. 33a). This is a simple but effective method to modify an electrode with a large amount of the molecular catalyst.[542–546] At the same time, the polymer coating can also be a protective layer for the VLA-SC film. The photocurrent density of this series of hybrid photocathodes for hydrogen evolution is around 1–2 mA cm^{-2}. For the example shown in Fig. 33b, the photocathode displayed a photocurrent density of 2.4 mA cm^{-2} at 0.31 V in 1 M phosphate buffer solution under 100 mW cm^{-2} illumination.[542] Comparable photocatalytic performance has also been achieved for the GaP electrode modified with metalloporphyrins by a UV-induced covalent grafting

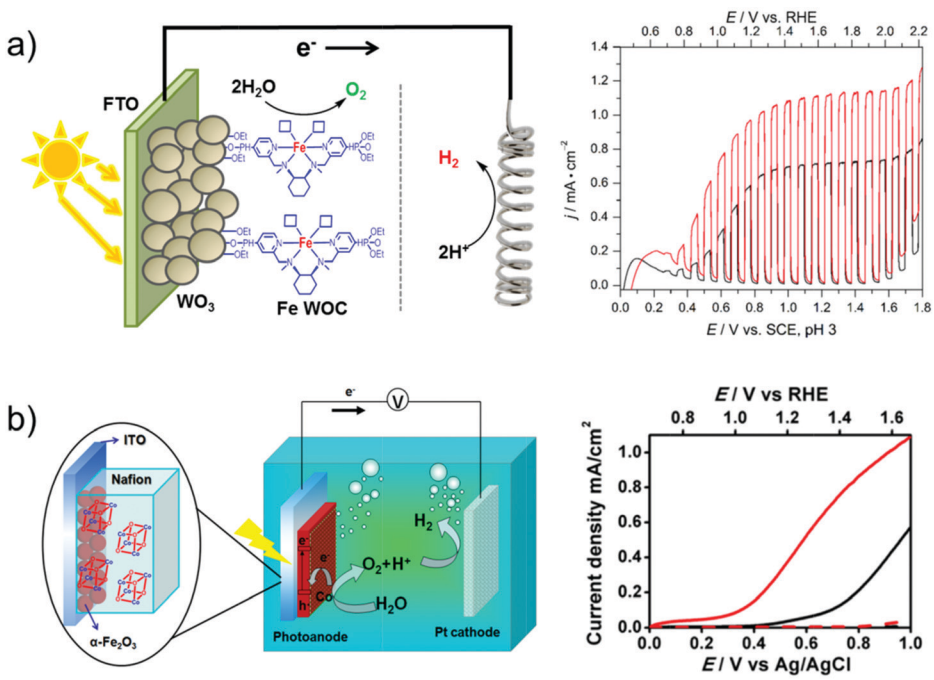

Fig. 32 Schematic representation and performances of PEC cells based on molecular-WOC-modified n-type VLA-SC photoanodes. (a) Fe-mcp-WOC-modified WO_3 photoanode. Adapted with permission from ref. 518. Copyright 2014 American Chemical Society. (b) "Co_4O_4 cubane"-WOC-immobilized α-Fe_2O_3 photoanode. Adapted with permission from ref. 235. Copyright 2014 American Chemical Society.

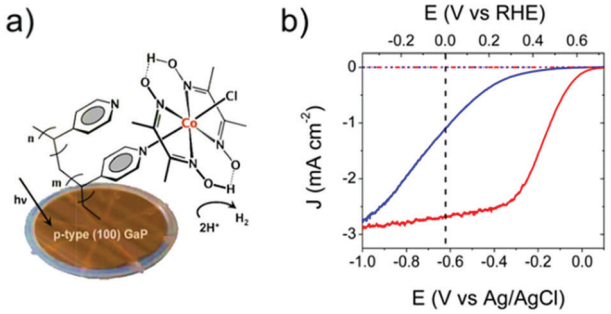

Fig. 33 (a) Schematic representation and (b) linear sweep voltammograms (LSVs) of a cobaltoxime-modified GaP photocathode for H_2 evolution. Adapted with permission from ref. 542. Copyright 2013 American Chemical Society.

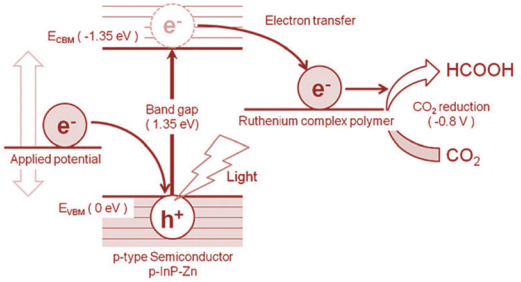

Fig. 35 Schematic energy diagram of the RCP/p-InP-Zn photocathode producing HCOOH under visible-light irradiation. Reproduced from ref. 553 with permission from The Royal Society of Chemistry.

approach.[547] Obviously, the modification of molecular HER catalysts on p-semiconductors can dramatically increase the photocatalytic current density and positively shift the onset potential for hydrogen evolution.

A breakthrough in this field was made by Turner and co-workers. The authors prepared a highly efficient p-$GaInP_2$ photocathode protected by a 35-nm TiO_2 layer immobilized with a cobaltoxime molecular catalyst ($GaInP_2$–TiO_2–cobaltoxime) (Fig. 34).[548] Atomic layer-deposited TiO_2 on top of the cobaltoxime catalyst layer makes the final $GaInP_2$–TiO_2–cobaltoxime–TiO_2 electrode corrosion resistant in a basic solution. In 0.1 M NaOH solution, the $GaInP_2$–TiO_2–cobaltoxime–TiO_2 electrode under 1 sun light illumination showed a photocurrent density of 11 mA cm^{-2} at 0 V_{RHE} and an onset potential at 0.75 V_{RHE}. Moreover, a TON of 1.39 $\times$ 10^5 was attained after 16 h of photoelectrolysis. The performance of the $GaInP_2$–TiO_2–cobaltoxime–TiO_2 electrode is comparable with that of Pt-modified $GaInP_2$. The most active and robust molecular catalysts for HER, Ni-based "DuBois catalysts", have also been investigated as a cocatalyst on the surface of VLA-SCs for photoelectrochemical hydrogen evolution.[549–552]

The modification of the CO_2 reduction catalyst enables p-type semiconductors to perform the photochemical reduction of CO_2 to form chemical fuels. Sato and co-workers reported the first example of molecular-catalyst-modified VLA-SC-based photocathodes with Zn-doped p-InP as a light absorber immobilized by a ruthenium complex polymer (RuCP) as a CO_2 reduction catalyst (Fig. 35).[553] CO_2 was successfully reduced into $HCOO^-$ by this device. This RuCP/p-InP photocathode was further investigated by Arai and co-workers for CO_2 reduction.[554–556]

5.2.3 Molecular-catalyst-modified VLA-SC based PEC tandem cells. Due to the high thermodynamic and kinetic barriers for the reactions in AP, a device based on a single semiconductor has not been found to reach high solar-to-fuel (STH) conversion efficiency. To finally overcome this limit, it is necessary to develop PEC tandem cells with both n-type VLA-SCs as a photoanode and p-type VLA-SCs as a photocathode. Several different designs have been realized to make VLA-SC based PEC tandem cells.[17]

The n-type VLA-SC photoanode and the p-type VLA-SC photocathode can be coupled by a wire. As the example shown in Fig. 36a, a $BiVO_4$/Cu_2O photoanode/photocathode tandem cell was reported for overall unassisted solar water splitting.[557] Another strategy is to fabricate a multijunction photoelectrode. The multijunction photoelectrode can be coupled with the counter electrode by a wire (Fig. 36b) or integrated with the counter electrode into a chip to form a monolithic PEC device (Fig. 36c). These spontaneous PEC devices have attracted attention since 1970s.[17] Efficiencies of a number of devices are high over 10%, and the highest reported efficiency is 18%.[511,559–562] However, the catalysts used in these devices still depended on precious-metal-based inorganic materials, which are rare and not atom-economic. One promising approach to change this situation is to employ molecular catalysts.

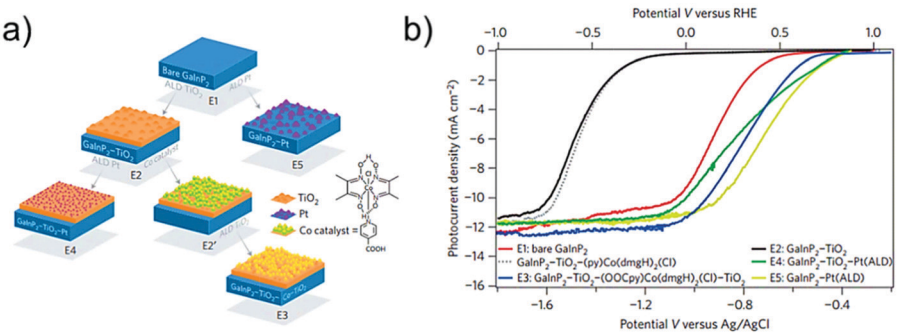

Fig. 34 (a) Schematic representation of surface modification for the p-$GaInP_2$ photoelectrodes; (b) LSVs of the cobaltoxime-modified p-$GaInP_2$ photoelectrodes and the control photoelectrodes. Adapted with permission from ref. 548. Copyright 2016 Nature publications.

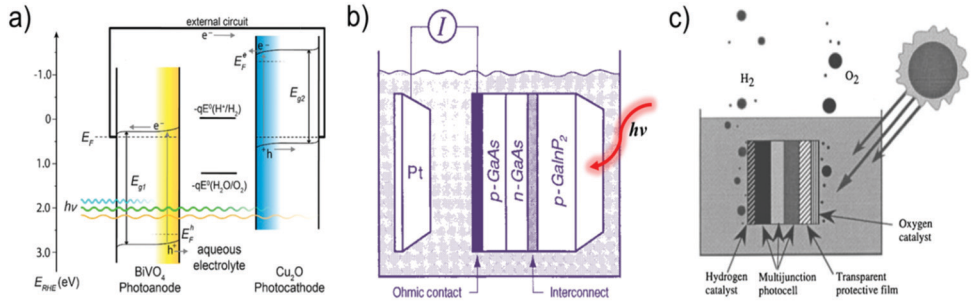

Fig. 36 Schematic representation of (a) PEC tandem cells based on wire-linked n-type VLA-SC photoanode and p-type VLA-SC photocathode. Reprinted with permission from ref. 557. Copyright 2014 American Chemical Society. (b) PEC cell with a p-GaAs–n-GaAs–p-$GaInP_2$ multijunction photoelectrode coupled with the counter electrode by a wire. Adapted with permission from ref. 511. Copyright 1998 American Association for the Advancement of Science (AAAS). (c) Monolithic PEC device integrated with a multijunction of different VLA-SCs and counter electrode for water splitting. Adapted with permission from ref. 558. Copyright 1998 American Chemical Society.

So far VLA-SC based PEC tandem cells modified by a molecular catalyst have rarely been reported. By coupling the RuCP/p-InP photocathode with a reduced $SrTiO_3$ (r-STO) photoanode, Arai and co-workers reported a full device for solar formate production from CO_2 and H_2O with no external electrical bias (Fig. 37).[554] A stable photocurrent of 140 μA cm^{-2} was achieved during 3 h of illumination for the r-STO//p-InP/RuCP system, which was seven times higher than that of the previous TiO_2(P25)//p-InP/RuCP system.[556] The conversion efficiency from solar to chemical energy was increased from 0.03% to 0.14%. A monolithic PEC device has also been fabricated with this r-STO//p-InP/RuCP system.

The same group further improved the solar-to-chemical-energy conversion efficiency to 4.6% by engineering a monolithic

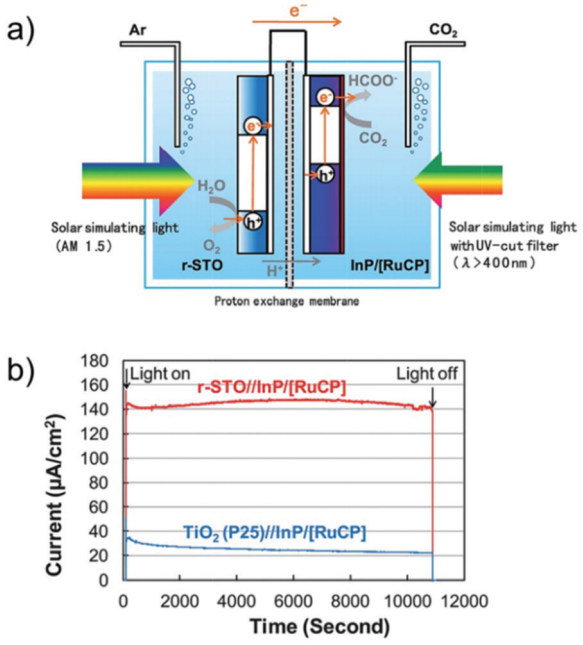

Fig. 37 (a) Schematic representation and (b) long-term photocurrent of the PEC tandem cells for reduction of CO_2 integrated with a reduced $SrTiO_3$ photoanode and a RuCP molecular CO_2RC decorated InP photocathode. Reproduced from ref. 554 with permission from The Royal Society of Chemistry.

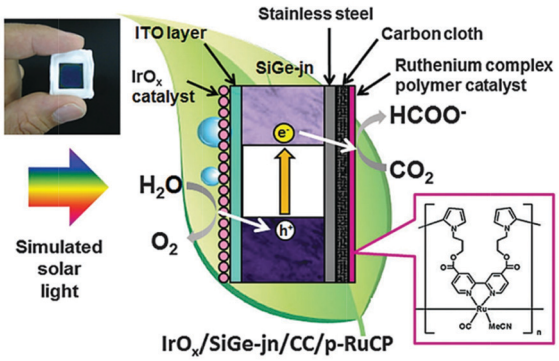

Fig. 38 Schematic representation of the IrO_x/SiGe-jn/CC/p-RuCP monolithic one-chip device for CO_2 photoreduction developed by Arai and co-workers. Reproduced from ref. 555 with permission from The Royal Society of Chemistry.

tablet-shaped device (IrO_x/SiGe-jn/CC/p-RuCP), which is composed of a porous RuCP as a CO_2 reduction catalyst, IrO_x as a WOC, and a triple-junction of amorphous silicon–germanium (Fig. 38).[555] In this efficient device, the first key technology is the selective CO_2 photoreduction in aqueous media, which was realized by the employment of the molecular CO_2 reduction catalyst. Therefore, the semiconductor–molecular catalyst hybrid system is a promising approach for the AP.

5.3 Application of molecular catalysts in PVE devices – a promising strategy

As an alternative of the PEC cell, the PVE device shown in Fig. 2 has become attractive in the past 5 years. Indeed, as the most direct and "brute force" approach, hydrogen production from water electrolysis driven by solar cells was proposed decades ago.[563] It consists of separated traditional photovoltaic solar cells wired to an electrolyzer for water splitting or water-oxidation-coupled CO_2 reduction. The separation of the light absorber part from an electrolyte offers several advantages: (1) two components, *i.e.*, solar cell and electrolyzer, can be investigated and developed separately; (2) light absorber can be protected from the damage of the electrochemical process.

In the past seven years, the prices of crystalline silicon (c-Si) solar cells and PV modules have dramatically decreased by 86% and 77%, respectively. In the meantime, average efficiencies of commercial c-Si solar cells have been improved to 17.5% for multicrystalline silicon and 19.5% for monocrystalline silicon.[564,565] Moreover, new generations of solar cells have been extensively developed, particularly perovskite solar cells with a simple preparation process, low-cost, and high laboratorial efficiency over 22%.[42,566]

On the other hand, there are commercially available technologies to produce hydrogen through water electrolysis on a large scale. Before the realization of hydrogen production *via* coal gasification and natural gas steam reforming in the 1950s, hydrogen was mainly produced by water electrolysis.[568] Two main commercial water-electrolysis technologies are the alkaline water electrolysis and proton exchange membrane (PEM) water electrolysis, as shown in Fig. 39a and b. Since the discovery of the electrolysis phenomenon by Troostwijk and Diemann in 1789,[569,570] alkaline electrolysis has become a matured technology for the production of H_2 up to the megawatt scale.[567] The most obvious advantage of alkaline water electrolysis is that both the anode and the cathode are noble-metal free materials, the anode is based on Ni–Co–Fe and the cathode is based on Ni–C. This is one of the important reasons that alkaline water electrolysis has been utilized on a commercial level worldwide for many years. However, for over a century, the employment of a strong alkaline electrolyte (30% KOH) and a low maximum achievable current density (0.2–0.4 A cm^{-2}) are the two major issues occurring in alkaline water electrolysis. To overcome these problems, PEM water electrolysis has been developed since the 1960s.[567] A typical PEM device requires only pure water as the reactant, and it is capable of obtaining a considerably higher current density (0.6–2 A cm^{-2}). In addition, the PEM device has a compact system design, which is suitable for domestic application. Like the commercialized PEC water electrolyzer displayed in Fig. 39c (size of the inside electrode is 10 cm diameter), it can produce H_2 at a rate of 18 L h^{-1}. PEM water electrolysis is an advanced and promising technology that can be combined with solar cells for practical application of AP. However, the broad application of PEM technology for water electrolysis is limited by its high cost arising from the usage of valuable materials. One of the major issues for this high cost is that only noble metal-based catalysts, such as RuO_2, IrO_2, and black Pt, can work well in the PEM cells because of their locally strong acidic corrosive environment. The development of efficient and stable catalysts that can function under acidic conditions is urgently required for PEM water electrolysis.

The development of applicable PVE devices for H_2 production from H_2O based on the available technologies is the best approach. To date, PVE devices, compared with the PEC cells, have been considered to be closer to their practical application. However, concerning the high cost and the huge demand, the replacement of noble-metal-based catalysts must be addressed. Molecular chemistry provides good opportunities for developing alternative cost-effective materials, sufficiently stable in strong acidic media. In this context, as discussed previously, the first challenge is to develop a low-cost and efficient molecular catalyst. The second challenge is to explore suitable electronic carriers for catalyst loading. The third challenge is to develop strategies for stable coating of molecular catalysts on the carrier (Fig. 40).

Many strategies have been developed to modify molecular catalysts on various conductive substrates in order to investigate their electrocatalytic properties. A direct and simple approach to place molecular catalysts onto the surface of solid electrodes is entrapping the catalysts within a film generated from polymeric materials, such as polyvinyl, hydrophilic polystyrene derivatives and Nafion™ (Fig. 39a).[222,235,361,571] This method is suitable for preliminary evaluation of electrocatalytic properties; however, it is not promising for the applicable design because of its obvious drawbacks, such as catalyst leaking and limited mass and charge transfer. Based on the many examples of PEC devices,[20,25] molecular catalysts can be immobilized on the surface of metal oxides, *e.g.*, TiO_2 and SnO_2, *via* acid groups such as carboxylic, phosphate and silicate groups (Fig. 39b).[78,457,572,573] The drawbacks of this methodology for catalyst immobilization are low loading amount and instability in aqueous media. A molecular catalyst functionalized with sulfur groups can be easily grafted on an Au electrode (Fig. 39c),[574,575]

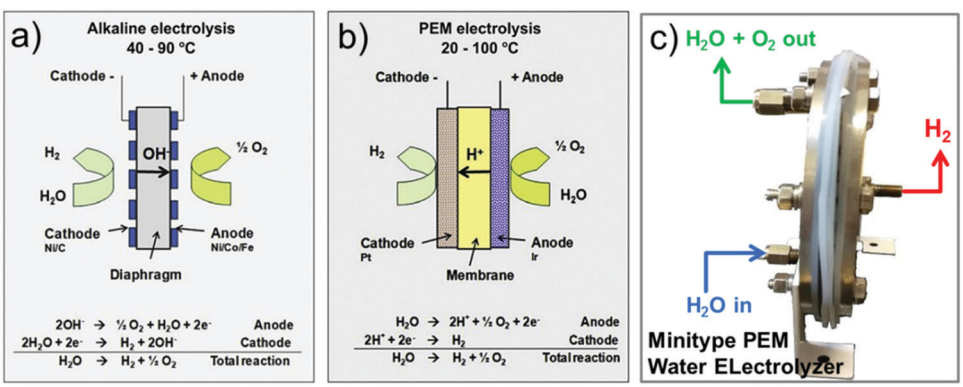

Fig. 39 Schematic representation of the operating principle of (a) an alkaline and (b) PEM water electrolysis cell. Reprinted with permission from ref. 567. Copyright 2013 Elsevier. (c) Photograph of a commercialized mini-type PEM electrolyzer for H_2 production.

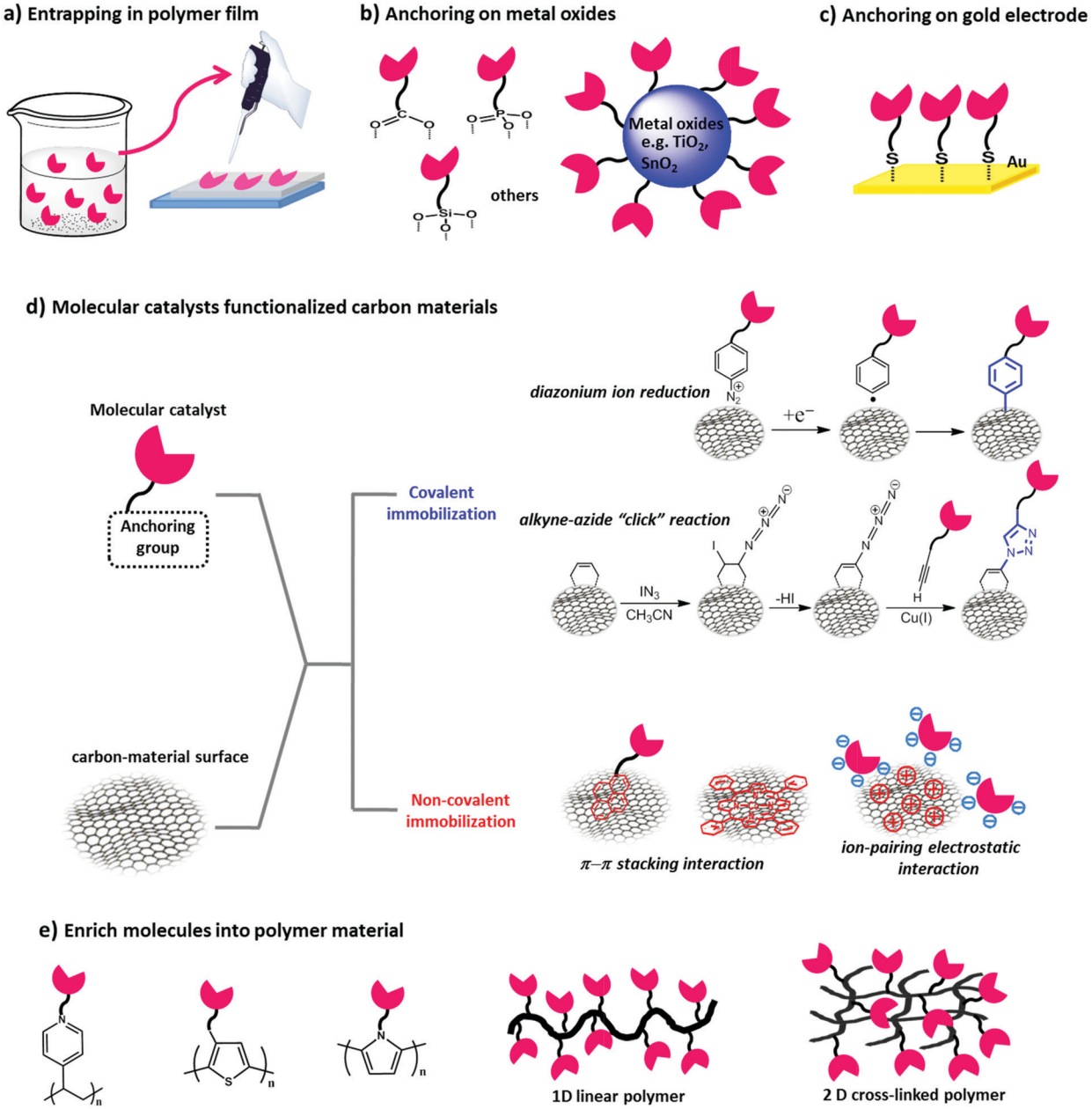

Fig. 40 Schematic representation of various strategies for heterogenizing molecular catalysts into materials.

which, like the glass carbon (GC) electrode, is a classic planar substrate electrode for investigating the monomolecular layer. There are several conventional strategies for the modification of the GC electrode *via* covalent attachment, *i.e.*, the "click" reaction route,[576,577] diazonium reduction route,[376,578–580] and methods designed by combining these two routes (Fig. 39d).[581,582] These covalent anchoring methods can also be employed to immobilize other advanced carbon materials, such as carbon nanotubes and graphene.[583–585] In addition, non-covalent immobilization of molecular catalysts on carbon nanotubes and graphene has also been realized by the introduction of pyrene substituents on target molecules to form π–π stacking interactions with the surface of carbon materials (Fig. 39d).[166,586–594] Because carbon nanotubes and graphene have good electro-oxidation stability, excellent charge transfer ability, high surface area and feasibility of modification, hybrid materials/electrodes made of carbon nanotube/graphene and molecular catalysts are promising to be employed by applicable devices for AP.

The strategy of involving the modification of a monomolecular layer on the porous carbon nanomaterial can provide sufficient exposure of active sites and increase the loading amount. However, in the view of application, the loading amount of the molecular catalyst should be further enhanced to a level higher than that of the monomolecular layer. The final solution is heterogenization of molecular catalysts into functional materials. Polymerization is an easy, tunable, and

effective route to enrich molecules into polymer materials, which can be conductive and processable. There are several reports on electrodes generated from polymerization of molecular catalysts.[482,595–598] For example, the Ru-bda WOC functionalized with a thiophene group is immobilized to the surface of electrodes by electropolymerization.[599] The polymer film of Ru-bda molecular WOC can electrochemically catalyze water oxidation under an overpotential of ~500 mV to reach a current density of 5 mA cm^{-2}. The first electropolymeric material incorporating the Fe–Fe hydrogenase mimic was reported by Pickett and co-workers although a high overpotential was required for this polymeric material; this work has taken several early steps toward a functional material containing a molecular catalyst.[595]

Metal–organic frameworks (MOFs) and covalent organic frameworks (COFs) are advanced materials formed by orderly accumulation of small-molecule units. The development of various structures of MOFs and COFs has attracted considerable attention in the material field, and significant improvement has been achieved on the design and synthesis of MOFs[601–603] and COFs.[604,605] MOFs and COFs have been widely investigated as catalysts because of their large porosities, uniform pore sizes, redox properties, diversified/tunable pore surfaces, and some other unique structural features.[606] Therefore, it is one of the promising approaches to heterogenize molecular catalysts into MOF or COF materials for AP.[164,435,600,607–613] As the examples shown in Fig. 41, MOFs and COFs generated from functionalized cobalt-porphyrins have been reported with a prominent performance of CO_2 electroreduction.[435,600] The latter displayed high Faradaic efficiency of 90% and TONs up to 2.9×10^5 (with initial TOF of 9400 h^{-1}) at pH 7 with an overpotential of −0.55 V with no degradation over 24 h, indicating the high potential of these structures.[435]

However, most polymers, MOFs and COFs have low stability and conductivity in aqueous solutions under electrochemical conditions.[601,614] In addition to promoting the intrinsic activity of molecular catalysts, the improvement of stability and electron conductivity of the materials heterogenized from molecular catalysts is another challenge to produce applicable AP devices based on molecular catalysts.

6. Underestimated power of molecular catalysts for AP

6.1 Intrinsic activity of molecular catalyst ≠ performance of AP device

The performance of an AP device is depended on many factors. However, an efficient catalyst is one of the most essential elements. This is also the reason why the development of catalysts with high intrinsic activity has become extensively attractive. A suitable system for the evaluation and comparison of a new catalyst is important for the development of the field. The most reliable parameter to judge a good catalyst is low overpotential, because the role of a catalyst in a certain reaction is to lower the activation energy, *i.e.*, facilitating the reaction under a lower overpotential. TONs and TOFs are also important direct parameters to evaluate a catalyst. However, TONs and TOFs are closely related to the testing systems and conditions, which need to be carefully considered when catalysts are compared based on TONs and TOFs.

Nevertheless, efficient catalysts with a high intrinsic activity are necessary but not the only factors attributable to the good performance of a device or an electrode.[30,615] At the initial stage in the development of molecular catalysts, the activity is evaluated by employing sacrificial reagents (*e.g.*, Ce^{4+} oxidant for water oxidation) and/or under homogeneous electrocatalytic

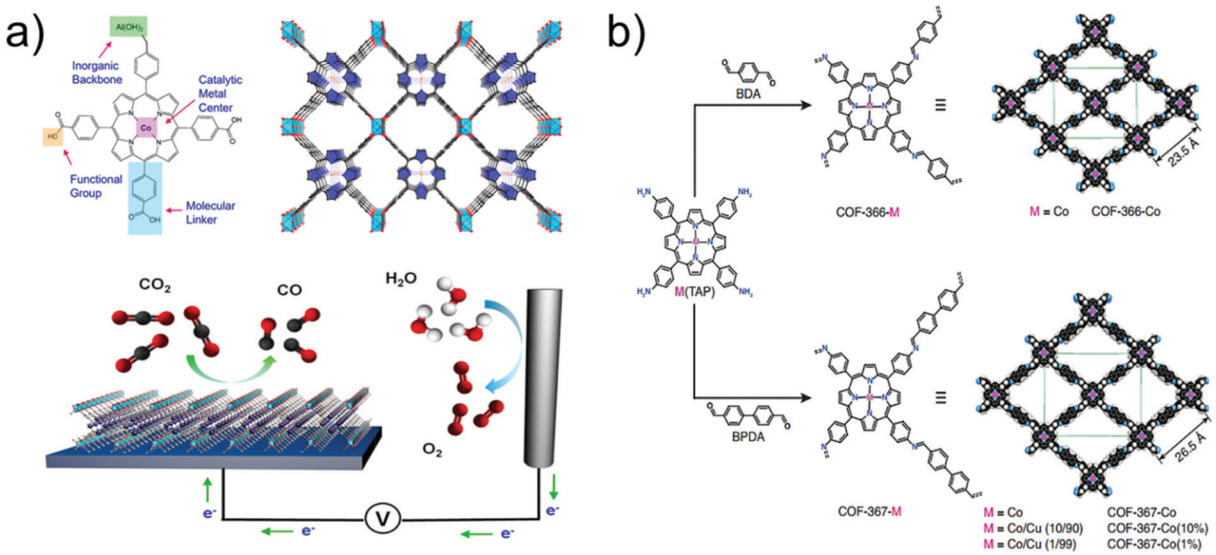

Fig. 41 Schematic representation of (a) MOFs generated from functionalized cobalt-porphyrins for efficient CO_2 electroreduction. Adapted with permission from ref. 600. Copyright 2015 American Chemical Society. (b) COFs generated from functionalized cobalt-porphyrins for efficient CO_2 electroreduction. Adapted with permission from ref. 435. Copyright 2015 American Association for the Advancement of Science (AAAS).

experiments, because these conditions can provide an adequate driving force and simple investigation systems. In many cases, when an efficient molecular catalyst is employed to construct a PEC cell or to modify an electrode, the device exhibits poor performance. However, this cannot indicate that the catalyst is not excellent or not promising for an applicable AP device, because the performance of a PEC cell or an electrolyzer is determined by a number of factors, such as catalyst loading amount, loading method, electrolyte, device design for mass transfer and proton transfer.

For example, the Ru-bda WOC exhibited an activity similar to the Nature's OEC when it is evaluated with Ce^{4+} as the oxidant under acidic conditions;[146–149] however, it exhibited very moderate performance under the three-component photocatalytic system.[145,616,617] In particular, when the Ru-bda WOC was employed for the first time to construct a DSPEC cell as shown in Fig. 20b, it yielded a photocurrent density of only 40 μA cm^{-2}.[453] However, after the photoanode was improved by the co-absorption strategy, a photocurrent density of 1.7 mA cm^{-2} was obtained.[163] A 40-fold enhancement of device performance was achieved with the same catalyst but different device design. Without Ru-bda as the catalyst, no other DSPEC cells have been reported with comparable performance. The super-low overpotential and super-high TOF guarantee the good performance of the DSPEC cell. As another example, the performance of photocatalytic H_2 evolution of the same [FeFe]-hydrogenase HECs has been investigated under systems using quantum dots (QDs) and the molecular photosensitizer $[Ru(bpy)_3]^{2+}$ in water. Under the same conditions, TONs of the [FeFe]-hydrogenase HECs working under the system with CdSe QDs are two orders of magnitude higher than those of the system with $[Ru(bpy)_3]^{2+}$.[618,619] The above examples clearly show that the activity of a catalyst cannot completely determine the efficiency of an AP device or a photocatalytic system, although an efficient catalyst is necessary for developing applicable AP devices in future.

6.2 Efficient molecular catalyst ≠ high catalytic current density of an electrode

Electrocatalytic water splitting has been a widely discussed topic since the past five years because it is believed that it can realize an applicable PVE device in the near future. Nowadays, electrocatalysts for AP are ranked on the basis of the current density (per geometric area of an electrode, *e.g.* 10 mA cm^{-2}) at a certain overpotential.[30] Although several super-efficient catalysts for reactions involved in AP, including water oxidation, proton reduction, and CO_2 reduction, have been developed, the current density of electrodes modified by molecular catalysts is still significantly lower than that of inorganic-material-based electrodes. This is one of the main reasons that make the development of molecular catalyst getting less attractive for applicable AP devices in recent years.

The unsatisfactory performance of molecular-catalyst-based electrodes can be attributed to the following two reasons: the challenge of heterogenization of molecular catalysts has not yet been overcome. Consequently, the low loading amount and the stability of immobilization dramatically limit the performance of molecular-catalyst-based electrodes. Secondly, the electrochemical testing system employed in the laboratory is not beneficial for exhibiting the activity of molecular-catalyst-based electrodes. Because water oxidation is the bottleneck of AP, we consider it as an example. Water oxidation involves the removal of four electrons and four protons. The electrons can be easily transported to a counter electrode, whereas the protons will accumulate in the diffuse double layer, instantly leading to a local pH drop, which will significantly increase the thermodynamic barrier and decrease the catalytic current. To date, the electrochemical water-oxidation performance of an electrode has been evaluated in a simple three-electrode electrochemical cell, *i.e.*, a beaker-like cell fixed with working, reference, and counter electrodes. However, in this kind of test system, the catalytic performance will be strongly limited by the proton and mass transfers.

To obtain high electrocatalytic efficiency, *i.e.*, high catalytic current density, the released protons must be fleetly transported to the bulk solution. For this, one possible solution is the employment of a highly concentrated strong alkaline electrolyte solution, such as 6 M KOH electrolyte solution used in the industrial alkaline water electrolysis[620] or 1 M KOH electrolyte solution widely employed in the laboratory beaker-like electrolyzer.[621] By using this strategy, the current density of the order of several hundreds of mA cm^{-2} (less than 500 mA cm^{-2}) can be achieved.[620,621] However, for most molecular WOCs based on organometallic compounds, maintaining the stability of compounds under electrooxidation conditions in a strong alkaline solution is already a considerable challenge, because OH^- is a strong σ-donating ligand, which may replace the ligand of the molecular catalyst when it is oxidized to high valence. For this reason, many molecular catalysts catalyzing under alkaline conditions are found transformed into metal oxide/hydroxide, serving as true catalysts, thereby imparting good stability and high catalytic activity because of the low thermodynamic requirement of water oxidation under high pH conditions.[308,622]

Nevertheless, without the alkaline condition, the performance of any type of water-oxidation electrodes is limited in a range of several mA cm^{-2} of current density under a moderate overpotential. Even with the state-of-the-art Ru-bda WOC, only 0.22 mA cm^{-2} has been obtained for the Ru-bda-modified carbon nanotube electrode at 0.58 V overpotential in a neutral Na_2SO_4 solution.[166] When the polymerization method was conducted to improve the catalyst loading amount, current density above 4.0 mA cm^{-2} at 0.48 V overpotential can be achieved in a phosphate buffer solution, where phosphate can functionalize as a proton shuttle.[599] The so called "Co-Pi" is an efficient inorganic WOC based on cobalt oxide. Although the "Co-Pi" is highly active under neutral conditions, even with a considerably higher loading amount, the catalytic current density of the Co-Pi electrode is also of the order of several mA cm^{-2}.[623]

Another methodology to solve the problem of proton transfer is the PEM electrolyzer. For the PEM electrolyzer, an electrolyte is avoided. With this technology, current density between 0.6 and 2 A cm^{-2} can be reached. However, because of its complicated

assembly process, the performance of the molecular-catalyst-based electrode has not been widely reported. The only available example was provided by Millet and co-workers demonstrating the incorporation of the Ru(tpy)(bpy) type WOC into a PEM cell.[624] A Ru(tpy)(bpy)-type WOC is far less efficient compared to a Ru-bda-type WOC. However, when it is incorporated into a PEM cell, a current density of 1 A cm^{-2} has been reached at 1.9 V, although this performance is not as good as that exhibited by the IrO_2 catalyst under the same testing conditions. It should be noted that the intrinsic activity of the Ru(tpy)(bpy)-type WOC is far lower than that of most of the efficient molecular WOCs. This report proves that high catalytic current can be anticipated by the molecular-catalyst-modified electrode.

Apparently, the power of molecular catalysts for AP is significantly underestimated because of the non-standard comparison. The current density normalized to the geometric area of an electrode is closely dependent on the loading amount of catalysts, the testing systems, and the actual electrochemically active surface area of the substrate electrode. For example, the actual surface area of the Ni foam electrode substrate is far higher than the value of its geometric area measured by a ruler. Therefore, it is not a valid parameter to indicate the intrinsic activity of a given electrocatalyst. Finally, the performance of an electrode is dominated by the intrinsic activity of the modified catalyst. Moreover, the application of an efficient molecular catalyst in an appropriate manner by careful design of the modification methods and the structure of the electrolyzer is also a great challenge.

6.3 The stability of molecular catalyst engineered devices

Low long-term-stability is one major limitation of AP devices based on molecular-catalyst-engineered electrodes. Many efficient molecular catalysts, including water oxidation catalysts, proton reduction catalysts, and CO_2 reduction catalysts, have been clearly reported to exhibit much lower overpotentials, extremely higher TOFs and TONs as compared to the conventional inorganic-material-based catalysts, such as metal alloys, oxides, and hydroxides.[4,43,55,313] In spite of this, there arises a question of why the stabilities of the electrodes engineered from these much more efficient molecular catalysts are not comparable with the electrodes generated from inorganic-material-based catalysts. To address this question, we propose here several reasons and possible solutions.

First, the stability of molecule-integrated electrodes should be distinguished from that of molecular catalysts. A molecular catalyst with a high TOF and TON certainly is a stable catalyst; however, it is very normal that the functional electrode fabricated from the molecular catalyst has very poor stability. Besides the intrinsic stability of the modified catalyst, many factors can impart low stability to an electrode, *e.g.*, detachment of an electrode film from the substrate, desorption of molecules, breaking of the linking bridge groups, and alteration of the catalytic mechanism on an electrode surface.

Second, catalytic kinetics, conditions, and local environments of molecular catalysts operating on an electrode surface are significantly different from those in homogeneous solutions. The performance of an electrode is dominated not only by the intrinsic activity of the molecular catalyst but also by the electron transfer rate between an active site and a supporting electrode, the reactant substrate transformation and binding to an active site, proton transfer between a catalyst and a solution phase, local pH change, and product removal from the electrode. If any of these steps is inefficient, the performance of the modified electrode will be dramatically limited, and the decomposition of catalysts will occur because of the accumulation of intermediates or the changes in local conditions. These types of decomposition occur in laboratory experiments, but they may be effectively prevented in practical industrial tests by the use of well-designed cells and technologies.

Third, the comparison of the stabilities of molecular-catalyst-engineered electrodes with those of inorganic-material-based electrodes is unequal if the loading amounts of catalysts are considered. The loading amounts of a molecular catalyst on an electrode are of the order of nmol cm^{-2},[166,298,592] in contrast, it is usually more than an order of μmol cm^{-2} for an inorganic-material-based catalyst.[621,625,626] It is noticed that the catalytic current is dramatically influenced by the loading amount of catalysts; therefore there is a factor called mass activity (A g^{-1}). Indeed, the stability of an electrode can also be dependent on the loading amounts of catalysts. The decomposition of 1 nmol catalyst is definitely much faster than that of 1 μmol catalyst. Therefore, if the loading amounts of catalysts are also considered and discussed during the stability comparison, the stability of molecular-catalyst-based electrodes may not be a real drawback and has a high possibility to be remarkably upgraded in future research.

In the present context, it is obvious that the power of molecular catalysts for AP has been under estimated, and the molecular catalyst is very promising for the realization of applicable AP devices. Because the mechanistic study of a molecular catalyst is relatively easier than material-based catalysis, it is more possible to protect the catalyst *via* blocking the decomposition pathways. Under suitable testing conditions, molecular catalysts will display not only superior intrinsic activity but also high working catalytic current density and stability.

7. Concluding remarks and outlook

Promising catalysts with high intrinsic activities are still the basis for producing chemical fuels from solar energy *via* AP. The development of molecular catalysts with plenty of specific advantages, as summarized above in this review, is the most effective way to understand catalytic mechanisms in detail and to obtain high intrinsic catalytic activities. The field of molecular AP, including the development of molecular catalysts (*e.g.*, WOCs, HECs, and CO_2RCs) and the assembly of molecular-catalyst-based AP devices, has thrived during the past 15 years. In this review, the history and the present developing state of AP based on molecules have been summarized to show the advantages and challenges of molecular catalysts, as

well as the future of molecular-catalyst-based AP for renewable energy conversion.

7.1 Present achievements in molecular-catalyst-based AP

In recent decades, abundant molecular catalysts for the reactions involved in AP, *i.e.*, water oxidation, hydrogen evolution, and CO_2 reduction, have been designed and investigated, and several successful catalysts with outstanding catalytic performances have been obtained. For the WOCs, the Ru-bda series can reach a catalytic TOF of 1000 s^{-1} and a TON of 100 000.[80,142,143] WOCs based on iron, which is the most cheap and abundant metal, can also achieve a considerable catalytic performance, with TOFs of 2.2 s^{-1} and TONs of 1000.[278] The structures of NiFe- and FeFe-hydrogenases have been successfully mimicked.[39,330,332] Although most of the mimics showed low activity and high overpotentials for hydrogen evolution, detailed studies of these molecular models have provided useful information for understanding the mechanism of hydrogen evolution *via* metal catalytic sites. Fortunately, several noble-metal-free HECs with excellent catalytic properties have been explored. Cobaltoxime HECs have overpotentials less than 100 mV towards hydrogen evolution.[325] With a high overpotential, Ni-diphosphine HECs can display catalytic TOFs over 100 000 s^{-1}.[312] Fe porphyrins have been, so far, the most efficient molecular catalysts for the reduction of CO_2 into CO, showing high catalytic rate, high selectivity, and high robustness. With an overpotential of only 220 mV, Fe porphyrin CO_2RCs can convert CO_2 into CO at a TOF of 10^6 s^{-1} for 80 h without obvious degradation.[432] On the other hand, studies to understand the catalytic mechanisms of these catalysts have also been fruitful. A toolbox is now available to allow rational design of more promising molecular catalysts for AP.

For an AP device based on molecular catalysis, a high intrinsic activity of the molecular catalyst, especially low overpotential, is an essential basis for obtaining high efficiency. Facilitated by the presence of plenty of efficient molecular catalysts, many design concepts for AP devices with molecular catalysts have been proven in the last five years, including DSPEC cells with photoanodes modified by molecules, DSPEC cells with photocathodes modified by molecules, DSPEC tandem cells based on molecule-modified photoelectrodes, molecular-catalyst–VLA-SC hybrid devices, and molecular-catalyst engineered materials as electrodes for PVE devices. The design and performance of AP devices with molecular catalysts have been much improved. For example, the successful development of the Ru-bda WOC with an extremely low potential allowed DSPEC cells based on molecular-WOC-modified photoanodes to flourish. The photocurrents generated by molecular DSPEC cells have been improved by about two orders of magnitude to 1.7 mA cm^{-2}.[163] With the modification of cobaltoxime HECs, a composite p-$GaInP_2$ photocathode mediates H_2 production with a current density of 11 mA cm^{-2}, which is close to the light-limited current of 12.5 mA cm^{-2}.[548] Several successful molecular-catalyst engineered electrode materials are readily available with very low overpotentials and good stabilities for PVE devices, for example, Ru-bda WOC functionalized MWCNTs,[166] cobaltoxime HECs/Ni-diphosphine functionalized MWCNTs,[579,581,586] and Fe-porphyrin CO_2RC constructed MOF materials.[435,600] In addition, the strategies advanced for the immobilization of molecular catalysts on electrodes, the mechanistic understanding of catalysis on the surface of electrodes, and the determination of the kinetics of electron transfer on photoelectrodes have also been gradually developed. This is extremely valuable for further development of AP devices based on molecular catalysts toward practical applications.

7.2 Challenges for the future of molecular-catalyst-based AP

Although the concept of AP was first proposed in 1912 by Giacomo Ciamician,[627] investigations into AP based on molecular catalysis were triggered much later, and intensive interest has only been aroused in recent 20 years. Moreover, most of the efforts of the community during this recent period have contributed to research for the development of efficient molecular catalysts. Work on assembling AP devices with molecular catalysts has been widely conducted in the last five to ten years. Most of these studies are only at the level of proof of concept. Because of the complexity of complete molecular-catalyst-based AP devices, the performance can be dominated by many different factors, as discussed in previous sections. Indeed, so far, there has not been even a set of standard cell designs or operating conditions for AP devices to be based on, which in turn is adverse to the development of molecular AP devices.

Apparently, the present research is largely insufficient to realize a practically applicable device because an ideal AP device for solar fuels is highly challenging involving not only the fundamentals of light absorption, charge transfer, and difficult catalysis but also engineering problems, such as device design and mass transfer. It is entirely understandable that, although some encouraging progress has been made in the past ten years in the development of molecular AP devices, none of these devices really satisfy the requirements for practical application or solve the issues of low stabilities of AP devices based on molecular catalysts. Therefore, it is too early to judge that AP devices based on molecular catalysts are not promising. Considering the prominent advantages of molecular catalysts, the construction of practically applicable AP devices based on molecular catalysts is still highly promising once the challenges are overcome. The development of molecular catalysts may still be the most effective way to solve the catalysis issues of AP.

In light of the above analysis and the present state of the field, the following challenges need to be addressed for the future of developing AP devices based on molecular catalysts:

(1) To develop earth-abundant metal based efficient catalysts working under aqueous conditions, especially under acidic conditions. WOCs with low overpotential and high TOF and TON are available. However, they are based on the noble metal ruthenium. Earth-abundant metal based WOCs are urgently needed now. For example, iron-based WOCs are promising candidates. To face the extremely low local pH problem, the development of WOCs that are efficient and stable under acidic conditions is necessary. For HECs, earth-abundant metal based catalysts with low overpotential and high TOF have been

obtained, but the big issue is that their best performances are highly dependent on organic solvent systems. The same problem also exists for the development of CO_2RCs. Moreover, the design of CO_2RCs to break through the limit of two-electron reduction to produce liquid fuels is another challenge.

(2) To enhance the development of molecular electrocatalysts for water oxidation. Over the last 30 years, the development of molecular catalyst has mainly been carried out under homogeneous catalytic conditions with sacrificial reagents, such as Ce^{4+} and Ru^{3+} complexes, sodium peroxodisulfate, oxone, or sodium periodate.[628] However, WOCs will finally be immobilized on electrodes for electrochemical water oxidation. Considering this point, the development of molecular electrocatalysts is closer to the aim of using molecular WOCs for AP devices. On the other hand, the investigation of catalysts is limited to the driving force of the sacrificial reagent and is also influenced by the instability of the sacrificial reagent, the involvement of active oxygen atom in the sacrificial reagent, and the special pH requirements of the sacrificial reagent. Harsh oxidative conditions may also lead to decomposition of the targeted catalysts. In contrast to the investigations with sacrificial reagents, the development of molecular electrocatalysts is much easier, milder and more adjustable.[629,630]

(3) To expand light absorbers, explore new transparent p-type semiconductors and upgrade the anchoring groups of functional molecules for PEC cells. In previous reports, Ru-based dyes have been the most used light absorber to build molecular-catalyst-modified PEC cells. Low stability, moderate light-absorption ability, and high cost mean they are not a good choice for practical applications. Inorganic semiconductors are a good replacement. The development of molecular catalyst-VLA-SC hybrid devices should be continued. With plenty of advantages, pure organic dyes can be more widely applied to PEC cells. In the reported PEC cells, the common anchoring groups of molecules are carboxylic or phosphate groups. However, in contrast to their utilization in dye-sensitized solar cells, these anchoring groups are not perfectly suited for use in PEC cells because the adsorption through carboxylic or phosphate groups cannot tolerate the aqueous electrolyte environment for long periods. Stronger binding groups should be designed and investigated for long-term stable PEC cells. Hydroxamate, acetylacetonate and 2,6-pyridinedicarboxylate groups are possible anchoring groups for stable PEC cells.

(4) To heterogenize molecular catalysts into materials. Heterogenization of molecular catalysts is an essential stage to bridge the gap between molecular catalysts and applicable AP devices. It could well remove the disadvantages of molecular catalysts, *e.g.*, low loading amounts and low stability, by merging homogeneous and heterogeneous catalysis. PVE devices can indirectly convert solar energy into fuels. General investigation into PVE devices began much earlier than the study of PEC cells, and the development of PVE devices is now closer to practical application. Alkaline water electrolysis has been a mature industrial technology for decades. Moreover, plenty of inorganic materials have been reported in the last five years as efficient catalysts for water splitting under alkaline conditions. On the other hand, the practical utilization of PEM electrolyzers, which are ideal for domestic applications, will be limited because of their dependency on noble-metal-based catalysts. Molecular chemistry offers new possibilities for this technology. For PEM water electrolyzers, inexpensive materials that can work in acidic environments are urgently required. Developing molecular-catalyst engineered materials will facilitate the advance of PEM technology. PEM technology can probably be further applied to convert CO_2 and N_2 into chemicals.

(5) To reveal the reasons for deactivation of molecular catalyst based AP devices, including the reasons for the decomposition of modified catalysts. The performance of a complete molecular-catalyst-based AP device is affected by many factors. Relative to homogeneous catalysis, more complicated reasons can lead to the decomposition of catalysts modified on electrodes. A deep understanding of the reasons for the deactivation of molecular-catalyst-based AP devices is essential to improve the stability and activity of AP devices for practical applications.

(6) To set the standards for comprehensive evaluation of molecular catalysts, molecular-catalyst engineered materials and molecular-catalyst-based devices. The performance of a catalyst can be completely different under different test systems, such as chemical catalysis, photochemical catalysis, electrochemical catalysis, or photoelectrochemical catalysis. For example, the TOF of a molecular catalyst evaluated by homogeneous electrochemical catalysis is normally several orders of magnitude higher than that obtained from homogeneous chemical catalysis. Comparisons should be made under the same test system with similar detailed parameters, such as oxidant/reductant, solvent, pH value and light intensity. The evaluation of the performance of electrodes needs to be conducted with comparable conductive substrates. The geometric area, electrochemically active surface area, and loading amount of catalysts must also be comparable and clearly stated; otherwise, any discussions based on the obtained current densities, *e.g.*, 10 mA cm^{-2}@η mV, are meaningless.

It is certain that AP based on molecular catalysts is promising. Much has been attained, but more challenges remain.

Conflicts of interest

The authors declare no competing interest.

Acknowledgements

We acknowledge financial support for this work from the Swedish Research Council (2017-00935), Swedish Energy Agency, Knut and Alice Wallenberg Foundation, and National Basic Research Program of China (973 program, 2014CB239402).

References

1 R. L. Purchase and H. J. de Groot, *Interface Focus*, 2015, **5**, 20150014.
2 V. Balzani, A. Credi and M. Venturi, *ChemSusChem*, 2008, **1**, 26–58.

3 H. Dau, E. Fujita and L. Sun, *ChemSusChem*, 2017, **10**, 4228–4235.
4 M. D. Kärkas, O. Verho, E. V. Johnston and B. Åkermark, *Chem. Rev.*, 2014, **114**, 11863–12001.
5 J. P. McEvoy and G. W. Brudvig, *Chem. Rev.*, 2006, **106**, 4455–4493.
6 E. S. Andreiadis, M. Chavarot-Kerlidou, M. Fontecave and V. Artero, *Photochem. Photobiol.*, 2011, **87**, 946–964.
7 S. A. Crowe, L. N. Dossing, N. J. Beukes, M. Bau, S. J. Kruger, R. Frei and D. E. Canfield, *Nature*, 2013, **501**, 535–538.
8 A. Amunts, O. Drory and N. Nelson, *Nature*, 2007, **447**, 58–63.
9 Y. Umena, K. Kawakami, J. R. Shen and N. Kamiya, *Nature*, 2011, **473**, 55–60.
10 K. E. Dalle, J. Warnan, J. J. Leung, B. Reuillard, I. S. Karmel and E. Reisner, *Chem. Rev.*, 2019, **119**, 2752–2875.
11 S. L. Foster, S. I. P. Bakovic, R. D. Duda, S. Maheshwari, R. D. Milton, S. D. Minteer, M. J. Janik, J. N. Renner and L. F. Greenlee, *Nat. Catal.*, 2018, **1**, 490–500.
12 W. M. Singh, D. Pegram, H. Duan, D. Kalita, P. Simone, G. L. Emmert and X. Zhao, *Angew. Chem., Int. Ed.*, 2012, **51**, 1653–1656.
13 H. Inoue, T. Shimada, Y. Kou, Y. Nabetani, D. Masui, S. Takagi and H. Tachibana, *ChemSusChem*, 2011, **4**, 173–179.
14 T. Shimada, A. Kumagai, S. Funyu, S. Takagi, D. Masui, Y. Nabetani, H. Tachibana, D. A. Tryk and H. Inoue, *Faraday Discuss.*, 2012, **155**, 145–163.
15 S. Fukuzumi, Y. M. Lee and W. Nam, *Chem. – Eur. J.*, 2018, **24**, 5016–5031.
16 K. Li and Y. Sun, *Chem. – Eur. J.*, 2018, **24**, 18258–18270.
17 J. W. Ager, M. R. Shaner, K. A. Walczak, I. D. Sharp and S. Ardo, *Energy Environ. Sci.*, 2015, **8**, 2811–2824.
18 X. Ding, L. Zhang, Y. Wang, A. Liu and Y. Gao, *Coord. Chem. Rev.*, 2018, **357**, 130–143.
19 A. Hagfeldt, G. Boschloo, L. Sun, L. Kloo and H. Pettersson, *Chem. Rev.*, 2010, **110**, 6595–6663.
20 D. L. Ashford, M. K. Gish, A. K. Vannucci, M. K. Brennaman, J. L. Templeton, J. M. Papanikolas and T. J. Meyer, *Chem. Rev.*, 2015, **115**, 13006–13049.
21 J. Seo, H. Nishiyama, T. Yamada and K. Domen, *Angew. Chem., Int. Ed.*, 2018, **57**, 8396–8415.
22 K. Sivula, F. Le Formal and M. Gratzel, *ChemSusChem*, 2011, **4**, 432–449.
23 S. S. Kalanur, L. T. Duy and H. Seo, *Top. Catal.*, 2018, **61**, 1043–1076.
24 Y. Park, K. J. McDonald and K. S. Choi, *Chem. Soc. Rev.*, 2013, **42**, 2321–2337.
25 E. A. Gibson, *Chem. Soc. Rev.*, 2017, **46**, 6194–6209.
26 M. Wang, Y. Yang, J. Shen, J. Jiang and L. Sun, *Sustainable Energy Fuels*, 2017, **1**, 1641–1663.
27 T. Nann, S. K. Ibrahim, P. M. Woi, S. Xu, J. Ziegler and C. J. Pickett, *Angew. Chem., Int. Ed.*, 2010, **49**, 1574–1577.
28 R. Wick and S. D. Tilley, *J. Phys. Chem. C*, 2015, **119**, 26243–26257.
29 B. Zhang, Q. Daniel, M. Cheng, L. Fan and L. Sun, *Faraday Discuss.*, 2017, **198**, 169–179.
30 C. Wei and Z. J. Xu, *Small Methods*, 2018, **2**, 1800168.
31 C. Jiang, S. J. A. Moniz, A. Wang, T. Zhang and J. Tang, *Chem. Soc. Rev.*, 2017, **46**, 4645–4660.
32 R. Argazzi, N. Y. Murakami Iha, H. Zabri, F. Odobel and C. A. Bignozzi, *Coord. Chem. Rev.*, 2004, **248**, 1299–1316.
33 J. T. Kirner and R. G. Finke, *J. Mater. Chem. A*, 2017, **5**, 19560–19592.
34 T. Yao, X. An, H. Han, J. Q. Chen and C. Li, *Adv. Energy Mater.*, 2018, **8**, 1800210.
35 H. L. Wu, X. B. Li, C. H. Tung and L. Z. Wu, *Adv. Sci.*, 2018, **5**, 1700684.
36 Y. Xu, X. Wang, W. L. Zhang, F. Lv and S. Guo, *Chem. Soc. Rev.*, 2018, **47**, 586–625.
37 Z. W. Seh, J. Kibsgaard, C. F. Dickens, I. Chorkendorff, J. K. Norskov and T. F. Jaramillo, *Science*, 2017, **355**, eaad4998.
38 X.-F. Yang, A. Wang, B. Qiao, J. Li, J. Liu and T. Zhang, *Acc. Chem. Res.*, 2013, **46**, 1740–1748.
39 F. Gloaguen, J. D. Lawrence and T. B. Rauchfuss, *J. Am. Chem. Soc.*, 2001, **123**, 9476–9477.
40 J. L. Fillol, Z. Codola, I. Garcia-Bosch, L. Gomez, J. J. Pla and M. Costas, *Nat. Chem.*, 2011, **3**, 807–813.
41 C. Costentin, S. Drouet, M. Robert and J.-M. Savéant, *Science*, 2012, **338**, 90–94.
42 A. Polman, M. Knight, E. C. Garnett, B. Ehrler and W. C. Sinke, *Science*, 2016, **352**, aad4424.
43 H. Takeda, C. Cometto, O. Ishitani and M. Robert, *ACS Catal.*, 2016, **7**, 70–88.
44 N. Elgrishi, M. B. Chambers, X. Wang and M. Fontecave, *Chem. Soc. Rev.*, 2017, **46**, 761–796.
45 B. Reuillard, K. H. Ly, T. E. Rosser, M. F. Kuehnel, I. Zebger and E. Reisner, *J. Am. Chem. Soc.*, 2017, **139**, 14425–14435.
46 X. Zhang, Z. Wu, X. Zhang, L. Li, Y. Li, H. Xu, X. Li, X. Yu, Z. Zhang, Y. Liang and H. Wang, *Nat. Commun.*, 2017, **8**, 14675.
47 A. Wang, J. Li and T. Zhang, *Nat. Rev. Chem.*, 2018, **2**, 65–81.
48 Y. Wang, J. Mao, X. Meng, L. Yu, D. Deng and X. Bao, *Chem. Rev.*, 2019, **119**, 1806–1854.
49 Y. Zhao, X. Yan, K. R. Yang, S. Cao, Q. Dong, J. E. Thorne, K. L. Materna, S. Zhu, X. Pan, M. Flytzani-Stephanopoulos, G. W. Brudvig, V. S. Batista and D. Wang, *ACS Cent. Sci.*, 2018, **4**, 1166–1172.
50 Y. Zhao, K. R. Yang, Z. Wang, X. Yan, S. Cao, Y. Yei, Q. Dong, X. Zhang, J. E. Thorne, L. Jin, K. L. Materna, A. Trimpalis, H. Bai, S. C. Fakra, X. Zhong, P. Wang, X. Pang, J. Guo, M. Flytzani-Stephanopoulos, G. W. Brudvig, V. S. Batista and D. Wang, *Proc. Natl. Acad. Sci. U. S. A.*, 2018, **115**, 2902–2907.
51 W. Lubitz, H. Ogata, O. Rudiger and E. Reijerse, *Chem. Rev.*, 2014, **114**, 4081–4148.
52 A. Dhingra, A. R. Portis and H. Daniell, *Proc. Natl. Acad. Sci. U. S. A.*, 2004, **101**, 6315–6320.
53 J.-M. Savéant, *Chem. Rev.*, 2008, **108**, 2348–2378.

54 S. Berardi, S. Drouet, L. Francas, C. Gimbert-Surinach, M. Guttentag, C. Richmond, T. Stoll and A. Llobet, *Chem. Soc. Rev.*, 2014, **43**, 7501–7519.
55 J. D. Blakemore, R. H. Crabtree and G. W. Brudvig, *Chem. Rev.*, 2015, **115**, 12974–13005.
56 H. Lv, Y. V. Geletii, C. Zhao, J. W. Vickers, G. Zhu, Z. Luo, J. Song, T. Lian, D. G. Musaev and C. L. Hill, *Chem. Soc. Rev.*, 2012, **41**, 7572–7589.
57 J. Limburg, J. S. Vrettos, L. M. Liable-Sands, A. L. Rheingold, R. H. Crabtree and G. W. Brudvig, *Science*, 1999, **283**, 1524–1527.
58 M. M. Najafpour, G. Renger, M. Holynska, A. N. Moghaddam, E. M. Aro, R. Carpentier, H. Nishihara, J. J. Eaton-Rye, J. R. Shen and S. I. Allakhverdiev, *Chem. Rev.*, 2016, **116**, 2886–2936.
59 N. Cox, D. A. Pantazis, F. Neese and W. Lubitz, *Acc. Chem. Res.*, 2013, **46**, 1588–1596.
60 J. R. Shen, *Annu. Rev. Plant Biol.*, 2015, **66**, 23–48.
61 B. Kok, B. Forbush and M. McGloin, *Photochem. Photobiol.*, 1970, **11**, 457–475.
62 V. Krewald, M. Retegan, N. Cox, J. Messinger, W. Lubitz, S. DeBeer, F. Neese and D. A. Pantazis, *Chem. Sci.*, 2015, **6**, 1676–1695.
63 D. A. Pantazis, W. Ames, N. Cox, W. Lubitz and F. Neese, *Angew. Chem., Int. Ed.*, 2012, **51**, 9935–9940.
64 T. Lohmiller, V. Krewald, A. Sedoud, A. W. Rutherford, F. Neese, W. Lubitz, D. A. Pantazis and N. Cox, *J. Am. Chem. Soc.*, 2017, **139**, 14412–14424.
65 M. Suga, F. Akita, K. Hirata, G. Ueno, H. Murakami, Y. Nakajima, T. Shimizu, K. Yamashita, M. Yamamoto, H. Ago and J. R. Shen, *Nature*, 2015, **517**, 99–103.
66 J. Yano and V. Yachandra, *Chem. Rev.*, 2014, **114**, 4175–4205.
67 M. Perez-Navarro, F. Neese, W. Lubitz, D. A. Pantazis and N. Cox, *Curr. Opin. Chem. Biol.*, 2016, **31**, 113–119.
68 D. J. Vinyard, S. Khan and G. W. Brudvig, *Faraday Discuss.*, 2015, **185**, 37–50.
69 P. E. M. Siegbahn, *Acc. Chem. Res.*, 2009, **42**, 1871–1880.
70 J. Barber, *Nat. Plants*, 2017, **3**, 17041.
71 B. Zhang and L. Sun, *Dalton Trans.*, 2018, **47**, 14381–14387.
72 B. Zhang, Q. Daniel, L. Fan, T. Liu, Q. Meng and L. Sun, *iScience*, 2018, **4**, 144–152.
73 B. Zhang, H. Chen, Q. Daniel, B. Philippe, F. Yu, M. Valvo, Y. Li, R. B. Ambre, P. Zhang, F. Li, H. Rensmo and L. Sun, *ACS Catal.*, 2017, **7**, 6311–6322.
74 P. Garrido-Barros, C. Gimbert-Surinach, R. Matheu, X. Sala and A. Llobet, *Chem. Soc. Rev.*, 2017, **46**, 6088–6098.
75 J. Hessels, R. J. Detz, M. T. M. Koper and J. N. H. Reek, *Chem. – Eur. J.*, 2017, **23**, 16413–16418.
76 S. Romanin, L. Vigara and A. Llobet, *Acc. Chem. Res.*, 2009, **42**, 1944–1953.
77 L. Duan, L. Tong, Y. Xu and L. Sun, *Energy Environ. Sci.*, 2011, **4**, 3296–3313.
78 T. J. Meyer, M. V. Sheridan and B. D. Sherman, *Chem. Soc. Rev.*, 2017, **46**, 6148–6169.
79 J. J. Concepcion, J. W. Jurss, M. K. Brennaman, P. G. Hoertz, A. O. T. Patrocinio, N. Y. M. Iha, J. L. Templeton and T. J. Meyer, *Acc. Chem. Res.*, 2009, **42**, 1954–1965.
80 L. Duan, F. Bozoglian, S. Mandal, B. Stewart, T. Privalov, A. Llobet and L. Sun, *Nat. Chem.*, 2012, **4**, 418–423.
81 J. Nyhlen, L. Duan, B. Akermark, L. Sun and T. Privalov, *Angew. Chem., Int. Ed.*, 2010, **49**, 1773–1777.
82 M. T. Zhang, Z. Chen, P. Kang and T. J. Meyer, *J. Am. Chem. Soc.*, 2013, **135**, 2048–2051.
83 L. Duan, A. Fischer, Y. Xu and L. Sun, *J. Am. Chem. Soc.*, 2009, **131**, 10397–10399.
84 S. W. Gersten, G. J. Samuels and T. J. Meyer, *J. Am. Chem. Soc.*, 1982, **104**, 4029–4030.
85 K. Nagoshi, S. Yamashita, M. Yagi and M. Kaneko, *J. Mol. Catal. A: Chem.*, 1999, **144**, 71–76.
86 J. P. Collin and J. P. Sauvage, *Inorg. Chem.*, 1986, **25**, 135–141.
87 L. Duan, L. Wang, F. Li, F. Li and L. Sun, *Acc. Chem. Res.*, 2015, **48**, 2084–2096.
88 D. Moonshiram, I. Alperovich, J. J. Concepcion, T. J. Meyer and Y. Pushkar, *Proc. Natl. Acad. Sci. U. S. A.*, 2013, **110**, 3765–3770.
89 J. A. Gilbert, D. S. Eggleston, W. R. Murphy Jr., D. A. Geselowitz, S. W. Gersten, D. J. Hodgson and T. J. Meyer, *J. Am. Chem. Soc.*, 1985, **107**, 3855–3864.
90 J. A. Stull, T. A. Stich, J. K. Hurst and R. D. Britt, *Inorg. Chem.*, 2013, **52**, 4578–4586.
91 D. Moonshiram, J. W. Jurss, J. J. Concepcion, T. Zakharova, I. Alperovich, T. J. Meyer and Y. Pushkar, *J. Am. Chem. Soc.*, 2012, **134**, 4625–4636.
92 H. Yamada and J. K. Hurst, *J. Am. Chem. Soc.*, 2000, **122**, 5303–5311.
93 H. Yamada, W. F. Siems, T. Koike and J. K. Hurst, *J. Am. Chem. Soc.*, 2004, **126**, 9786–9795.
94 J. L. Cape and J. K. Hurst, *J. Am. Chem. Soc.*, 2008, **130**, 827–829.
95 F. Liu, J. J. Concepcion, J. W. Jurss, T. Cardolaccia, J. L. Templeton and T. J. Meyer, *Inorg. Chem.*, 2008, **47**, 1727–1752.
96 R. A. Binstead, C. W. Chronister, J. Ni, C. M. Hartshorn and T. J. Meyer, *J. Am. Chem. Soc.*, 2000, **122**, 8464–8473.
97 J. J. Concepcion, J. W. Jurss, J. L. Templeton and T. J. Meyer, *Proc. Natl. Acad. Sci. U. S. A.*, 2008, **105**, 17632–17635.
98 X. Yang and M.-H. Baik, *J. Am. Chem. Soc.*, 2006, **128**, 7476–7485.
99 H. Seo, K. H. Cho, H. Ha, S. Park, J. S. Hong, K. Jin and K. T. Nam, *J. Korean Ceram. Soc.*, 2017, **54**, 1–8.
100 B. M. Hunter, H. B. Gray and A. M. Muller, *Chem. Rev.*, 2016, **116**, 14120–14136.
101 B. A. Moyer and T. J. Meyer, *Inorg. Chem.*, 1981, **20**, 436–444.
102 B. A. Moyer and T. J. Meyer, *J. Am. Chem. Soc.*, 1978, **100**, 3601–3603.
103 L. Tong and R. P. Thummel, *Chem. Sci.*, 2016, **7**, 6591–6603.
104 C. J. Gagliardi, A. K. Vannucci, J. J. Concepcion, Z. Chen and T. J. Meyer, *Energy Environ. Sci.*, 2012, **5**, 7704–7717.
105 C. Sens, I. Romero, M. Rodriguez, A. Llobet, T. Parella and J. Benet-Buchholz, *J. Am. Chem. Soc.*, 2004, **126**, 7798–7799.

106 S. Romain, F. Bozoglian, X. Sala and A. Llobet, *J. Am. Chem. Soc.*, 2009, **131**, 2768–2769.
107 X. Sala, S. Maji, R. Bofill, J. García-Antón, L. Escriche and A. Llobet, *Acc. Chem. Res.*, 2014, **47**, 504–516.
108 C. Sens, M. Rodríguez, I. Romero and A. Llobet, *Inorg. Chem.*, 2003, **42**, 2040–2048.
109 L. Francas, X. Sala, E. Escudero-Adan, J. Benet-Buchholz, L. Escriche and A. Llobet, *Inorg. Chem.*, 2011, **50**, 2771–2781.
110 J. Mola, C. Dinoi, X. Sala, M. Rodriguez, I. Romero, T. Parella, X. Fontrodona and A. Llobet, *Dalton Trans.*, 2011, **40**, 3640–3646.
111 C. Sens, M. Rodríguez, I. Romero and A. Llobet, *Inorg. Chem.*, 2003, **42**, 8385–8394.
112 J. Aguiló, L. Francàs, H. J. Liu, R. Bofill, J. García-Antón, J. Benet-Buchholz, A. Llobet, L. Escriche and X. Sala, *Catal. Sci. Technol.*, 2014, **4**, 190–199.
113 L. Francas, X. Sala, J. Benet-Buchholz, L. Escriche and A. Llobet, *ChemSusChem*, 2009, **2**, 321–329.
114 Z. Deng, H.-W. Tseng, R. Zong, D. Wang and R. Thummel, *Inorg. Chem.*, 2008, **47**, 1835–1848.
115 R. Zong and R. P. Thummel, *J. Am. Chem. Soc.*, 2005, **127**, 12802–12803.
116 T. Wada, K. Tsuge and K. Tanaka, *Angew. Chem., Int. Ed.*, 2000, **39**, 1479–1482.
117 T. A. Betley, Q. Wu, T. V. Voorhis and D. G. Nocera, *Inorg. Chem.*, 2008, **47**, 1849–1861.
118 L. Chen, M. Wang, K. Han, P. Zhang, F. Gloaguen and L. Sun, *Energy Environ. Sci.*, 2014, **7**, 329–334.
119 T. Wada, J. T. Muckerman, E. Fujitab and K. Tanaka, *Dalton Trans.*, 2011, **40**, 2225–2233.
120 T. Wada, H. Ohtsu and K. Tanaka, *Chem. – Eur. J.*, 2012, **18**, 2374–2381.
121 H. Y. Du, S. C. Chen, X. J. Su, L. Jiao and M. T. Zhang, *J. Am. Chem. Soc.*, 2018, **140**, 1557–1565.
122 P. Garrido-Barros, I. Funes-Ardoiz, S. Drouet, J. Benet-Buchholz, F. Maseras and A. Llobet, *J. Am. Chem. Soc.*, 2015, **137**, 6758–6761.
123 D. J. Wasylenko, C. Ganesamoorthy, B. D. Koivisto and C. P. Berlinguette, *Eur. J. Inorg. Chem.*, 2010, 3135–3142.
124 J. J. Concepcion, M.-K. Tsai, J. T. Muckerman and T. J. Meyer, *J. Am. Chem. Soc.*, 2010, **132**, 1545–1557.
125 J. J. Concepcion, J. W. Jurss, J. L. Templeton and T. J. Meyer, *J. Am. Chem. Soc.*, 2008, **130**, 16462–16463.
126 H.-W. Tseng, R. Zong, J. T. Muckerman and R. Thummel, *Inorg. Chem.*, 2008, **47**, 11763–11773.
127 N. Kaveevivitchai, R. Zong, H. W. Tseng, R. Chitta and R. P. Thummel, *Inorg. Chem.*, 2012, **51**, 2930–2939.
128 Y. M. Badiei, D. E. Polyansky, J. T. Muckerman, D. J. Szalda, R. Haberdar, R. Zong, R. P. Thummel and E. Fujita, *Inorg. Chem.*, 2013, **52**, 8845–8850.
129 D. E. Polyansky, J. T. Muckerman, J. Rochford, R. Zong, R. P. Thummel and E. Fujita, *J. Am. Chem. Soc.*, 2011, **133**, 14649–14665.
130 S. Masaoka and K. Sakai, *Chem. Lett.*, 2009, **38**, 182–183.
131 A. Kimoto, K. Yamauchi, M. Yoshida, S. Masaoka and K. Sakai, *Chem. Commun.*, 2012, **48**, 239–241.
132 J. J. Concepcion, J. W. Jurss, M. R. Norris, Z. Chen, J. L. Templeton and T. J. Meyer, *Inorg. Chem.*, 2010, **49**, 1277–1279.
133 D. J. Wasylenko, C. Ganesamoorthy, B. D. Koivisto, M. A. Henderson and C. P. Berlinguette, *Inorg. Chem.*, 2010, **49**, 2202–2209.
134 D. J. Wasylenko, C. Ganesamoorthy, M. A. Henderson and C. P. Berlinguette, *Inorg. Chem.*, 2011, **50**, 3662–3672.
135 D. J. Wasylenko, C. Ganesamoorthy, M. A. Henderson, B. D. Koivisto, H. D. Osthoff and C. P. Berlinguette, *J. Am. Chem. Soc.*, 2010, **132**, 16094–16106.
136 M. Yagi, S. Tajima, M. Komia and H. Yamazaki, *Dalton Trans.*, 2011, **40**, 3802–3804.
137 Y. Tamaki, A. K. Vannucci, C. J. Dares, R. A. Binstead and T. J. Meyer, *J. Am. Chem. Soc.*, 2014, **136**, 6854–6857.
138 Z. Chen, J. J. Concepcion, X. Hu, W. Yang, P. G. Hoertz and T. J. Meyer, *Proc. Natl. Acad. Sci. U. S. A.*, 2010, **107**, 7225–7229.
139 Y. Xu, T. Åkermark, V. Gyollai, D. Zou, L. Eriksson, L. Duan, R. Zhang, B. Åkermark and L. Sun, *Inorg. Chem.*, 2009, **48**, 2717–2719.
140 Y. Xu, L. Duan, L. Tong, B. Akermark and L. Sun, *Chem. Commun.*, 2010, **46**, 6506–6508.
141 Y. Xu, A. Fischer, L. Duan, L. Tong, E. Gabrielsson, B. Åkermark and L. Sun, *Angew. Chem., Int. Ed.*, 2010, **49**, 8934–8937.
142 L. Wang, L. Duan, Y. Wang, M. S. Ahlquist and L. Sun, *Chem. Commun.*, 2014, **50**, 12947–12950.
143 L. Duan, C. M. Araujob, M. S. G. Ahlquist and L. Sun, *Proc. Natl. Acad. Sci. U. S. A.*, 2012, **109**, 15584–15588.
144 L. Wang, L. Duan, B. Stewart, M. Pu, J. Liu, T. Privalov and L. Sun, *J. Am. Chem. Soc.*, 2012, **134**, 18868–18880.
145 L. Duan, Y. Xu, P. Zhang, M. Wang and L. Sun, *Inorg. Chem.*, 2010, **49**, 209–215.
146 Y. Jiang, F. Li, F. Huang, B. Zhang and L. Sun, *Chin. J. Catal.*, 2013, **34**, 1489–1495.
147 Y. Sato, S.-y. Takizawa and S. Murata, *Eur. J. Inorg. Chem.*, 2015, 5495–5502.
148 L. Duan, L. Wang, A. K. Inge, A. Fischer, X. Zou and L. Sun, *Inorg. Chem.*, 2013, **52**, 7844–7852.
149 Y. Xie, D. W. Shaffer and J. J. Concepcion, *Inorg. Chem.*, 2018, **57**, 10533–10542.
150 Q. Daniel, P. Huang, T. Fan, Y. Wang, L. Duan, L. Wang, F. Li, Z. Rinkevicius, F. Mamedov, M. S. G. Ahlquist, S. Styring and L. Sun, *Coord. Chem. Rev.*, 2017, **346**, 206–215.
151 D. Lebedev, Y. Pineda-Galvan, Y. Tokimaru, A. Fedorov, N. Kaeffer, C. Coperet and Y. Pushkar, *J. Am. Chem. Soc.*, 2018, **140**, 451–458.
152 N. Song, J. J. Concepcion, R. A. Binstead, J. A. Rudd, A. K. Vannucci, C. J. Dares, M. K. Coggins and T. J. Meyer, *Proc. Natl. Acad. Sci. U. S. A.*, 2015, **112**, 4935–4940.
153 S. Zhan, D. Martensson, M. Purg, S. C. L. Kamerlin and M. S. G. Ahlquist, *Angew. Chem., Int. Ed.*, 2017, **56**, 6962–6965.
154 T. Fan, S. Zhan and M. S. G. Ahlquist, *ACS Catal.*, 2016, **6**, 8308–8312.

155 B. Zhang, F. Li, R. Zhang, C. Ma, L. Chen and L. Sun, *Chem. Commun.*, 2016, **52**, 8619–8622.
156 R. Matheu, A. Ghaderian, L. Francàs, P. Chernev, M. Z. Ertem, J. Benet-Buchholz, V. S. Batista, M. Haumann, C. Gimbert-Suriñach, X. Sala and A. Llobet, *Chem. – Eur. J.*, 2018, **24**, 12838–12847.
157 M. Schulze, V. Kunz, P. D. Frischmann and F. Wurthner, *Nat. Chem.*, 2016, **8**, 576–583.
158 Y. Xie, D. W. Shaffer, A. Lewandowska-Andralojc, D. J. Szalda and J. J. Concepcion, *Angew. Chem., Int. Ed.*, 2016, **55**, 8067–8071.
159 R. Matheu, M. Z. Ertem, J. Benet-Buchholz, E. Coronado, V. S. Batista, X. Sala and A. Llobet, *J. Am. Chem. Soc.*, 2015, **137**, 10786–10795.
160 D. W. Shaffer, Y. Xie, D. J. Szalda and J. J. Concepcion, *J. Am. Chem. Soc.*, 2017, **139**, 15347–15355.
161 D. Wang, S. L. Marquard, L. Troian-Gautier, M. V. Sheridan, B. D. Sherman, Y. Wang, M. S. Eberhart, B. H. Farnum, C. J. Dares and T. J. Meyer, *J. Am. Chem. Soc.*, 2018, **140**, 719–726.
162 Y. K. Eom, L. Nhon, G. Leem, B. D. Sherman, D. Wang, L. Troian-Gautier, S. Kim, J. Kim, T. J. Meyer, J. R. Reynolds and K. S. Schanze, *ACS Energy Lett.*, 2018, **3**, 2114–2119.
163 Y. Gao, X. Ding, J. Liu, L. Wang, Z. Lu, L. Li and L. Sun, *J. Am. Chem. Soc.*, 2013, **135**, 4219–4222.
164 A. Bhunia, B. A. Johnson, J. Czapla-Masztafiak, J. Sa and S. Ott, *Chem. Commun.*, 2018, **54**, 7770–7773.
165 D. Wang, M. S. Eberhart, M. V. Sheridan, K. Hu, B. D. Sherman, A. Nayak, Y. Wang, S. L. Marquard, C. J. Dares and T. J. Meyer, *Proc. Natl. Acad. Sci. U. S. A.*, 2018, **115**, 8523–8528.
166 F. Li, B. Zhang, X. Li, Y. Jiang, L. Chen, Y. Li and L. Sun, *Angew. Chem., Int. Ed.*, 2011, **50**, 12276–12279.
167 B. Yang, X. Jiang, Q. Guo, T. Lei, L. P. Zhang, B. Chen, C. H. Tung and L. Z. Wu, *Angew. Chem., Int. Ed.*, 2016, **55**, 6229–6234.
168 B. Li, F. Li, S. Bai, Z. Wang, L. Sun, Q. Yang and C. Li, *Energy Environ. Sci.*, 2012, **5**, 8229–8233.
169 F. Yu, D. Poole, 3rd, S. Mathew, N. Yan, J. Hessels, N. Orth, I. Ivanovic-Burmazovic and J. N. H. Reek, *Angew. Chem., Int. Ed.*, 2018, **57**, 11247–11251.
170 C. J. Richmond, R. Matheu, A. Poater, L. Falivene, J. Benet-Buchholz, X. Sala, L. Cavallo and A. Llobet, *Chem. – Eur. J.*, 2014, **20**, 17282–17286.
171 Y. Jiang, F. Li, B. Zhang, X. Li, X. Wang, F. Huang and L. Sun, *Angew. Chem., Int. Ed.*, 2013, **52**, 3398–3401.
172 L. L. Zhang, Y. Gao, Z. Liu, X. Ding, Z. Yu and L. C. Sun, *Dalton Trans.*, 2016, **45**, 3814–3819.
173 S. Zhan, R. Zou and M. S. G. Ahlquist, *ACS Catal.*, 2018, **8**, 8642–8648.
174 T. Fan, L. Duan, P. Huang, H. Chen, Q. Daniel, M. S. G. Ahlquist and L. Sun, *ACS Catal.*, 2017, **7**, 2956–2966.
175 L. Duan, Y. Xu, M. Gorlov, L. Tong, S. Andersson and L. Sun, *Chem. – Eur. J.*, 2010, **16**, 4659–4668.
176 Q. Daniel, L. Duan, B. J. J. Timmer, H. Chen, X. Luo, R. Ambre, Y. Wang, B. Zhang, P. Zhang, L. Wang, F. Li, J. Sun, M. Ahlquist and L. Sun, *ACS Catal.*, 2018, **8**, 4375–4382.
177 R. Matheu, M. Z. Ertem, M. Pipelier, J. Lebreton, D. Dubreuil, J. Benet-Buchholz, X. Sala, A. Tessier and A. Llobet, *ACS Catal.*, 2018, **8**, 2039–2048.
178 R. Matheu, M. Z. Ertem, C. Gimbert-Suriñach, J. Benet-Buchholz, X. Sala and A. Llobet, *ACS Catal.*, 2017, **7**, 6525–6532.
179 L. Tong, L. Duan, Y. Xu, T. Privalov and L. Sun, *Angew. Chem., Int. Ed.*, 2011, **50**, 445–449.
180 V. Kunz, M. Schulze, D. Schmidt and F. Würthner, *ACS Energy Lett.*, 2017, **2**, 288–293.
181 V. Kunz, J. O. Lindner, M. Schulze, M. I. S. Röhr, D. Schmidt, R. Mitrić and F. Würthner, *Energy Environ. Sci.*, 2017, **10**, 2137–2153.
182 V. Kunz, D. Schmidt, M. I. S. Röhr, R. Mitrić and F. Würthner, *Adv. Energy Mater.*, 2017, **7**, 1602939.
183 J. M. Thomsen, D. L. Huang, R. H. Crabtree and G. W. Brudvig, *Dalton Trans.*, 2015, **44**, 12452–12472.
184 N. D. McDaniel, F. J. Coughlin, L. L. Tinker and S. Bernhard, *J. Am. Chem. Soc.*, 2008, **130**, 210–217.
185 J. F. Hull, D. Balcells, J. D. Blakemore, C. D. Incarvito, O. Eisenstein, G. W. Brudvig and R. H. Crabtree, *J. Am. Chem. Soc.*, 2009, **131**, 8730–8731.
186 J. D. Blakemore, N. D. Schley, D. Balcells, J. F. Hull, G. W. Olack, C. D. Incarvito, O. Eisenstein, G. W. Brudvig and R. H. Crabtree, *J. Am. Chem. Soc.*, 2010, **132**, 16017–16029.
187 T. P. Brewster, J. D. Blakemore, N. D. Schley, C. D. Incarvito, N. Hazari, G. W. Brudvig and R. H. Crabtree, *Organometallics*, 2011, **30**, 965–973.
188 M. Navarro, C. A. Smith, M. Li, S. Bernhard and M. Albrecht, *Chem. – Eur. J.*, 2018, **24**, 6386–6398.
189 R. Lalrempuia, N. D. McDaniel, H. Muller-Bunz, S. Bernhard and M. Albrecht, *Angew. Chem., Int. Ed.*, 2010, **49**, 9765–9768.
190 A. Savini, G. Bellachioma, G. Ciancaleoni, C. Zuccaccia, D. Zuccaccia and A. Macchioni, *Chem. Commun.*, 2010, **46**, 9218–9219.
191 D. G. Hetterscheid and J. N. Reek, *Chem. Commun.*, 2011, **47**, 2712–2714.
192 S. B. Sinha, D. Y. Shopov, L. S. Sharninghausen, C. J. Stein, B. Q. Mercado, D. Balcells, T. B. Pedersen, M. Reiher, G. W. Brudvig and R. H. Crabtree, *J. Am. Chem. Soc.*, 2017, **139**, 9672–9683.
193 L. S. Sharninghausen, S. B. Sinha, D. Y. Shopov, B. Choi, B. Q. Mercado, X. Roy, D. Balcells, G. W. Brudvig and R. H. Crabtree, *J. Am. Chem. Soc.*, 2016, **138**, 15917–15926.
194 J. E. Post, *Proc. Natl. Acad. Sci. U. S. A.*, 1999, **96**, 3447–3454.
195 Y. Naruta, M. Sasayama and T. Sasaki, *Angew. Chem., Int. Ed.*, 1994, **33**, 1839–1841.
196 Y. Shimazaki, T. Nagano, H. Takesue, B. H. Ye, F. Tani and Y. Naruta, *Angew. Chem., Int. Ed.*, 2004, **43**, 98–100.
197 J. Limburg, J. S. Vrettos, H. Chen, J. C. de Paula, R. H. Crabtree and G. W. Brudvig, *J. Am. Chem. Soc.*, 2001, **123**, 423–430.
198 J. Limburg, G. W. Brudvig and R. H. Crabtree, *J. Am. Chem. Soc.*, 1997, **119**, 2761–2762.

199 C. Baffert, S. Romain, A. Richardot, J.-C. Leprêtre, B. Lefebvre, A. Deronzier and M.-N. Collomb, *J. Am. Chem. Soc.*, 2005, **127**, 13694–13704.
200 M. Hirahara, H. Yamazaki, S. Yamada, K. Matsubara, K. Saito, T. Yui and M. Yagi, *Catal. Sci. Technol.*, 2013, **3**, 1776–1781.
201 M. Yagi and K. Narita, *J. Am. Chem. Soc.*, 2004, **126**, 8084–8085.
202 M. Yagi, M. Toda, S. Yamada and H. Yamazaki, *Chem. Commun.*, 2010, **46**, 8594–8596.
203 G. Li, E. M. Sproviero, R. C. Snoeberger Iii, N. Iguchi, J. D. Blakemore, R. H. Crabtree, G. W. Brudvig and V. S. Batista, *Energy Environ. Sci.*, 2009, **2**, 230–238.
204 G. Li, E. M. Sproviero, W. R. McNamara, R. C. Snoeberger III, R. H. Crabtree, G. W. Brudvig and V. S. Batista, *J. Phys. Chem. B*, 2010, **114**, 14214–14222.
205 B. Nepal and S. Das, *Angew. Chem., Int. Ed.*, 2013, **52**, 7224–7227.
206 C. Baffert, J.-M. Latour, L. P. Nielsenb, M.-N. Collomb, K. H. Lund and N. Thorup, *Dalton Trans.*, 2003, 1765–1772.
207 Y. Gao, T. Åkermark, J. Liu, L. Sun and B. Åkermark, *J. Am. Chem. Soc.*, 2009, **131**, 8726–8727.
208 E. A. Karlsson, B. L. Lee, T. Akermark, E. V. Johnston, M. D. Karkas, J. Sun, O. Hansson, J. E. Backvall and B. Akermark, *Angew. Chem., Int. Ed.*, 2011, **50**, 11715–11718.
209 L. Ma, Q. Wang, W. L. Man, H. K. Kwong, C. C. Ko and T. C. Lau, *Angew. Chem., Int. Ed.*, 2015, **54**, 5246–5249.
210 M. D. Kärkäs, E. V. Johnston, O. Verho and B. Åkermark, *Acc. Chem. Res.*, 2014, **47**, 100–111.
211 C. Chen, Y. Li, G. Zhao, R. Yao and C. Zhang, *ChemSusChem*, 2017, **10**, 4403–4408.
212 P. Huang, A. Magnuson, R. Lomoth, M. Abrahamsson, M. Tamm, L. Sun, B. van Rotterdam, J. Park, L. Hammarström, B. Åkermark and S. Styring, *J. Inorg. Biochem.*, 2002, **91**, 159–172.
213 A. Magnuson, M. Anderlund, O. Johansson, P. Lindblad, R. Lomoth, T. Polivka, S. Ott, K. Stensjö, S. Styring, V. Sundström and L. Hammarström, *Acc. Chem. Res.*, 2009, **42**, 1899–1909.
214 L. Sun, H. Berglund, R. Davydov, T. Norrby, L. Hammarström, P. Korall, A. Börje, C. Philouze, K. Berg, A. Tran, M. Andersson, G. Stenhagen, J. Mårtensson, M. Almgren, S. Styring and B. Åkermark, *J. Am. Chem. Soc.*, 1997, **119**, 6996–7004.
215 A. Johansson, M. Abrahamsson, A. Magnuson, P. Huang, J. Mårtensson, S. Styring, L. Hammarström, L. Sun and B. Åkermark, *Inorg. Chem.*, 2003, **42**, 7502–7511.
216 J. S. Kanady, E. Y. Tsui, M. W. Day and T. Agapie, *Science*, 2011, **333**, 733–736.
217 J. S. Kanady, P. H. Lin, K. M. Carsch, R. J. Nielsen, M. K. Takase, W. A. Goddard, 3rd and T. Agapie, *J. Am. Chem. Soc.*, 2014, **136**, 14373–14376.
218 C. Zhang, C. Chen, H. Dong, J.-R. Shen, H. Dau and J. Zhao, *Science*, 2015, **348**, 690–693.
219 G. Maayan, N. Gluz and G. Christou, *Nat. Catal.*, 2017, **1**, 48–54.
220 M. Anbar and I. Pecht, *J. Am. Chem. Soc.*, 1967, **89**, 2553–2556.
221 D. J. Wasylenko, R. D. Palmer, E. Schott and C. P. Berlinguette, *Chem. Commun.*, 2012, **48**, 2107–2109.
222 D. K. Dogutan, R. McGuire, Jr. and D. G. Nocera, *J. Am. Chem. Soc.*, 2011, **133**, 9178–9180.
223 H. Lei, A. Han, F. Li, M. Zhang, Y. Han, P. Du, W. Lai and R. Cao, *Phys. Chem. Chem. Phys.*, 2014, **16**, 1883–1893.
224 T. Nakazono, A. R. Parent and K. Sakai, *Chem. Commun.*, 2013, **49**, 6325–6327.
225 D. Hong, J. Jung, J. Park, Y. Yamada, T. Suenobu, Y.-M. Lee, W. Nam and S. Fukuzumi, *Energy Environ. Sci.*, 2012, **5**, 7606–7616.
226 C.-F. Leung, S.-M. Ng, C.-C. Ko, W.-L. Man, J. Wu, L. Chen and T.-C. Lau, *Energy Environ. Sci.*, 2012, **5**, 7903–7907.
227 H. Chen, Z. Sun, X. Liu, A. Han and P. Du, *J. Phys. Chem. C*, 2015, **119**, 8998–9004.
228 E. Pizzolato, M. Natali, B. Posocco, A. Montellano Lopez, I. Bazzan, M. Di Valentin, P. Galloni, V. Conte, M. Bonchio, F. Scandola and A. Sartorel, *Chem. Commun.*, 2013, **49**, 9941–9943.
229 D. Wang and J. T. Groves, *Proc. Natl. Acad. Sci. U. S. A.*, 2013, **110**, 15579–15584.
230 N. S. McCool, D. M. Robinson, J. E. Sheats and G. C. Dismukes, *J. Am. Chem. Soc.*, 2011, **133**, 11446–11449.
231 G. La Ganga, F. Puntoriero, S. Campagna, I. Bazzan, S. Berardi, M. Bonchio, A. Sartorel, M. Natali and F. Scandola, *Faraday Discuss.*, 2012, **155**, 177–190.
232 S. Berardi, G. La Ganga, M. Natali, I. Bazzan, F. Puntoriero, A. Sartorel, F. Scandola, S. Campagna and M. Bonchio, *J. Am. Chem. Soc.*, 2012, **134**, 11104–11107.
233 M. D. Symes, D. A. Lutterman, T. S. Teets, B. L. Anderson, J. J. Breen and D. G. Nocera, *ChemSusChem*, 2013, **6**, 65–69.
234 X. Zhou, F. Li, H. Li, B. Zhang, F. Yu and L. Sun, *ChemSusChem*, 2014, **7**, 2453–2456.
235 B. Zhang, F. Li, F. Yu, X. Wang, X. Zhou, H. Li, Y. Jiang and L. Sun, *ACS Catal.*, 2014, **4**, 804–809.
236 Y. Wang, F. Li, H. Li, L. Bai and L. Sun, *Chem. Commun.*, 2016, **52**, 3050–3053.
237 S. Ye, C. Ding, R. Chen, F. Fan, P. Fu, H. Yin, X. Wang, Z. Wang, P. Du and C. Li, *J. Am. Chem. Soc.*, 2018, **140**, 3250–3256.
238 Y. Wang, F. Li, X. Zhou, F. Yu, J. Du, L. Bai and L. Sun, *Angew. Chem., Int. Ed.*, 2017, **56**, 6911–6915.
239 P. F. Smith, L. Hunt, A. B. Laursen, V. Sagar, S. Kaushik, K. U. D. Calvinho, G. Marotta, E. Mosconi, F. De Angelis and G. C. Dismukes, *J. Am. Chem. Soc.*, 2015, **137**, 15460–15468.
240 A. I. Nguyen, M. S. Ziegler, P. Ona-Burgos, M. Sturzbecher-Hohne, W. Kim, D. E. Bellone and T. D. Tilley, *J. Am. Chem. Soc.*, 2015, **137**, 12865–12872.
241 C. N. Brodsky, R. G. Hadt, D. Hayes, B. J. Reinhart, N. Li, L. X. Chen and D. G. Nocera, *Proc. Natl. Acad. Sci. U. S. A.*, 2017, **114**, 3855–3860.
242 R. G. Hadt, D. Hayes, C. N. Brodsky, A. M. Ullman, D. M. Casa, M. H. Upton, D. G. Nocera and L. X. Chen, *J. Am. Chem. Soc.*, 2016, **138**, 11017–11030.

243 F. Evangelisti, R. More, F. Hodel, S. Luber and G. R. Patzke, *J. Am. Chem. Soc.*, 2015, **137**, 11076–11084.
244 M. Kondo and S. Masaoka, *Chem. Lett.*, 2016, **45**, 1220–1231.
245 S. M. Barnett, K. I. Goldberg and J. M. Mayer, *Nat. Chem.*, 2012, **4**, 498–502.
246 T. Zhang, C. Wang, S. Liu, J. L. Wang and W. Lin, *J. Am. Chem. Soc.*, 2014, **136**, 273–281.
247 D. L. Gerlach, S. Bhagan, A. A. Cruce, D. B. Burks, I. Nieto, H. T. Truong, S. P. Kelley, C. J. Herbst-Gervasoni, K. L. Jernigan, M. K. Bowman, S. Pan, M. Zeller and E. T. Papish, *Inorg. Chem.*, 2014, **53**, 12689–12698.
248 J. S. Pap, L. Szyrwiel, D. Sranko, Z. Kerner, B. Setner, Z. Szewczuk and W. Malinka, *Chem. Commun.*, 2015, **51**, 6322–6324.
249 K. J. Fisher, K. L. Materna, B. Q. Mercado, R. H. Crabtree and G. W. Brudvig, *ACS Catal.*, 2017, **7**, 3384–3387.
250 B. Rudshteyn, K. J. Fisher, H. M. C. Lant, K. R. Yang, B. Q. Mercado, G. W. Brudvig, R. H. Crabtree and V. S. Batista, *ACS Catal.*, 2018, **8**, 7952–7960.
251 X. J. Su, M. Gao, L. Jiao, R. Z. Liao, P. E. Siegbahn, J. P. Cheng and M. T. Zhang, *Angew. Chem., Int. Ed.*, 2015, **54**, 4909–4914.
252 J.-W. Wang, W.-J. Liu, D.-C. Zhong and T.-B. Lu, *Coord. Chem. Rev.*, 2019, **378**, 237–261.
253 M. Zhang, M. T. Zhang, C. Hou, Z. F. Ke and T. B. Lu, *Angew. Chem., Int. Ed.*, 2014, **53**, 13042–13048.
254 J.-W. Wang, C. Hou, H.-H. Huang, W.-J. Liu, Z.-F. Ke and T.-B. Lu, *Catal. Sci. Technol.*, 2017, **7**, 5585–5593.
255 Y. Han, Y. Wu, W. Lai and R. Cao, *Inorg. Chem.*, 2015, **54**, 5604–5613.
256 L. Wang, L. Duan, R. B. Ambre, Q. Daniel, H. Chen, J. Sun, B. Das, A. Thapper, J. Uhlig, P. Dinér and L. Sun, *J. Catal.*, 2016, **335**, 72–78.
257 J. Lin, P. Kang, X. Liang, B. Ma and Y. Ding, *Electrochim. Acta*, 2017, **258**, 353–359.
258 G. Y. Luo, H. H. Huang, J. W. Wang and T. B. Lu, *ChemSusChem*, 2016, **9**, 485–491.
259 D. Wang and C. O. Bruner, *Inorg. Chem.*, 2017, **56**, 13638–13641.
260 A. Singh, S. L. Y. Chang, R. K. Hocking, U. Bach and L. Spiccia, *Energy Environ. Sci.*, 2013, **6**, 579–586.
261 A. Singh, S. L. Y. Chang, R. K. Hocking, U. Bach and L. Spiccia, *Catal. Sci. Technol.*, 2013, **3**, 1725–1732.
262 D. Wang, G. Ghirlanda and J. P. Allen, *J. Am. Chem. Soc.*, 2014, **136**, 10198–10201.
263 C. E. Tinberg and S. J. Lippard, *Acc. Chem. Res.*, 2011, **44**, 280–288.
264 B. Meunier, S. P. de Visser and S. Shaik, *Chem. Rev.*, 2004, **104**, 3947–3980.
265 M. Costas, K. Chen and L. Que Jr., *Coord. Chem. Rev.*, 2000, **200–202**, 517–544.
266 T. Liu, B. Zhang and L. Sun, *Chem. – Asian J.*, 2019, **14**, 31–43.
267 W. C. Ellis, N. D. McDaniel, S. Bernhard and T. J. Collins, *J. Am. Chem. Soc.*, 2010, **132**, 10990–10991.
268 E. L. Demeter, S. L. Hilburg, N. R. Washburn, T. J. Collins and J. R. Kitchin, *J. Am. Chem. Soc.*, 2014, **136**, 5603–5606.
269 R.-Z. Liao, X.-C. Li and P. E. M. Siegbahn, *Eur. J. Inorg. Chem.*, 2014, 728–741.
270 M. Z. Ertem, L. Gagliardi and C. J. Cramer, *Chem. Sci.*, 2012, **3**, 1293–1299.
271 G. Panchbhai, W. M. Singh, B. Das, R. T. Jane and A. Thapper, *Eur. J. Inorg. Chem.*, 2016, 3262–3268.
272 W. A. Hoffert, M. T. Mock, A. M. Appel and J. Y. Yang, *Eur. J. Inorg. Chem.*, 2013, 3846–3857.
273 Z. Codola, I. Garcia-Bosch, F. Acuna-Pares, I. Prat, J. M. Luis, M. Costas and J. Lloret-Fillol, *Chem. – Eur. J.*, 2013, **19**, 8042–8047.
274 F. Acuna-Pares, M. Costas, J. M. Luis and J. Lloret-Fillol, *Inorg. Chem.*, 2014, **53**, 5474–5485.
275 F. Acuna-Pares, Z. Codola, M. Costas, J. M. Luis and J. Lloret-Fillol, *Chem. – Eur. J.*, 2014, **20**, 5696–5707.
276 Z. Codola, L. Gomez, S. T. Kleespies, L. Que, Jr., M. Costas and J. Lloret-Fillol, *Nat. Commun.*, 2015, **6**, 5865.
277 E. E. Kasapbasi and M. H. Whangbo, *Inorg. Chem.*, 2012, **51**, 10850–10855.
278 L. D. Wickramasinghe, R. Zhou, R. Zong, P. Vo, K. J. Gagnon and R. P. Thummel, *J. Am. Chem. Soc.*, 2015, **137**, 13260–13263.
279 M. M. Najafpour, A. N. Moghaddam, D. J. Sedigh and M. Hołyńska, *Catal. Sci. Technol.*, 2014, **4**, 30–33.
280 A. R. Parent, T. Nakazono, S. Lin, S. Utsunomiya and K. Sakai, *Dalton Trans.*, 2014, **43**, 12501–12513.
281 Y. Liu, R. Xiang, X. Du, Y. Ding and B. Ma, *Chem. Commun.*, 2014, **50**, 12779–12782.
282 B. Zhang, F. Li, F. Yu, H. Cui, X. Zhou, H. Li, Y. Wang and L. Sun, *Chem. – Asian J.*, 2014, **9**, 1515–1518.
283 W. P. To, T. Wai-Shan Chow, C. W. Tse, X. Guan, J. S. Huang and C. M. Che, *Chem. Sci.*, 2015, **6**, 5891–5903.
284 M. K. Coggins, M. T. Zhang, A. K. Vannucci, C. J. Dares and T. J. Meyer, *J. Am. Chem. Soc.*, 2014, **136**, 5531–5534.
285 M. Okamura, M. Kondo, R. Kuga, Y. Kurashige, T. Yanai, S. Hayami, V. K. Praneeth, M. Yoshida, K. Yoneda, S. Kawata and S. Masaoka, *Nature*, 2016, **530**, 465–468.
286 Y. V. Geletii, B. Botar, P. Kogerler, D. A. Hillesheim, D. G. Musaev and C. L. Hill, *Angew. Chem., Int. Ed.*, 2008, **47**, 3896–3899.
287 A. Sartorel, M. Carraro, G. Scorrano, R. De Zorzi, S. Geremia, N. D. McDaniel, S. Bernhard and M. Bonchio, *J. Am. Chem. Soc.*, 2008, **130**, 5006–5007.
288 Q. Yin, J. M. Tan, C. Besson, Y. V. Geletii, D. G. Musaev, A. E. Kuznetsov, Z. Luo, K. I. Hardcastle and C. L. Hill, *Science*, 2010, **328**, 342–345.
289 C. Besson, Z. Huang, Y. V. Geletii, S. Lense, K. I. Hardcastle, D. G. Musaev, T. Lian, A. Proust and C. L. Hill, *Chem. Commun.*, 2010, **46**, 2784–2786.
290 M. Murakami, D. Hong, T. Suenobu, S. Yamaguchi, T. Ogura and S. Fukuzumi, *J. Am. Chem. Soc.*, 2011, **133**, 11605–11613.
291 P.-E. Car, M. Guttentag, K. K. Baldridge, R. Alberto and G. R. Patzke, *Green Chem.*, 2012, **14**, 1680–1688.

292 R. Cao, H. Ma, Y. V. Geletii, K. I. Hardcastle and C. L. Hill, *Inorg. Chem.*, 2009, **48**, 5596–5598.
293 G. Zhu, E. N. Glass, C. Zhao, H. Lv, J. W. Vickers, Y. V. Geletii, D. G. Musaev, J. Song and C. L. Hill, *Dalton Trans.*, 2012, **41**, 13043–13049.
294 A. E. Kuznetsov, Y. V. Geletii, C. L. Hill, K. Morokuma and D. G. Musaev, *J. Am. Chem. Soc.*, 2009, **131**, 6844–6854.
295 A. Sartorel, P. Miró, E. Salvadori, S. Romain, M. Carraro, G. Scorrano, M. D. Valentin, A. Llobet, C. Bo and M. Bonchio, *J. Am. Chem. Soc.*, 2009, **131**, 16051–16053.
296 Y. V. Geletii, C. Besson, Y. Hou, Q. Yin, D. G. Musaev, D. Quiñonero, R. Cao, K. I. Hardcastle, A. Proust, P. Kögerler and C. L. Hill, *J. Am. Chem. Soc.*, 2009, **131**, 17360–17370.
297 F. M. Toma, A. Sartorel, M. Iurlo, M. Carraro, S. Rapino, L. Hoober-Burkhardt, T. Da Ros, M. Marcaccio, G. Scorrano, F. Paolucci, M. Bonchio and M. Prato, *ChemSusChem*, 2011, **4**, 1447–1451.
298 F. M. Toma, A. Sartorel, M. Iurlo, M. Carraro, P. Parisse, C. Maccato, S. Rapino, B. R. Gonzalez, H. Amenitsch, T. Da Ros, L. Casalis, A. Goldoni, M. Marcaccio, G. Scorrano, G. Scoles, F. Paolucci, M. Prato and M. Bonchio, *Nat. Chem.*, 2010, **2**, 826–831.
299 A. Sartorel, M. Carraro, F. M. Toma, M. Prato and M. Bonchio, *Energy Environ. Sci.*, 2012, **5**, 5592–5603.
300 E. Anxolabehere-Mallart, C. Costentin, M. Fournier, S. Nowak, M. Robert and J. M. Saveant, *J. Am. Chem. Soc.*, 2012, **134**, 6104–6107.
301 T. W. Woolerton, S. Sheard, Y. S. Chaudhary and F. A. Armstrong, *Energy Environ. Sci.*, 2012, **5**, 7470–7490.
302 K. S. Joya and H. J. M. de Groot, *Int. J. Hydrogen Energy*, 2012, **37**, 8787–8799.
303 J. J. Stracke and R. G. Finke, *J. Am. Chem. Soc.*, 2011, **133**, 14872–14875.
304 L. Yu, Y. Ding and M. Zheng, *Appl. Catal., B*, 2017, **209**, 45–52.
305 R. Al-Oweini, A. Sartorel, B. S. Bassil, M. Natali, S. Berardi, F. Scandola, U. Kortz and M. Bonchio, *Angew. Chem., Int. Ed.*, 2014, **53**, 11182–11185.
306 M. Blasco-Ahicart, J. Soriano-Lopez, J. J. Carbo, J. M. Poblet and J. R. Galan-Mascaros, *Nat. Chem.*, 2018, **10**, 24–30.
307 M. D. Karkas and B. Akermark, *Dalton Trans.*, 2016, **45**, 14421–14461.
308 X. Wu, F. Li, B. Zhang and L. Sun, *J. Photochem. Photobiol., C*, 2015, **25**, 71–89.
309 Q. Daniel, R. B. Ambre, B. Zhang, B. Philippe, H. Chen, F. Li, K. Fan, S. Ahmadi, H. Rensmo and L. Sun, *ACS Catal.*, 2017, **7**, 1143–1149.
310 J. Li, R. Guttinger, R. More, F. Song, W. Wan and G. R. Patzke, *Chem. Soc. Rev.*, 2017, **46**, 6124–6147.
311 M. Frey, *ChemBioChem*, 2002, **3**, 153–160.
312 M. L. Helm, M. P. Stewart, R. M. Bullock, M. R. DuBois and D. L. DuBois, *Science*, 2011, **333**, 863–866.
313 M. Wang, L. Chen and L. Sun, *Energy Environ. Sci.*, 2012, **5**, 6763–6778.
314 J. W. Peters, G. J. Schut, E. S. Boyd, D. W. Mulder, E. M. Shepard, J. B. Broderick, P. W. King and M. W. Adams, *Biochim. Biophys. Acta*, 2015, **1853**, 1350–1369.
315 J. C. Fontecilla-Camps, A. Volbeda, C. Cavazza and Y. Nicolet, *Chem. Rev.*, 2007, **107**, 4273–4303.
316 C. Baffert, V. Artero and M. Fontecave, *Inorg. Chem.*, 2007, **46**, 1817–1824.
317 J. T. Muckerman and E. Fujita, *Chem. Commun.*, 2011, **47**, 12456–12458.
318 J. L. Dempsey, J. R. Winkler and H. B. Gray, *J. Am. Chem. Soc.*, 2010, **132**, 16774–16776.
319 B. H. Solis and S. Hammes-Schiffer, *J. Am. Chem. Soc.*, 2011, **133**, 19036–19039.
320 M. Kirch, J.-M. Lehn and J.-P. Sauvage, *Helv. Chim. Acta*, 1979, **62**, 1345–1384.
321 S. Fukuzumi, T. Kobayashi and T. Suenobu, *Angew. Chem., Int. Ed.*, 2011, **50**, 728–731.
322 T. Stoll, M. Gennari, I. Serrano, J. Fortage, J. Chauvin, F. Odobel, M. Rebarz, O. Poizat, M. Sliwa, A. Deronzier and M. N. Collomb, *Chem. – Eur. J.*, 2013, **19**, 782–792.
323 E. D. Cline, S. E. Adamson and S. Bernhard, *Inorg. Chem.*, 2008, **47**, 10378–10388.
324 K. Sakai and H. Ozawa, *Coord. Chem. Rev.*, 2007, **251**, 2753–2766.
325 J. R. McKone, S. C. Marinescu, B. S. Brunschwig, J. R. Winkler and H. B. Gray, *Chem. Sci.*, 2014, **5**, 865–878.
326 V. S. Thoi, Y. Sun, J. R. Long and C. J. Chang, *Chem. Soc. Rev.*, 2013, **42**, 2388–2400.
327 N. Coutard, N. Kaeffer and V. Artero, *Chem. Commun.*, 2016, **52**, 13728–13748.
328 V. Fourmond, S. Canaguier, B. Golly, M. J. Field, M. Fontecave and V. Artero, *Energy Environ. Sci.*, 2011, **4**, 2417–2427.
329 S. Canaguier, M. Field, Y. Oudart, J. Pecaut, M. Fontecave and V. Artero, *Chem. Commun.*, 2010, **46**, 5876–5878.
330 B. E. Barton, C. M. Whaley, T. B. Rauchfuss and D. L. Gray, *J. Am. Chem. Soc.*, 2009, **131**, 6942–6943.
331 D. Sil, Z. Martinez, S. Ding, N. Bhuvanesh, D. J. Darensbourg, M. B. Hall and M. Y. Darensbourg, *J. Am. Chem. Soc.*, 2018, **140**, 9904–9911.
332 B. E. Barton and T. B. Rauchfuss, *J. Am. Chem. Soc.*, 2010, **132**, 14877–14885.
333 D. Schilter, J. M. Camara, M. T. Huynh, S. Hammes-Schiffer and T. B. Rauchfuss, *Chem. Rev.*, 2016, **116**, 8693–8749.
334 M. Rakowski DuBois and D. L. DuBois, *Chem. Soc. Rev.*, 2009, **38**, 62–72.
335 A. D. Wilson, R. H. Newell, M. J. McNevin, J. T. Muckerman, M. R. DuBois and D. L. DuBois, *J. Am. Chem. Soc.*, 2006, **128**, 358–366.
336 C. J. Curtis, A. Miedaner, W. W. Ellis and D. L. DuBois, *J. Am. Chem. Soc.*, 2002, **124**, 1918–1925.
337 M. R. Dubois and D. L. Dubois, *Acc. Chem. Res.*, 2009, **42**, 1974–1982.
338 D. H. Pool and D. L. DuBois, *J. Organomet. Chem.*, 2009, **694**, 2858–2865.
339 U. J. Kilgore, J. A. Roberts, D. H. Pool, A. M. Appel, M. P. Stewart, M. R. DuBois, W. G. Dougherty, W. S. Kassel, R. M. Bullock and D. L. DuBois, *J. Am. Chem. Soc.*, 2011, **133**, 5861–5872.

340 J. Hawecker, J. M. Lehn and R. Ziessel, *Nouv. J. Chim.*, 1983, **7**, 271–277.
341 P. Connolly and J. H. Espenson, *Inorg. Chem.*, 1986, **25**, 2684–2688.
342 X. Hu, B. M. Cossairt, B. S. Brunschwig, N. S. Lewis and J. C. Peters, *Chem. Commun.*, 2005, 4723–4725.
343 M. Razavet, V. Artero and M. Fontecave, *Inorg. Chem.*, 2005, **44**, 4786–4795.
344 J. L. Dempsey, B. S. Brunschwig, J. R. Winkler and H. B. Gray, *Acc. Chem. Res.*, 2009, **42**, 1995–2004.
345 P. A. Jacques, V. Artero, J. Pecaut and M. Fontecave, *Proc. Natl. Acad. Sci. U. S. A.*, 2009, **106**, 20627–20632.
346 N. Kaeffer, M. Chavarot-Kerlidou and V. Artero, *Acc. Chem. Res.*, 2015, **48**, 1286–1295.
347 C. C. McCrory, C. Uyeda and J. C. Peters, *J. Am. Chem. Soc.*, 2012, **134**, 3164–3170.
348 B. H. Solis, Y. Yu and S. Hammes-Schiffer, *Inorg. Chem.*, 2013, **52**, 6994–6999.
349 A. Bhattacharjee, E. S. Andreiadis, M. Chavarot-Kerlidou, M. Fontecave, M. J. Field and V. Artero, *Chem. – Eur. J.*, 2013, **19**, 15166–15174.
350 H. I. Karunadasa, E. Montalvo, Y. Sun, M. Majda, J. R. Long and C. J. Chang, *Science*, 2012, **335**, 698–702.
351 H. I. Karunadasa, C. J. Chang and J. R. Long, *Nature*, 2010, **464**, 1329–1333.
352 E. J. Sundstrom, X. Yang, V. S. Thoi, H. I. Karunadasa, C. J. Chang, J. R. Long and M. Head-Gordon, *J. Am. Chem. Soc.*, 2012, **134**, 5233–5242.
353 V. S. Thoi, H. I. Karunadasa, Y. Surendranath, J. R. Long and C. J. Chang, *Energy Environ. Sci.*, 2012, **5**, 7762–7770.
354 B. Hinnemann, P. G. Moses, J. Bonde, K. P. Jørgensen, J. H. Nielsen, S. Horch, I. Chorkendorff and J. K. Nørskov, *J. Am. Chem. Soc.*, 2005, **127**, 5308–5309.
355 J.-P. Cao, T. Fang, L.-L. Zhou, L.-Z. Fu and S. Zhan, *Electrochim. Acta*, 2014, **147**, 129–135.
356 J.-P. Cao, L.-L. Zhou, L.-Z. Fu and S. Zhan, *J. Power Sources*, 2014, **272**, 169–175.
357 W. Zhang, W. Lai and R. Cao, *Chem. Rev.*, 2017, **117**, 3717–3797.
358 I. Bhugun, D. Lexa and J.-M. Savéant, *J. Am. Chem. Soc.*, 1996, **118**, 3982–3983.
359 D. J. Graham and D. G. Nocera, *Organometallics*, 2014, **33**, 4994–5001.
360 R. M. Kellett and T. G. Spiro, *Inorg. Chem.*, 1985, **24**, 2373–2377.
361 R. M. Kellett and T. G. Spiro, *Inorg. Chem.*, 1985, **24**, 2378–2382.
362 C. H. Lee, D. K. Dogutan and D. G. Nocera, *J. Am. Chem. Soc.*, 2011, **133**, 8775–8777.
363 D. K. Bediako, B. H. Solis, D. K. Dogutan, M. M. Roubelakis, A. G. Maher, C. H. Lee, M. B. Chambers, S. Hammes-Schiffer and D. G. Nocera, *Proc. Natl. Acad. Sci. U. S. A.*, 2014, **111**, 15001–15006.
364 C. Costentin, H. Dridi and J. M. Saveant, *J. Am. Chem. Soc.*, 2014, **136**, 13727–13734.
365 M. M. Roubelakis, D. K. Bediako, D. K. Dogutan and D. G. Nocera, *Energy Environ. Sci.*, 2012, **5**, 7737–7740.
366 P. Zhang, M. Wang, Y. Yang, T. Yao and L. Sun, *Angew. Chem., Int. Ed.*, 2014, **53**, 13803–13807.
367 N. Queyriaux, R. T. Jane, J. Massin, V. Artero and M. Chavarot-Kerlidou, *Coord. Chem. Rev.*, 2015, **304-305**, 3–19.
368 D. Brazzolotto, M. Gennari, N. Queyriaux, T. R. Simmons, J. Pecaut, S. Demeshko, F. Meyer, M. Orio, V. Artero and C. Duboc, *Nat. Chem.*, 2016, **8**, 1054–1060.
369 T. Straistari, R. Hardre, J. Fize, S. Shova, M. Giorgi, M. Reglier, V. Artero and M. Orio, *Chem. – Eur. J.*, 2018, **24**, 8779–8786.
370 B. J. Fisher and R. Eisenberg, *J. Am. Chem. Soc.*, 1980, **102**, 7361–7363.
371 J.-P. Collin, A. Jouaiti and J.-P. Sauvage, *Inorg. Chem.*, 1988, **27**, 1986–1990.
372 W. M. Singh, T. Baine, S. Kudo, S. Tian, X. A. Ma, H. Zhou, N. J. DeYonker, T. C. Pham, J. C. Bollinger, D. L. Baker, B. Yan, C. E. Webster and X. Zhao, *Angew. Chem., Int. Ed.*, 2012, **51**, 5941–5944.
373 W. R. McNamara, Z. Han, P. J. Alperin, W. W. Brennessel, P. L. Holland and R. Eisenberg, *J. Am. Chem. Soc.*, 2011, **133**, 15368–15371.
374 W. R. McNamara, Z. Han, C.-J. M. Yin, W. W. Brennessel, P. L. Holland and R. Eisenberg, *Proc. Natl. Acad. Sci. U. S. A.*, 2012, **109**, 15594–15599.
375 B. D. Stubbert, J. C. Peters and H. B. Gray, *J. Am. Chem. Soc.*, 2011, **133**, 18070–18073.
376 J. Pinson and F. Podvorica, *Chem. Soc. Rev.*, 2005, **34**, 429–439.
377 F. Wang, *ChemSusChem*, 2017, **10**, 4393–4402.
378 S. Meshitsuka, M. Ichikawa and K. Tamaru, *J. Chem. Soc., Chem. Commun.*, 1974, 158–159.
379 M. Beley, J.-P. Collin, R. Ruppert and J.-P. Sauvage, *J. Chem. Soc., Chem. Commun.*, 1984, 1315–1316.
380 H. Hori, F. P. A. Johnson, K. Koike, O. Ishitani and T. Ibusuki, *J. Photochem. Photobiol., A*, 1996, **96**, 171–174.
381 J. Hawecker, J.-M. Lehn and R. Ziessel, *J. Chem. Soc., Chem. Commun.*, 1984, 328–330.
382 J. Hawecker, J.-M. Lehn and R. Ziessel, *J. Chem. Soc., Chem. Commun.*, 1983, 536–538.
383 B. P. Sullivan, C. M. Bolinger, D. Conrad, W. J. Vining and T. J. Meyer, *J. Chem. Soc., Chem. Commun.*, 1985, 1414–1416.
384 J. R. Pugh, M. R. M. Bruce, B. P. Sullivan and T. J. Meyer, *Inorg. Chem.*, 1991, **30**, 86–91.
385 H. Ishida, H. Tanaka, K. Tanaka and T. Tanaka, *J. Chem. Soc., Chem. Commun.*, 1987, 131–132.
386 H. Ishida, K. Tanaka and T. Tanaka, *Organometallics*, 1987, **6**, 181–186.
387 H. Ishida, T. Terada, K. Tanaka and T. Tanaka, *Inorg. Chem.*, 1990, **29**, 905–911.
388 S. Chardon-Noblat, M.-N. Collomb-Dunand-Sauthier, A. Deronzier, R. Ziessel and D. Zsoldos, *Inorg. Chem.*, 1994, **33**, 4410–4412.
389 M.-N. Collomb-Dunand-Sauthier, A. Deronzier and R. Ziessel, *J. Phys. Chem.*, 1993, **97**, 5973–5979.

390 C. Caix, S. Chardon-Noblat and A. Deronzier, *J. Electroanal. Chem.*, 1997, **434**, 163–170.
391 C. M. Bolinger, B. P. Sullivan, D. Conrad, J. A. Gilbert, N. Story and T. J. Meyer, *J. Chem. Soc., Chem. Commun.*, 1985, 796–797.
392 L. Duan, G. F. Manbeck, M. Kowalczyk, D. J. Szalda, J. T. Muckerman, Y. Himeda and E. Fujita, *Inorg. Chem.*, 2016, **55**, 4582–4594.
393 P. Paul, B. Tyagi, A. K. Bilakhiya, M. M. Bhadbhade, E. Suresh and G. Ramachandraiah, *Inorg. Chem.*, 1998, **37**, 5733–5742.
394 A. Sinopoli, N. T. La Porte, J. F. Martinez, M. R. Wasielewski and M. Sohail, *Coord. Chem. Rev.*, 2018, **365**, 60–74.
395 J. Hawecker, J.-M. Lehn and R. Ziessel, *Helv. Chim. Acta*, 1986, **69**, 1990–2012.
396 F. P. A. Johnson, M. W. George, F. Hartl and J. J. Turner, *Organometallics*, 1996, **15**, 3374–3387.
397 J. M. Smieja and C. P. Kubiak, *Inorg. Chem.*, 2010, **49**, 9283–9289.
398 S. A. Chabolla, E. A. Dellamary, C. W. Machan, F. A. Tezcan and C. P. Kubiak, *Inorg. Chim. Acta*, 2014, **422**, 109–113.
399 E. E. Benson and C. P. Kubiak, *Chem. Commun.*, 2012, **48**, 7374–7376.
400 H. Takeda, K. Koike, H. Inoue and O. Ishitani, *J. Am. Chem. Soc.*, 2008, **130**, 2023–2031.
401 Y. Yamazaki, H. Takeda and O. Ishitani, *J. Photochem. Photobiol., C*, 2015, **25**, 106–137.
402 G. Sahara and O. Ishitani, *Inorg. Chem.*, 2015, **54**, 5096–5104.
403 B. A. Johnson, S. Maji, H. Agarwala, T. A. White, E. Mijangos and S. Ott, *Angew. Chem., Int. Ed.*, 2016, **55**, 1825–1829.
404 C. M. Bolinger, N. Story, B. P. Sullivan and T. J. Meyer, *Inorg. Chem.*, 1988, **27**, 4582–4587.
405 C. W. Machan, M. D. Sampson and C. P. Kubiak, *J. Am. Chem. Soc.*, 2015, **137**, 8564–8571.
406 Z. Chen, C. Chen, D. R. Weinberg, P. Kang, J. J. Concepcion, D. P. Harrison, M. S. Brookhart and T. J. Meyer, *Chem. Commun.*, 2011, **47**, 12607–12609.
407 M. R. M. Bruce, E. Megehee, B. P. Sullivan, H. Thorp, T. R. O'Toole, A. Downard and T. J. Meyer, *Organometallics*, 1988, **7**, 238–240.
408 J. Chauvin, F. Lafolet, S. Chardon-Noblat, A. Deronzier, M. Jakonen and M. Haukka, *Chem. – Eur. J.*, 2011, **17**, 4313–4322.
409 M. R. M. Bruce, E. Megehee, B. P. Sullivan, H. H. Thorp, T. R. O'Toole, A. Downard, J. R. Pugh and T. J. Meyer, *Inorg. Chem.*, 1992, **31**, 4864–4873.
410 S. Sato, T. Morikawa, T. Kajino and O. Ishitani, *Angew. Chem., Int. Ed.*, 2013, **52**, 988–992.
411 Y. Kuramochi, M. Kamiya and H. Ishida, *Inorg. Chem.*, 2014, **53**, 3326–3332.
412 P. Voyame, K. E. Toghill, M. A. Mendez and H. H. Girault, *Inorg. Chem.*, 2013, **52**, 10949–10957.
413 Y. Kuramochi, J. Itabashi, K. Fukaya, A. Enomoto, M. Yoshida and H. Ishida, *Chem. Sci.*, 2015, **6**, 3063–3074.
414 J. W. Raebiger, J. W. Turner, B. C. Noll, C. J. Curtis, A. Miedaner, B. Cox and D. L. DuBois, *Organometallics*, 2006, **25**, 3345–3351.
415 D. L. DuBois, A. Miedaner and R. C. Haltiwanger, *J. Am. Chem. Soc.*, 1991, **113**, 8753–8764.
416 J.-M. Lehn and R. Ziessel, *Proc. Natl. Acad. Sci. U. S. A.*, 1982, **79**, 701–704.
417 T. Hirose, S. Shigaki, M. Hirose and A. Fushimi, *J. Fluorine Chem.*, 2010, **131**, 915–921.
418 A. G. M. M. Hossain, T. Nagaoka and K. Ogura, *Electrochim. Acta*, 1997, **42**, 2577–2585.
419 S. Matsuoka, K. Yamamoto, T. Ogata, M. Kusaba, N. Nakashima, E. Fujita and S. Yanagida, *J. Am. Chem. Soc.*, 1993, **115**, 601–609.
420 C.-M. Che, S.-T. Mak, W.-O. Lee and K.-W. Fung, *J. Chem. Soc., Dalton Trans.*, 1988, 2153–2159.
421 K. Mochizuki, S. Manaka, I. Takeda and T. Kondo, *Inorg. Chem.*, 1996, **35**, 5132–5136.
422 A. Chapovetsky, T. H. Do, R. Haiges, M. K. Takase and S. C. Marinescu, *J. Am. Chem. Soc.*, 2016, **138**, 5765–5768.
423 M. Beley, J.-P. Collin, R. Ruppert and J.-P. Sauvage, *J. Am. Chem. Soc.*, 1986, **108**, 7461–7467.
424 M. Bourrez, F. Molton, S. Chardon-Noblat and A. Deronzier, *Angew. Chem., Int. Ed.*, 2011, **50**, 9903–9906.
425 M. D. Sampson, A. D. Nguyen, K. A. Grice, C. E. Moore, A. L. Rheingold and C. P. Kubiak, *J. Am. Chem. Soc.*, 2014, **136**, 5460–5471.
426 K. T. Ngo, M. McKinnon, B. Mahanti, R. Narayanan, D. C. Grills, M. Z. Ertem and J. Rochford, *J. Am. Chem. Soc.*, 2017, **139**, 2604–2618.
427 C. Costentin, M. Robert and J. M. Saveant, *Acc. Chem. Res.*, 2015, **48**, 2996–3006.
428 H. Rao, L. C. Schmidt, J. Bonin and M. Robert, *Nature*, 2017, **548**, 74–77.
429 M. Hammouche, D. Lexa, M. Momenteau and J. M. Saveant, *J. Am. Chem. Soc.*, 1991, **113**, 8455–8466.
430 I. Bhugun, D. Lexa and J.-M. Savéant, *J. Am. Chem. Soc.*, 1996, **118**, 1769–1776.
431 C. Costentin, G. Passard, M. Robert and J.-M. Savéant, *Proc. Natl. Acad. Sci. U. S. A.*, 2014, **111**, 14990–14994.
432 I. Azcarate, C. Costentin, M. Robert and J. M. Saveant, *J. Am. Chem. Soc.*, 2016, **138**, 16639–16644.
433 Y. Wu, J. Jiang, Z. Weng, M. Wang, D. L. J. Broere, Y. Zhong, G. W. Brudvig, Z. Feng and H. Wang, *ACS Cent. Sci.*, 2017, **3**, 847–852.
434 Z. Weng, J. Jiang, Y. Wu, Z. Wu, X. Guo, K. L. Materna, W. Liu, V. S. Batista, G. W. Brudvig and H. Wang, *J. Am. Chem. Soc.*, 2016, **138**, 8076–8079.
435 S. Lin, C. S. Diercks, Y.-B. Zhang, N. Kornienko, E. M. Nichols, Y. Zhao, A. R. Paris, D. Kim, P. Yang, O. M. Yaghi and C. J. Chang, *Science*, 2015, **349**, 1208–1213.
436 J. Jiang, A. J. Matula, J. R. Swierk, N. Romano, Y. Wu, V. S. Batista, R. H. Crabtree, J. S. Lindsey, H. Wang and G. W. Brudvig, *ACS Catal.*, 2018, **8**, 10131–10136.
437 K. A. Grice, *Coord. Chem. Rev.*, 2017, **336**, 78–95.
438 R. Angamuthu, P. Byers, M. Lutz, A. L. Spek and E. Bouwman, *Science*, 2010, **327**, 313–315.
439 J. Grodkowski, P. Neta, E. Fujita, A. Mahammed, L. Simkhovich and Z. Gross, *J. Phys. Chem. A*, 2002, **106**, 4772–4778.

440 G. Seshadri, C. Lin and A. B. Bocarsly, *J. Electroanal. Chem.*, 1994, **372**, 145–150.
441 E. E. Barton, D. M. Rampulla and A. B. Bocarsly, *J. Am. Chem. Soc.*, 2008, **130**, 6342–6344.
442 E. B. Cole, P. S. Lakkaraju, D. M. Rampulla, A. J. Morris, E. Abelev and A. B. Bocarsly, *J. Am. Chem. Soc.*, 2010, **132**, 11539–11551.
443 Z. Lu and T. J. Williams, *ACS Catal.*, 2016, **6**, 6670–6673.
444 P. Wang, G. Liang, M. R. Reddy, M. Long, K. Driskill, C. Lyons, B. Donnadieu, J. C. Bollinger, C. E. Webster and X. Zhao, *J. Am. Chem. Soc.*, 2018, **140**, 9219–9229.
445 X. Liu, S. Inagaki and J. Gong, *Angew. Chem., Int. Ed.*, 2016, **55**, 14924–14950.
446 B. O'Regan and M. Grätzel, *Nature*, 1991, **353**, 737–740.
447 J. A. Treadway, J. A. Moss and T. J. Meyer, *Inorg. Chem.*, 1999, **38**, 4386–4387.
448 B. C. O'Regan and J. R. Durrant, *Acc. Chem. Res.*, 2009, **42**, 1799–1808.
449 W. J. Youngblood, S. H. Lee, Y. Kobayashi, E. A. Hernandez-Pagan, P. G. Hoertz, T. A. Moore, A. L. Moore, D. Gust and T. E. Mallouk, *J. Am. Chem. Soc.*, 2009, **131**, 926–927.
450 Y. Zhao, J. R. Swierk, J. D. Megiatto Jr, B. Sherman, W. J. Youngblood, D. Qin, D. M. Lentz, A. L. Moore, T. A. Moore, D. Gust and T. E. Mallouk, *Proc. Natl. Acad. Sci. U. S. A.*, 2012, **109**, 15612–15616.
451 W. J. Youngblood, S.-H. A. Lee, K. Maeda and T. E. Mallouk, *Acc. Chem. Res.*, 2009, **42**, 1966–1973.
452 R. Brimblecombe, A. Koo, G. C. Dismukes, G. F. Swiegers and L. Spiccia, *J. Am. Chem. Soc.*, 2010, **132**, 2892–2894.
453 L. Li, L. Duan, Y. Xu, M. Gorlov, A. Hagfeldt and L. Sun, *Chem. Commun.*, 2010, **46**, 7307–7309.
454 G. F. Moore, J. D. Blakemore, R. L. Milot, J. F. Hull, H.-E. Song, L. Cai, C. A. Schmuttenmaer, R. H. Crabtree and G. W. Brudvig, *Energy Environ. Sci.*, 2011, **4**, 2389–2392.
455 F. Li, H. Yang, W. Li and L. Sun, *Joule*, 2018, **2**, 36–60.
456 Z. Yu, F. Li and L. Sun, *Energy Environ. Sci.*, 2015, **8**, 760–775.
457 J. J. Concepcion, J. W. Jurss, P. G. Hoertz and T. J. Meyer, *Angew. Chem., Int. Ed.*, 2009, **48**, 9473–9476.
458 B. D. Sherman, Y. Xie, M. V. Sheridan, D. Wang, D. W. Shaffer, T. J. Meyer and J. J. Concepcion, *ACS Energy Lett.*, 2016, **2**, 124–128.
459 W. Song, C. R. K. Glasson, H. Luo, K. Hanson, M. K. Brennaman, J. J. Concepcion and T. J. Meyer, *J. Phys. Chem. Lett.*, 2011, **2**, 1808–1813.
460 M. R. Norris, J. J. Concepcion, Z. Fang, J. L. Templeton and T. J. Meyer, *Angew. Chem., Int. Ed.*, 2013, **52**, 13580–13583.
461 D. L. Ashford, W. Song, J. J. Concepcion, C. R. Glasson, M. K. Brennaman, M. R. Norris, Z. Fang, J. L. Templeton and T. J. Meyer, *J. Am. Chem. Soc.*, 2012, **134**, 19189–19198.
462 M. V. Sheridan, B. D. Sherman, R. L. Coppo, D. Wang, S. L. Marquard, K.-R. Wee, N. Y. Murakami Iha and T. J. Meyer, *ACS Energy Lett.*, 2016, **1**, 231–236.
463 X. Ding, Y. Gao, L. Zhang, Z. Yu, J. Liu and L. Sun, *ACS Catal.*, 2014, **4**, 2347–2350.
464 K. Hanson, D. A. Torelli, A. K. Vannucci, M. K. Brennaman, H. Luo, L. Alibabaei, W. Song, D. L. Ashford, M. R. Norris, C. R. K. Glasson, J. J. Concepcion and T. J. Meyer, *Angew. Chem., Int. Ed.*, 2012, **51**, 12782–12785.
465 D. L. Ashford, B. D. Sherman, R. A. Binstead, J. L. Templeton and T. J. Meyer, *Angew. Chem., Int. Ed.*, 2015, **54**, 4778–4781.
466 D. L. Ashford, A. M. Lapides, A. K. Vannucci, K. Hanson, D. A. Torelli, D. P. Harrison, J. L. Templeton and T. J. Meyer, *J. Am. Chem. Soc.*, 2014, **136**, 6578–6581.
467 A. M. Lapides, D. L. Ashford, K. Hanson, D. A. Torelli, J. L. Templeton and T. J. Meyer, *J. Am. Chem. Soc.*, 2013, **135**, 15450–15458.
468 L. Wang, D. L. Ashford, D. W. Thompson, T. J. Meyer and J. M. Papanikolas, *J. Phys. Chem. C*, 2013, **117**, 24250–24258.
469 A. M. Lapides, B. D. Sherman, M. K. Brennaman, C. J. Dares, K. R. Skinner, J. L. Templeton and T. J. Meyer, *Chem. Sci.*, 2015, **6**, 6398–6406.
470 A. K. Vannuccia, L. Alibabaeia, M. D. Losegob, J. J. Concepciona, B. Kalanyanb, G. N. Parsonsb and T. J. Meyer, *Proc. Natl. Acad. Sci. U. S. A.*, 2013, **110**, 20918–20922.
471 K. R. Wee, M. K. Brennaman, L. Alibabaei, B. H. Farnum, B. Sherman, A. M. Lapides and T. J. Meyer, *J. Am. Chem. Soc.*, 2014, **136**, 13514–13517.
472 K. L. Materna, B. Rudshteyn, B. J. Brennan, M. H. Kane, A. J. Bloomfield, D. L. Huang, D. Y. Shopov, V. S. Batista, R. H. Crabtree and G. W. Brudvig, *ACS Catal.*, 2016, **6**, 5371–5377.
473 B. J. Brennan, M. J. Llansola Portoles, P. A. Liddell, T. A. Moore, A. L. Moore and D. Gust, *Phys. Chem. Chem. Phys.*, 2013, **15**, 16605–16614.
474 K. L. Materna, B. J. Brennan and G. W. Brudvig, *Dalton Trans.*, 2015, **44**, 20312–20315.
475 K. Szpakolski, K. Latham, C. Rix, R. A. Rani and K. Kalantar-zadeh, *Polyhedron*, 2013, **52**, 719–732.
476 D. G. Brown, P. A. Schauer, J. Borau-Garcia, B. R. Fancy and C. P. Berlinguette, *J. Am. Chem. Soc.*, 2013, **135**, 1692–1695.
477 S. M. Zakeeruddin, M. K. Nazeeruddin, R. Humphry-Baker, P. Péchy, P. Quagliotto, C. Barolo, G. Viscardi and M. Grätzel, *Langmuir*, 2002, **18**, 952–954.
478 K. Hanson, M. D. Losego, B. Kalanyan, D. L. Ashford, G. N. Parsons and T. J. Meyer, *Chem. Mater.*, 2012, **25**, 3–5.
479 K. Hanson, M. D. Losego, B. Kalanyan, G. N. Parsons and T. J. Meyer, *Nano Lett.*, 2013, **13**, 4802–4809.
480 M. Yamamoto, L. Wang, F. Li, T. Fukushima, K. Tanaka, L. Sun and H. Imahori, *Chem. Sci.*, 2016, **7**, 1430–1439.
481 L. Zhang, Y. Gao, X. Ding, Z. Yu and L. Sun, *ChemSusChem*, 2014, **7**, 2801–2804.
482 F. Li, K. Fan, L. Wang, Q. Daniel, L. Duan and L. Sun, *ACS Catal.*, 2015, **5**, 3786–3790.
483 X. Ding, Y. Gao, L. Ye, L. Zhang and L. Sun, *ChemSusChem*, 2015, **8**, 3992–3995.
484 Y. Gao, L. Zhang, X. Ding and L. Sun, *Phys. Chem. Chem. Phys.*, 2014, **16**, 12008–12013.
485 D. Wang, M. V. Sheridan, B. Shan, B. H. Farnum, S. L. Marquard, B. D. Sherman, M. S. Eberhart, A. Nayak,

C. J. Dares, A. K. Das, R. M. Bullock and T. J. Meyer, *J. Am. Chem. Soc.*, 2017, **139**, 14518–14525.
486 M. S. Eberhart, D. Wang, R. N. Sampaio, S. L. Marquard, B. Shan, M. K. Brennaman, G. J. Meyer, C. Dares and T. J. Meyer, *J. Am. Chem. Soc.*, 2017, **139**, 16248–16255.
487 H. Tian, *ChemSusChem*, 2015, **8**, 3746–3759.
488 J. He, H. Lindström, A. Hagfeldt and S.-E. Lindquist, *Sol. Energy Mater. Sol. Cells*, 2000, **62**, 265–273.
489 J. Willkomm, K. L. Orchard, A. Reynal, E. Pastor, J. R. Durrant and E. Reisner, *Chem. Soc. Rev.*, 2016, **45**, 9–23.
490 L. Li, L. Duan, F. Wen, C. Li, M. Wang, A. Hagfeldt and L. Sun, *Chem. Commun.*, 2012, **48**, 988–990.
491 L. J. Antila, P. Ghamgosar, S. Maji, H. Tian, S. Ott and L. Hammarström, *ACS Energy Lett.*, 2016, **1**, 1106–1111.
492 C. E. Creissen, J. Warnan and E. Reisner, *Chem. Sci.*, 2018, **9**, 1439–1447.
493 N. Kaeffer, C. D. Windle, R. Brisse, C. Gablin, D. Leonard, B. Jousselme, M. Chavarot-Kerlidou and V. Artero, *Chem. Sci.*, 2018, **9**, 6721–6738.
494 J. M. Gardner, M. Beyler, M. Karnahl, S. Tschierlei, S. Ott and L. Hammarström, *J. Am. Chem. Soc.*, 2012, **134**, 19322–19325.
495 P. B. Pati, L. Zhang, B. Philippe, R. Fernández-Terán, S. Ahmadi, L. Tian, H. Rensmo, L. Hammarström and H. Tian, *ChemSusChem*, 2017, **10**, 2480–2495.
496 Z. Ji, M. He, Z. Huang, U. Ozkan and Y. Wu, *J. Am. Chem. Soc.*, 2013, **135**, 11696–11699.
497 N. Kaeffer, J. Massin, C. Lebrun, O. Renault, M. Chavarot-Kerlidou and V. Artero, *J. Am. Chem. Soc.*, 2016, **138**, 12308–12311.
498 B. Shan, A. K. Das, S. Marquard, B. H. Farnum, D. Wang, R. M. Bullock and T. J. Meyer, *Energy Environ. Sci.*, 2016, **9**, 3693–3697.
499 M. A. Gross, C. E. Creissen, K. L. Orchard and E. Reisner, *Chem. Sci.*, 2016, **7**, 5537–5546.
500 M. G. Gatty, S. Pullen, E. Sheibani, H. Tian, S. Ott and L. Hammarström, *Chem. Sci.*, 2018, **9**, 4983–4991.
501 A. M. Brown, L. J. Antila, M. Mirmohades, S. Pullen, S. Ott and L. Hammarström, *J. Am. Chem. Soc.*, 2016, **138**, 8060–8063.
502 K. A. Click, D. R. Beauchamp, Z. Huang, W. Chen and Y. Wu, *J. Am. Chem. Soc.*, 2016, **138**, 1174–1179.
503 G. Sahara, R. Abe, M. Higashi, T. Morikawa, K. Maeda, Y. Ueda and O. Ishitani, *Chem. Commun.*, 2015, **51**, 10722–10725.
504 Y. Kou, S. Nakatani, G. Sunagawa, Y. Tachikawa, D. Masui, T. Shimada, S. Takagi, D. A. Tryk, Y. Nabetani, H. Tachibana and H. Inoue, *J. Catal.*, 2014, **310**, 57–66.
505 H. Kumagai, G. Sahara, K. Maeda, M. Higashi, R. Abe and O. Ishitani, *Chem. Sci.*, 2017, **8**, 4242–4249.
506 R. Kamata, H. Kumagai, Y. Yamazaki, G. Sahara and O. Ishitani, *ACS Appl. Mater. Interfaces*, 2019, **11**, 5632–5641.
507 K. Fan, F. Li, L. Wang, Q. Daniel, E. Gabrielsson and L. Sun, *Phys. Chem. Chem. Phys.*, 2014, **16**, 25234–25240.
508 F. Li, K. Fan, B. Xu, E. Gabrielsson, Q. Daniel, L. Li and L. Sun, *J. Am. Chem. Soc.*, 2015, **137**, 9153–9159.
509 G. Sahara, H. Kumagai, K. Maeda, N. Kaeffer, V. Artero, M. Higashi, R. Abe and O. Ishitani, *J. Am. Chem. Soc.*, 2016, **138**, 14152–14158.
510 A. Fujishima and K. Honda, *Nature*, 1972, **238**, 37–38.
511 O. Khaselev and J. A. Turner, *Science*, 1998, **280**, 425–427.
512 A. G. Tamirat, J. Rick, A. A. Dubale, W.-N. Su and B.-J. Hwang, *Nanoscale Horiz.*, 2016, **1**, 243–267.
513 J. Yang, D. Wang, H. Han and C. Li, *Acc. Chem. Res.*, 2013, **46**, 1900–1909.
514 D. Li, J. Shi and C. Li, *Small*, 2018, **14**, 1704179.
515 U. T. Mueller-Westerhoff and A. Nazzal, *J. Am. Chem. Soc.*, 1984, **106**, 5381–5382.
516 D. K. Zhong, S. Zhao, D. E. Polyansky and E. Fujita, *J. Catal.*, 2013, **307**, 140–147.
517 X. Chen, X. Ren, Z. Liu, L. Zhuang and J. Lu, *Electrochem. Commun.*, 2013, **27**, 148–151.
518 B. M. Klepser and B. M. Bartlett, *J. Am. Chem. Soc.*, 2014, **136**, 1694–1697.
519 T. E. Rosser, M. A. Gross, Y. H. Lai and E. Reisner, *Chem. Sci.*, 2016, **7**, 4024–4035.
520 G. Liu, S. Ye, P. Yan, F. Xiong, P. Fu, Z. Wang, Z. Chen, J. Shi and C. Li, *Energy Environ. Sci.*, 2016, **9**, 1327–1334.
521 K. Fan, F. Li, L. Wang, Q. Daniel, H. Chen, E. Gabrielsson, J. Sun and L. Sun, *ChemSusChem*, 2015, **8**, 3242–3247.
522 W. Li, D. He, S. W. Sheehan, Y. He, J. E. Thorne, X. Yao, G. W. Brudvig and D. Wang, *Energy Environ. Sci.*, 2016, **9**, 1794–1802.
523 L. Badia-Bou, E. Mas-Marza, P. Rodenas, E. M. Barea, F. Fabregat-Santiago, S. Gimenez, E. Peris and J. Bisquert, *J. Phys. Chem. C*, 2013, **117**, 3826–3833.
524 S. W. Sheehan, J. M. Thomsen, U. Hintermair, R. H. Crabtree, G. W. Brudvig and C. A. Schmuttenmaer, *Nat. Commun.*, 2015, **6**, 6469.
525 K. S. Joya, N. Morlanes, E. Maloney, V. Rodionov and K. Takanabe, *Chem. Commun.*, 2015, **51**, 13481–13484.
526 B. Liu, J. Li, H. L. Wu, W. Q. Liu, X. Jiang, Z. J. Li, B. Chen, C. H. Tung and L. Z. Wu, *ACS Appl. Mater. Interfaces*, 2016, **8**, 18577–18583.
527 Y. Liu, Y. Jiang, F. Li, F. Yu, W. Jiang and L. Xia, *J. Mater. Chem. A*, 2018, **6**, 10761–10768.
528 S. Nakashima, R. Negishi and H. Tada, *Chem. Commun.*, 2016, **52**, 3665–3668.
529 Y. Hou, B. L. Abrams, P. C. Vesborg, M. E. Bjorketun, K. Herbst, L. Bech, A. M. Setti, C. D. Damsgaard, T. Pedersen, O. Hansen, J. Rossmeisl, S. Dahl, J. K. Norskov and I. Chorkendorff, *Nat. Mater.*, 2011, **10**, 434–438.
530 B. Seger, K. Herbst, T. Pedersen, B. Abrams, P. C. K. Vesborg, O. Hansen and I. Chorkendorff, *J. Electrochem. Soc.*, 2014, **161**, H722–H724.
531 J. J. Leung, J. Warnan, D. H. Nam, J. Z. Zhang, J. Willkomm and E. Reisner, *Chem. Sci.*, 2017, **8**, 5172–5180.
532 Y. H. Lai, H. S. Park, J. Z. Zhang, P. D. Matthews, D. S. Wright and E. Reisner, *Chem. – Eur. J.*, 2015, **21**, 3919–3923.
533 C.-Y. Lee, H. S. Park, J. C. Fontecilla-Camps and E. Reisner, *Angew. Chem., Int. Ed.*, 2016, **55**, 5971–5974.

534 N. Kornienko, J. Z. Zhang, K. K. Sakimoto, P. Yang and E. Reisner, *Nat. Nanotechnol.*, 2018, **13**, 890–899.
535 M. Kato, J. Z. Zhang, N. Paul and E. Reisner, *Chem. Soc. Rev.*, 2014, **43**, 6485–6497.
536 K. K. Sakimoto, A. B. Wong and P. Yang, *Science*, 2016, **351**, 74–77.
537 K. A. Brown, D. F. Harris, M. B. Wilker, A. Rasmussen, N. Khadka, H. Hamby, S. Keable, G. Dukovic, J. W. Peters, L. C. Seefeldt and P. W. King, *Science*, 2016, **352**, 448–450.
538 J. Z. Zhang, K. P. Sokol, N. Paul, E. Romero, R. van Grondelle and E. Reisner, *Nat. Chem. Biol.*, 2016, **12**, 1046–1052.
539 D. Mersch, C. Y. Lee, J. Z. Zhang, K. Brinkert, J. C. Fontecilla-Camps, A. W. Rutherford and E. Reisner, *J. Am. Chem. Soc.*, 2015, **137**, 8541–8549.
540 D. H. Nam, J. Z. Zhang, V. Andrei, N. Kornienko, N. Heidary, A. Wagner, K. Nakanishi, K. P. Sokol, B. Slater, I. Zebger, S. Hofmann, J. C. Fontecilla-Camps, C. B. Park and E. Reisner, *Angew. Chem., Int. Ed.*, 2018, **57**, 10595–10599.
541 K. P. Sokol, W. E. Robinson, A. R. Oliveira, J. Warnan, M. M. Nowaczyk, A. Ruff, I. A. C. Pereira and E. Reisner, *J. Am. Chem. Soc.*, 2018, **140**, 16418–16422.
542 A. Krawicz, J. Yang, E. Anzenberg, J. Yano, I. D. Sharp and G. F. Moore, *J. Am. Chem. Soc.*, 2013, **135**, 11861–11868.
543 D. Cedeno, A. Krawicz, P. Doak, M. Yu, J. B. Neaton and G. F. Moore, *J. Phys. Chem. Lett.*, 2014, **5**, 3222–3226.
544 A. M. Beiler, D. Khusnutdinova, S. I. Jacob and G. F. Moore, *Ind. Eng. Chem. Res.*, 2016, **55**, 5306–5314.
545 A. M. Beiler, D. Khusnutdinova, S. I. Jacob and G. F. Moore, *ACS Appl. Mater. Interfaces*, 2016, **8**, 10038–10047.
546 A. Krawicz, D. Cedeno and G. F. Moore, *Phys. Chem. Chem. Phys.*, 2014, **16**, 15818–15824.
547 D. Khusnutdinova, A. M. Beiler, B. L. Wadsworth, S. I. Jacob and G. F. Moore, *Chem. Sci.*, 2017, **8**, 253–259.
548 J. Gu, Y. Yan, J. L. Young, K. X. Steirer, N. R. Neale and J. A. Turner, *Nat. Mater.*, 2016, **15**, 456–460.
549 G. F. Moore and I. D. Sharp, *J. Phys. Chem. Lett.*, 2013, **4**, 568–572.
550 H. J. Kim, J. Seo and M. J. Rose, *ACS Appl. Mater. Interfaces*, 2016, **8**, 1061–1066.
551 J. Seo, R. T. Pekarek and M. J. Rose, *Chem. Commun.*, 2015, **51**, 13264–13267.
552 D. Cedeno, A. Krawicz and G. F. Moore, *Interface Focus*, 2015, **5**, 20140085.
553 T. Arai, S. Sato, K. Uemura, T. Morikawa, T. Kajino and T. Motohiro, *Chem. Commun.*, 2010, **46**, 6944–6946.
554 T. Arai, S. Sato, T. Kajino and T. Morikawa, *Energy Environ. Sci.*, 2013, **6**, 1274–1282.
555 T. Arai, S. Sato and T. Morikawa, *Energy Environ. Sci.*, 2015, **8**, 1998–2002.
556 S. Sato, T. Arai, T. Morikawa, K. Uemura, T. M. Suzuki, H. Tanaka and T. Kajino, *J. Am. Chem. Soc.*, 2011, **133**, 15240–15243.
557 P. Bornoz, F. F. Abdi, S. D. Tilley, B. Dam, R. van de Krol, M. Graetzel and K. Sivula, *J. Phys. Chem. C*, 2014, **118**, 16959–16966.
558 R. E. Rocheleau, E. L. Miller and A. Misra, *Energy Fuels*, 1998, **12**, 3–10.
559 O. Khaselev, A. Bansal and J. A. Turner, *Int. J. Hydrogen Energy*, 2001, **26**, 127–132.
560 R. C. Kainthla, B. Zelenay and J. O. M. Bockris, *J. Electrochem. Soc.*, 1987, **134**, 841–845.
561 G. Peharz, F. Dimroth and U. Wittstadt, *Int. J. Hydrogen Energy*, 2007, **32**, 3248–3252.
562 S. Licht, B. Wang, S. Mukerji, T. Soga, M. Umeno and H. Tributsch, *J. Phys. Chem. B*, 2000, **104**, 8920–8924.
563 A. Heller, *Science*, 1984, **223**, 1141–1148.
564 S. Chu and A. Majumdar, *Nature*, 2012, **488**, 294–303.
565 D. M. Powell, M. T. Winkler, H. J. Choi, C. B. Simmons, D. B. Needleman and T. Buonassisi, *Energy Environ. Sci.*, 2012, **5**, 5874–5883.
566 F. Sahli, J. Werner, B. A. Kamino, M. Brauninger, R. Monnard, B. Paviet-Salomon, L. Barraud, L. Ding, J. J. Diaz Leon, D. Sacchetto, G. Cattaneo, M. Despeisse, M. Boccard, S. Nicolay, Q. Jeangros, B. Niesen and C. Ballif, *Nat. Mater.*, 2018, **17**, 820–826.
567 M. Carmo, D. L. Fritz, J. Mergel and D. Stolten, *Int. J. Hydrogen Energy*, 2013, **38**, 4901–4934.
568 W. Kreuter and H. Hofmann, *Int. J. Hydrogen Energy*, 1998, **23**, 661–666.
569 S. Trasatti, *J. Electroanal. Chem.*, 1999, **476**, 90–91.
570 A. Ursua, L. M. Gandia and P. Sanchis, *Proc. IEEE*, 2012, **100**, 410–426.
571 F. Zhao, J. Zhang, T. Abe, D. Wohrle and M. Kaneko, *J. Mol. Catal. A: Chem.*, 1999, **145**, 245–256.
572 K. L. Materna, R. H. Crabtree and G. W. Brudvig, *Chem. Soc. Rev.*, 2017, **46**, 6099–6110.
573 A. Reynal, J. Willkomm, N. M. Muresan, F. Lakadamyali, M. Planells, E. Reisner and J. R. Durrant, *Chem. Commun.*, 2014, **50**, 12768–12771.
574 B. R. Lydon, A. Germann and J. Y. Yang, *Inorg. Chem. Front.*, 2016, **3**, 836–841.
575 S. Mukherjee, A. Mukherjee, A. Bhagi-Damodaran, M. Mukherjee, Y. Lu and A. Dey, *Nat. Commun.*, 2015, **6**, 8467.
576 M. Meldal and C. W. Tornøe, *Chem. Rev.*, 2008, **108**, 2952–3015.
577 A. K. Das, M. H. Engelhard, S. Lense, J. A. Roberts and R. M. Bullock, *Dalton Trans.*, 2015, **44**, 12225–12233.
578 P. Allongue, M. Delamar, B. Desbat, O. Fagebaume, R. Hitmi, J. Pinson and J.-M. Savéant, *J. Am. Chem. Soc.*, 1997, **119**, 201–207.
579 A. Le Goff, V. Artero, B. Jousselme, P. D. Tran, N. Guillet, R. Metaye, A. Fihri, S. Palacin and M. Fontecave, *Science*, 2009, **326**, 1384–1387.
580 M. A. Alonso-Lomillo, O. Rüdiger, A. Maroto-Valiente, M. Velez, I. Rodríguez-Ramos, F. J. Muñoz, V. M. Fernández and A. L. De Lacey, *Nano Lett.*, 2007, **7**, 1603–1608.
581 E. S. Andreiadis, P. A. Jacques, P. D. Tran, A. Leyris, M. Chavarot-Kerlidou, B. Jousselme, M. Matheron, J. Pecaut, S. Palacin, M. Fontecave and V. Artero, *Nat. Chem.*, 2013, **5**, 48–53.

582 L. Tong, M. Gothelid and L. Sun, *Chem. Commun.*, 2012, **48**, 10025–10027.
583 K. E. deKrafft, C. Wang, Z. Xie, X. Su, B. J. Hinds and W. Lin, *ACS Appl. Mater. Interfaces*, 2012, **4**, 608–613.
584 M. Tavakkoli, M. Nosek, J. Sainio, F. Davodi, T. Kallio, P. M. Joensuu and K. Laasonen, *ACS Catal.*, 2017, **7**, 8033–8041.
585 X. Zhou, T. Zhang, C. W. Abney, Z. Li and W. Lin, *ACS Appl. Mater. Interfaces*, 2014, **6**, 18475–18479.
586 P. D. Tran, A. Le Goff, J. Heidkamp, B. Jousselme, N. Guillet, S. Palacin, H. Dau, M. Fontecave and V. Artero, *Angew. Chem., Int. Ed.*, 2011, **50**, 1371–1374.
587 B. Reuillard, J. Warnan, J. J. Leung, D. W. Wakerley and E. Reisner, *Angew. Chem., Int. Ed.*, 2016, **55**, 3952–3957.
588 H. Lei, C. Liu, Z. Wang, Z. Zhang, M. Zhang, X. Chang, W. Zhang and R. Cao, *ACS Catal.*, 2016, **6**, 6429–6437.
589 P. Kang, S. Zhang, T. J. Meyer and M. Brookhart, *Angew. Chem., Int. Ed.*, 2014, **53**, 8709–8713.
590 R. Matheu, I. A. Moreno-Hernandez, X. Sala, H. B. Gray, B. S. Brunschwig, A. Llobet and N. S. Lewis, *J. Am. Chem. Soc.*, 2017, **139**, 11345–11348.
591 P. Garrido-Barros, C. Gimbert-Surinach, D. Moonshiram, A. Picon, P. Monge, V. S. Batista and A. Llobet, *J. Am. Chem. Soc.*, 2017, **139**, 12907–12910.
592 J. Creus, R. Matheu, I. Peñafiel, D. Moonshiram, P. Blondeau, J. Benet-Buchholz, J. García-Antón, X. Sala, C. Godard and A. Llobet, *Angew. Chem., Int. Ed.*, 2016, **55**, 15382–15386.
593 J. D. Blakemore, A. Gupta, J. J. Warren, B. S. Brunschwig and H. B. Gray, *J. Am. Chem. Soc.*, 2013, **135**, 18288–18291.
594 X. Li, H. Lei, X. Guo, X. Zhao, S. Ding, X. Gao, W. Zhang and R. Cao, *ChemSusChem*, 2017, **10**, 4632–4641.
595 S. K. Ibrahim, X. Liu, C. Tard and C. J. Pickett, *Chem. Commun.*, 2007, 1535–1537.
596 W. W. Kramer and C. C. L. McCrory, *Chem. Sci.*, 2016, **7**, 2506–2515.
597 X. M. Hu, Z. Salmi, M. Lillethorup, E. B. Pedersen, M. Robert, S. U. Pedersen, T. Skrydstrup and K. Daasbjerg, *Chem. Commun.*, 2016, **52**, 5864–5867.
598 L. Wang, K. Fan, Q. Daniel, L. Duan, F. Li, B. Philippe, H. Rensmo, H. Chen, J. Sun and L. Sun, *Chem. Commun.*, 2015, **51**, 7883–7886.
599 L. Wang, K. Fan, H. Chen, Q. Daniel, B. Philippe, H. Rensmo and L. Sun, *Catal. Today*, 2017, **290**, 73–77.
600 N. Kornienko, Y. Zhao, C. S. Kley, C. Zhu, D. Kim, S. Lin, C. J. Chang, O. M. Yaghi and P. Yang, *J. Am. Chem. Soc.*, 2015, **137**, 14129–14135.
601 S. Yuan, L. Feng, K. Wang, J. Pang, M. Bosch, C. Lollar, Y. Sun, J. Qin, X. Yang, P. Zhang, Q. Wang, L. Zou, Y. Zhang, L. Zhang, Y. Fang, J. Li and H. C. Zhou, *Adv. Mater.*, 2018, **30**, 1704303.
602 B. Zhu, R. Zou and Q. Xu, *Adv. Energy Mater.*, 2018, **8**, 1801193.
603 C.-C. Hou and Q. Xu, *Adv. Energy Mater.*, 2018, 1801307.
604 C. Y. Lin, D. Zhang, Z. Zhao and Z. Xia, *Adv. Mater.*, 2018, **30**, 1703646.
605 M. S. Lohse and T. Bein, *Adv. Funct. Mater.*, 2018, **28**, 1705553.
606 P.-Q. Liao, J.-Q. Shen and J.-P. Zhang, *Coord. Chem. Rev.*, 2018, **373**, 22–48.
607 M. B. Chambers, X. Wang, N. Elgrishi, C. H. Hendon, A. Walsh, J. Bonnefoy, J. Canivet, E. A. Quadrelli, D. Farrusseng, C. Mellot-Draznieks and M. Fontecave, *ChemSusChem*, 2015, **8**, 603–608.
608 C. S. Diercks, S. Lin, N. Kornienko, E. A. Kapustin, E. M. Nichols, C. Zhu, Y. Zhao, C. J. Chang and O. M. Yaghi, *J. Am. Chem. Soc.*, 2018, **140**, 1116–1122.
609 T. Zheng and L. Li, *New J. Chem.*, 2018, **42**, 2526–2536.
610 C. Wang, Z. Xie, K. E. deKrafft and W. Lin, *J. Am. Chem. Soc.*, 2011, **133**, 13445–13454.
611 S. Cui, M. Qian, X. Liu, Z. Sun and P. Du, *ChemSusChem*, 2016, **9**, 2365–2373.
612 S. Zhao, Y. Wang, J. Dong, C.-T. He, H. Yin, P. An, K. Zhao, X. Zhang, C. Gao, L. Zhang, J. Lv, J. Wang, J. Zhang, A. M. Khattak, N. A. Khan, Z. Wei, J. Zhang, S. Liu, H. Zhao and Z. Tang, *Nat. Energy*, 2016, **1**, 16184.
613 M. Wang, J. Liu, C. Guo, X. Gao, C. Gong, Y. Wang, B. Liu, X. Li, G. G. Gurzadyan and L. Sun, *J. Mater. Chem. A*, 2018, **6**, 4768–4775.
614 N. Li, J. Xu, R. Feng, T. L. Hu and X. H. Bu, *Chem. Commun.*, 2016, **52**, 8501–8513.
615 S. Sun, H. Li and Z. J. Xu, *Joule*, 2018, **2**, 1024–1027.
616 H. Li, F. Li, B. Zhang, X. Zhou, F. Yu and L. Sun, *J. Am. Chem. Soc.*, 2015, **137**, 4332–4335.
617 F. Li, Y. Jiang, B. Zhang, F. Huang, Y. Gao and L. Sun, *Angew. Chem., Int. Ed.*, 2012, **51**, 2417–2420.
618 J.-X. Jian, C. Ye, X.-Z. Wang, M. Wen, Z.-J. Li, X.-B. Li, B. Chen, C.-H. Tung and L.-Z. Wu, *Energy Environ. Sci.*, 2016, **9**, 2083–2089.
619 L. Z. Wu, B. Chen, Z. J. Li and C. H. Tung, *Acc. Chem. Res.*, 2014, **47**, 2177–2185.
620 S. Marini, P. Salvi, P. Nelli, R. Pesenti, M. Villa, M. Berrettoni, G. Zangari and Y. Kiros, *Electrochim. Acta*, 2012, **82**, 384–391.
621 M. Tahir, L. Pan, F. Idrees, X. Zhang, L. Wang, J.-J. Zou and Z. L. Wang, *Nano Energy*, 2017, **37**, 136–157.
622 P. Zhang, L. Li, D. Nordlund, H. Chen, L. Fan, B. Zhang, X. Sheng, Q. Daniel and L. Sun, *Nat. Commun.*, 2018, **9**, 381.
623 M. W. Kanan and D. G. Nocera, *Science*, 2008, **321**, 1072–1075.
624 N. Mbemba Kiele, C. Herrero, A. Ranjbari, A. Aukauloo, S. A. Grigoriev, A. Villagra and P. Millet, *Int. J. Hydrogen Energy*, 2013, **38**, 8590–8596.
625 K. Fan, H. Chen, Y. Ji, H. Huang, P. M. Claesson, Q. Daniel, B. Philippe, H. Rensmo, F. Li, Y. Luo and L. Sun, *Nat. Commun.*, 2016, **7**, 11981.
626 F. Dionigi and P. Strasser, *Adv. Eng. Mater.*, 2016, **6**, 1600621.
627 G. Ciamician, *Science*, 1912, **36**, 385–394.
628 A. R. Parent, R. H. Crabtree and G. W. Brudvig, *Chem. Soc. Rev.*, 2013, **42**, 2247–2252.
629 C. Costentin, S. Drouet, M. Robert and J. M. Saveant, *J. Am. Chem. Soc.*, 2012, **134**, 11235–11242.
630 E. S. Rountree, B. D. McCarthy, T. T. Eisenhart and J. L. Dempsey, *Inorg. Chem.*, 2014, **53**, 9983–10002.

